UNIVERSITÀ DEGLI STUDI DI PADOVA

Dipartimento di Fisica e Astronomia "Galileo Galilei"

Master Degree in Physics

Final Dissertation

Probing Light Dark Sectors via New Macroscopic Forces

Thesis supervisor

Dr. Luca Di Luzio

Candidate

Enrico Scantamburlo

Academic Year 2022/2023

Dedicated to my parents. Without them I would never have come this far.

CONTENTS

ABSTRACT

New dynamics from light and weakly-coupled sectors beyond the Standard Model may manifest as long-range forces between visible matter particles. Such new forces can be searches for by means of a variety of experimental approaches. In this thesis, we re-examine the calculation of non-relativistic potentials mediated by new light particles coupled to the Standard Model, employing a general parametrization of the new interactions and going beyond the leading order Born approximation. We correct and integrate previous results, and point out as well the presence of new relevant contact terms arising at next-to-leading order in the non-relativistic expansion.

CHAPTER 1

INTRODUCTION

The Standard Model (SM) is the foremost modern theory regarding the physics of the fundamental interactions. Developed during the second half of the twentieth century, its predictions are still tested nowadays both at the intensity and the energy frontiers, with experiments such as the LHC at CERN [1]. The discovery of the Higgs boson [2, 3] at the LHC was one of the most important advances of the past decade, confirming a fundamental prediction of the SM. Conversely, neutrino masses, the observations of dark matter and dark energy, the matter-antimatter asymmetry of the universe and the inclusion of gravity, provide experimental evidences for physics beyond the SM [4, 5]. The particle physics explanations of the previously mentioned phenomena can span an enormous range of scales, from the subnuclear to the cosmological one. While heavy new physics around the TeV scale has been often invoked, e.g. in order to address the Hierarchy Problem of the electroweak scale, the absence of new physics signals at the LHC has recently triggered a shift of interest towards light and weakly coupled extensions of the SM. Popular proposals include axions, dark photons, and sterile neutrinos [6, 7, 8]. Such new particles have been proposed in order to address possible shortcomings of the SM, as in the case of the QCD axion addressing the strong CP problem, and they belong to a hypothetical light dark sector, which is connected to the SM via new portal interactions.

The exchange of new light particles by ordinary matter (e.g. nucleons) would generate an additional, and potentially observable, "fifth" force between them. Searches for long-range spin-independent forces have a long history (see e.g. [9]), and they can be searched for via precision measurements of Newton's law, searches for violations of the equivalence principle, torsion balance techniques, etc. On the other hand, long-range spin-dependent forces could lead to a broader variety of observable effects, such as e.g. shifts in atomic energy levels. A well-studied and paradigmatic scenario is given by the QCD axion in the presence of extra sources of CP violation, in which case the axion develops both scalar and pseudo-scalar couplings to nucleons. This leads to so-called monopole-dipole forces, given by the product of a scalar and a pseudo-scalar vertex, which provide a promising experimental approach in order to test the QCD axion. In fact, a new detection concept by the ARIADNE collaboration [10] proposes to use nuclear magnetic resonance to probe the monopole-dipole force between an unpolarized material and a sample of nucleon spins, with projected sensitivities going much beyond current astrophysical limits.

The calculation of non-relativistic potentials mediated by scalar/pseudo-scalar exchange can be extended to more general Lorentz structures, including vector and axial-vector as well as tensor and pseudo-tensor interactions (see e.g. [11]). A model-independent approach actually requires only rotational invariance in the non-relativistic limit, and a more general classification of long-range potentials has been proposed in Ref. [12]. This approach potentially encodes also contributions arising from the exchange of new light particles at the loop level, the most known case being that of a neutrino pair exchange [13, 14].

It is the purpose of this thesis to critically re-examine the calculation of the non-relativistic potentials discussed above, within a general setup and going beyond the usually employed leading order Born approximation. Apart for pointing out few discrepancies with respect to the existing literature (cf. Section 4.2), the main novel result of the present work consists in the calculation of tree-level potentials beyond the leading order in the non-relativistic expansion, discussed in Chapter (5). In particular, we find the presence of new contact terms (proportional to the Dirac's delta function) which can provide a sizeable contribution when compared to their long-range counterparts arising at leading order.

The thesis is structured as follows. We will first introduce in Chapter (3) the formalism of scattering theory in non-relativistic quantum mechanics and give the formal definition of scattering potential in terms of a Fourier transform of the scattering amplitude expanded in the non-relativistic limit. Moreover, we will also discuss an alternative derivation of the long-range potential by means of a dispersion relation, that is well-suited for the calculation of loop-induced potentials. In Chapter (4) we will review the calculations of tree-level mediated potentials within a general class simplified models, encoding (pseudo)scalar, (axial)vector and (pseudo)tensor interactions. Next, we will relax the exact elasticity hypothesis and consider in Chapter (5) novel contributions arising at the next-to-leading order in the non-relativistic expansion, always assuming a general class of simplified models at tree level. Chapter (6) deals instead with loop-mediated potentials, where we extend some previous results obtained in [15]. In (7) we discuss the model-independent approach of [12], also in relation to the rotationally-invariant structure of the previously computed potentials. We offer our conclusions in Chapter (8), while more technical details and further results are deferred to Appendices (A,B,C).

CHAPTER 2

PHYSICS OF LIGHT DARK SECTORS

The search for very light and weakly coupled new particles [16] has considerably increased in the recent years, both from an experimental and theoretical point of view [17]. The SM of particle physics is considered to be an incomplete theory, and among the open questions [18] we are still trying to answer, the cosmological observations of Dark Matter [19] and the so-called strong-CP Problem [20], represent two main issues which require physics beyond the SM.
In this Chapter we introduce two popular frameworks regarding the physics of light dark sectors, including the QCD axion and the dark photon. Then we discuss some phenomenological aspects related to long-range force observables associated to those light particles and conclude with a generalization of the framework which sets the targets for the calculation of the non-relativistic potentials that will be main subject of the present thesis.

2.1 The QCD Axion

Hypothetical new particles called Axions [21, 22, 23] have been suggested in the literature as a solution of the strong-CP Problem [24, 25] and they turn out also to be ideal candidates for Dark Matter [26, 27, 28].

The Strong CP Problem

The strong-CP Problem arises from the non-trivial vacuum structure [29] of the QCD Lagrangian

$$\mathcal{L}_{QCD} = \sum_q \bar{q}(i\not{D} - m_q e^{i\theta_q\gamma^5})q - \frac{1}{4}G^a_{\mu\nu}G^{a\mu\nu} + \theta\frac{g_s^2}{32\pi^2}G^a_{\mu\nu}\tilde{G}^{a\mu\nu}\,, \tag{2.1}$$

where the linear combination of the phases $\bar{\theta} \equiv \theta + \sum_q \theta_q$ is responsible for CP violation in the strong sector. Among the CP-violating observables induced by $\bar{\theta}$, the neutron electric dipole moment [30] is the most sensitive one, as reviewed in the following.
The neutron electric dipole moment operator is given by the Lorentz-invariant Lagrangian

$$\mathcal{L}_n = -d_n\frac{i}{2}\bar{n}\sigma_{\mu\nu}\gamma^5 n F^{\mu\nu} \tag{2.2}$$

which is responsible at low-energies for the non-relativistic Hamiltonian

$$\hat{H}_n = -d_n\mathbf{E}\cdot\hat{\mathbf{S}} \tag{2.3}$$

that describes the electrostatic potential to which the nucleon spin **S** is subjected into an external electric field **E**. To relate d_n to the phase $\bar{\theta}$, it is worth noting that the effective contribution of the 5-dimensional operator of eq. (2.2) can be deduced from dimensional analysis and loop power counting, and it is given by

$$\mathcal{L}_n \sim \frac{e}{16\pi^2}\frac{m_q e^{i\bar{\theta}}}{m_n}\frac{1}{m_n}\bar{n}\sigma_{\mu\nu}\gamma^5 n F^{\mu\nu}\,. \tag{2.4}$$

Expanding for $\bar{\theta} \ll 1$ and matching the Lagrangians, the theoretical estimate yields

$$|d_n| \sim \frac{e}{16\pi^2}\frac{m_q}{m_n}\frac{\bar{\theta}}{m_n} \sim 10^{-4}\bar{\theta}\,\mathrm{e\,GeV}^{-1}\,, \tag{2.5}$$

to be compared to the experimental bound of $|d_n| \lesssim 10^{-26}\mathrm{e\,cm}$ [31] leading to the following limit on the CP-violating phase

$$|\bar{\theta}| \lesssim 10^{-10}\,. \tag{2.6}$$

Explaining the smallness of $\bar{\theta}$ constitutes the strong-CP Problem. The axion provides a dynamical solution to the strong-CP Problem by promoting $\bar{\theta}$ to a dynamical field, $a(x)$, which aquires a potential in the background of QCD dynamics and relaxes to zero.

Axion Effective Lagrangians

The axion is a periodic spin-0 field

$$a(x) = a(x) + 2\pi f_a \tag{2.7}$$

that always comes together with a mass scale f_a, called Axion Decay Constant, and it is endowed with a pseudo-shift symmetry, as dictated by the Peccei-Quinn mechanism

$$U(1)_{PQ}:\ a(x) \to a(x) + \kappa f_a \tag{2.8}$$

that leaves the action invariant up to the term

$$\delta\mathcal{S} = \frac{\kappa}{32\pi^2}\int d^4x\, G^a_{\mu\nu}\tilde{G}^{a\mu\nu}\,. \tag{2.9}$$

In this way, in the following effective Lagrangian

$$\mathcal{L}_a = \frac{1}{2}\partial_\mu a \partial^\mu a + \mathcal{L}(\partial_\mu a, \psi) + \frac{a}{f_a}\frac{g_s^2}{32\pi^2}G^a_{\mu\nu}\tilde{G}^{a\mu\nu} \tag{2.10}$$

a specific choice of the shifting parameter, $\kappa = -\bar{\theta}$, is able to cancel the strong CP-violating source. The shift symmetry indicates the Goldstone nature of the axion that originates from the spontaneous symmetry breaking of $U(1)_{PQ}$, also anomalous under $SU(3)_C$.
The brief review just given above involve a correction to the SM Lagrangian, which is more involved to rely on if we focus on the low energy behaviour of hadronic physics. To uncover other properties of the axion, it is better to change the point of view, studying the axion effective Lagrangian at the level of the chiral perturbation theory (χPT) [32, 33], whose validity lies below about 1 GeV.
Let us consider for definiteness the axion QCD Lagrangian with two flavours, $q = (u, d)^T$, give by

$$\mathcal{L}^a_{QCD} = \frac{a}{f_a}\frac{g_s^2}{32\pi^2}G^a_{\mu\nu}\tilde{G}^{a\mu\nu} - \bar{q}_L M_q q_R + h.c. + \dots\ ,\quad M_q = \begin{pmatrix} m_u & 0 \\ 0 & m_d \end{pmatrix}. \tag{2.11}$$

To pass into the χPT description, it is useful to perform an axion-dependent field transformation on the quark field

$$q \mapsto e^{i\gamma^5\frac{a}{2f_a}Q_a}q \tag{2.12}$$

with Q_a a generic matrix in flavour space with $\mathrm{Tr}\,Q_a = 1$. This anomalous rotation allows to get rid of the $aG\tilde{G}$ operator, and recast all the dependence of the axion into a dressed quark mass matrix

$$M_a = e^{i\frac{a}{2f_a}Q_a}M_q e^{i\frac{a}{2f_a}Q_a}\,. \tag{2.13}$$

Now we can perform the matching with the axion Chiral Lagrangian as

$$\mathcal{L}^a_{\chi\mathrm{PT}} = \frac{f_\pi^2}{4}\left(\mathrm{Tr}[(D_\mu\Sigma)^\dagger(D^\mu\Sigma)] + 2B\mathrm{Tr}[\Sigma M_a^\dagger + M_a\Sigma^\dagger]\right) + \dots\,, \tag{2.14}$$

where D_μ is the covariant derivative, f_π is the Pion Decay Constant, B is related to the chiral condensate, while the pion fields are in included into the matrix

$$\Sigma = e^{i\frac{\pi}{f_\pi}} \quad , \quad \pi = \begin{pmatrix} \pi^0 & \sqrt{2}\pi^+ \\ \sqrt{2}\pi^- & -\pi^0 \end{pmatrix}. \tag{2.15}$$

The specific choice of $Q_a = \mathbb{1}/2$ allows to simplify the calculations of the axion-pion potential, that reads indeed the axion potential acquires the simple analytic form (see e.g. [34])

$$V(a,\pi^0) = -m_\pi^2 f_\pi^2\sqrt{1 - \frac{4m_u m_d}{(m_u+m_d)^2}\sin^2\left(\frac{a}{2f_a}\right)}\cos\left(\frac{\pi^0}{f_\pi} - \frac{m_u - m_d}{m_u+m_d}\tan\left(\frac{a}{2f_a}\right)\right) \tag{2.16}$$

and its absolute minima satisfy the constraints

$$\begin{cases} \langle a\rangle = 0 \\ \langle\pi^0\rangle = 0 \end{cases}, \tag{2.17}$$

thus providing a solution to the strong CP-problem. An expansion around the vacuum shows the explicit expression of the axion mass, i.e.

$$m_a = \sqrt{\frac{m_\pi^2 f_\pi^2}{f_a^2}\frac{m_u m_d}{(m_u+m_d)^2}} \simeq 5.7\left(\frac{10^{12}\mathrm{GeV}}{f_a}\right)\mu\mathrm{eV}\,, \tag{2.18}$$

and since the astrophysical bounds on the axion decay constant typically imply $f_a \gtrsim 10^9$GeV (see e.g. [35, 36]), the axion mass is expected to be

$$m_a \lesssim 10^{-2\div 3}\mathrm{eV}\,. \tag{2.19}$$

Among other possible coupling that can be constructed between axions and matter fields, the axion can have derivative couplings with matter fields of the form [34]

$$\mathcal{L}(\partial_\mu a, \Psi) \supset \bar\Psi(i\partial\!\!\!/ - m_\Psi)\Psi + \frac{c_\Psi}{2}\frac{\partial_\mu a}{f_a}\bar\Psi\gamma^\mu\gamma^5\Psi\,, \tag{2.20}$$

where c_Ψ is an order one adimensional coupling and $\Psi = p, n, e$. This interaction can be rewritten in a different form via an axion-dependent field redefinition of the matter fields of the type

$$\begin{cases} \Psi \longrightarrow e^{ic_\Psi\frac{a}{2f_a}\gamma^5}\Psi \\ \bar\Psi \longrightarrow \bar\Psi e^{ic_\Psi\frac{a}{2f_a}\gamma^5} \end{cases}. \tag{2.21}$$

Thereby the operator in eq. (2.20) is traded for

$$\mathcal{L}(\partial_\mu a, \Psi) \supset \bar\Psi(i\partial\!\!\!/ - m_\Psi e^{ic_\Psi\frac{a}{f_a}\gamma^5})\Psi \tag{2.22}$$

and expanding the exponential, keeping only the linear terms in a, yields the pseudo-scalar interaction

$$-\frac{m_\Psi c_\Psi}{f_a}a\bar\Psi i\gamma^5\Psi \equiv -g_\Psi^P a\bar\Psi i\gamma^5\Psi\,. \tag{2.23}$$

In the presence of new sources of CP-violation beyond QCD the axion can also acquire a scalar coupling to matter fields [37]

$$\mathcal{L}^a \supset -g_\Psi^S a\bar\Psi\Psi\,. \tag{2.24}$$

Those couplings break the axion shift symmetry, and hence they are expected to be more suppressed compared to the standard pseudo-scalar couplings. For nucleons, $N = p, n$, the typical expectation is (see e.g. [38, 39])

$$g_N^S \sim 10^{-12}\theta_{\mathrm{eff}}\left(\frac{10^{10}\ \mathrm{GeV}}{f_a}\right), \tag{2.25}$$

where $\theta_{\mathrm{eff}} \equiv \langle a\rangle/f_a$, with $|\theta_{\mathrm{eff}}| \lesssim 10^{-10}$, is due to an axion vacuum expectation value induced by new sources of CP violation at high energies.

2.2 Dark Photons

Dark Photons [7] are another type of hypothetical particles engineered in a way to interact through a portal with ordinary matter. The vector portal allows for interactions with the SM due to the kinetic mixing between a new $\mathrm{U(1)_X}$ gauge boson $\hat{X}_\mu$ and the hypercharge $\mathrm{U(1)_Y}$ gauge boson $\hat{B}_\mu$, as described by the following renormalizable Lagrangian

$$\mathcal{L}_{mix} = -\frac{1}{4}\hat{X}_{\mu\nu}\hat{X}^{\mu\nu} + \frac{1}{2}M_X^2\hat{X}_\mu\hat{X}^\mu - \frac{1}{4}\hat{B}_{\mu\nu}\hat{B}^{\mu\nu} - \frac{\epsilon}{2}\hat{B}_{\mu\nu}\hat{X}^{\mu\nu} - g' J_\mu^Y \hat{B}^\mu \,. \tag{2.26}$$

Here, $\hat{X}_{\mu\nu}$ and $\hat{B}_{\mu\nu}$ are the respective fields strength, whereas g' is the hypercharge guage coupling and J_μ^Y the hypercharge current. Due to the kinetic mixing, the hat fields inside the Lagrangian are not canonically normalized and the corresponding gauge fields need to be redefined. The first step consists of a non-orthogonal rotation $G(\epsilon)$ in the space of the fields, such that

$$\begin{pmatrix} \hat{B}_\mu \\ \hat{W}_\mu^3 \\ \hat{X}_\mu \end{pmatrix} = G(\epsilon') \begin{pmatrix} B_\mu \\ W_\mu^3 \\ X_\mu \end{pmatrix} \,, \tag{2.27}$$

in which W_μ^3 denotes the $SU(2)_L$ gauge boson, and

$$G(\epsilon') = \begin{pmatrix} 1 & 0 & -\frac{\epsilon'}{\sqrt{1-\epsilon'^2}} \\ 0 & 1 & 0 \\ 0 & 0 & \frac{1}{\sqrt{1-\epsilon'^2}} \end{pmatrix} . \tag{2.28}$$

With such transformation, the mass matrix of the massive gauge boson is altered and in the $\epsilon' \ll 1$ limit becomes

$$M^2 = \frac{v^2}{4}\begin{pmatrix} g'^2 & -gg' & -g'^2\epsilon' \\ -gg' & g^2 & gg'\epsilon \\ -g'^2\epsilon' & gg'\epsilon' & \frac{4M_x^2}{v^2}(1+\epsilon'^2) + g'^2\epsilon'^2 \end{pmatrix} + \mathcal{O}(\epsilon'^3) \tag{2.29}$$

where g the $SU(2)_L$ gauge coupling and v the Higgs vacuum expectation value. The mass eigenstates are reached through a combination of two block-diagonal rotations around the Weinberg angle θ_w and an additional angle ξ, in this way

$$R_1(\xi)R_2(\theta_w)M^2 R_2(\theta_w)^{\mathrm{T}} R_1(\xi)^{\mathrm{T}} = \begin{pmatrix} M_\gamma^2 & 0 & 0 \\ 0 & M_Z^2 & 0 \\ 0 & 0 & M_{A'}^2 \end{pmatrix} , \tag{2.30}$$

with

$$\tan 2\xi = \frac{2\epsilon' \sin\theta_w}{1 - \hat{M}_X^2/\hat{M}_Z^2} + \mathcal{O}(\epsilon'^2) \;\;, \quad \hat{M}_Z = \frac{v\sqrt{g^2+g'^2}}{2} \,. \tag{2.31}$$

To the leading order (LO) in ϵ the masses of the new vector boson remain unaltered before and after the transformation, i.e.

$$M_{A'}^2 = M_{\hat{X}}^2(1 + \mathcal{O}(\epsilon'^2)) \,. \tag{2.32}$$

As a result, the couplings between the gauge boson mass eigenstates and the fermion currents are given by the interaction

$$\begin{pmatrix} eJ_{em}^\mu & \frac{e}{\sin\theta_w\cos\theta_w}J_Z^\mu & 0 \end{pmatrix} K \begin{pmatrix} A_\mu \\ Z_\mu \\ A'_\mu \end{pmatrix} , \tag{2.33}$$

in which

$$K \equiv \left(R_1(\xi)R_2(\theta_w)G^{-1}(\epsilon')R_2(\theta_w)^{-1}\right)^{-1} = \begin{pmatrix} 1 & 0 & -\epsilon \\ 0 & 1 & 0 \\ 0 & \epsilon\tan\theta_w & 1 \end{pmatrix} + \mathcal{O}(\epsilon\delta, \epsilon^2) \tag{2.34}$$

and $\epsilon \equiv \epsilon' \cos\theta_w$. Dealing with canonically normalized fields, the interaction between the hidden photon and the matter fields is represented by

$$\mathcal{L}_{int} = -g^V_{A'\psi} J^\mu_{em} A'_\mu \,, \tag{2.35}$$

by further defining $g^V_{A'\psi} \equiv \epsilon e$.
In extensions of the dark photon framework, there could also be direct couplings to SM fields and in particular to axial currents, as described by the following interaction term

$$\mathcal{L}_{int} \supset -g^A_{A'\psi} \bar{\psi}\gamma^\mu\gamma^5\psi A'_\mu \,. \tag{2.36}$$

2.3 Phenomenology of New Macroscopic Forces

As suggested long ago by Moody and Wilczek [37], a possible way to detect light particles (axions, dark photons, etc.) coupled with ordinary matter, is to look for new macroscopic forces mediated by the exchange of such light new particles (see also [12, 40]). These forces are associated to non-relativistic potentials acting at laboratory scales. First of all, we must define between which objects, and at which scales, these forces could act. Throughout the work we will remain general about which fermions might be involved in these new processes, merely saying that they are particles belonging to the SM. Macroscopic objects consist of electrons, neutrons and protons. Consequently, the total potential between these objects must be a sum of the pairwise interactions of fermions belonging to the two different bodies. However, we should keep in mind that this is only an approximation since a part to the total masses come from the nuclear binding energies, so the effect of long-range forces would not be taken into account only by summing over fermion pairs.
Long-range forces are searched for via different type of experiments, based on precision measurements of Newton's law, searches for violations of the equivalence principle, torsion balance techniques, shifts in atomic energy levels and nuclear magnetic resonance (for a review see e.g. [41]). However, the theroertical interpretation of those bounds has been mostly focussed on setting limits for axion-like particles and dark photons, as reviwed in the following.

2.3.1 Axion-mediated Forces

Axion-mediated potentials give rise to interactions among nucleons of three types: monopole-monopole (g^S_N-g^S_N), monopole-dipole (g^S_N-g^P_N) and dipole-dipole (g^P_N-g^P_N). Long-range spinless interaction between monopoles arises from the exchange of scalar particles at the LO of the non-relativistic expansion. The effectiveness of the force lies nearby distances comparable to Compton wavelength $\lambda \sim 1/m_a$. It can therefore be tested in laboratory searches, as reported in fig.(2.1), where the best experimental constraints on its parameter space are highlighted. The main potentials upon which the experimental research has focused so far concern interactions between monopoles and dipoles. Anticipating our results of Chapter (4), at the LO in the non-relativistic expansion they are given by

$$V_{MM}(r) = -\frac{g^S_N g^S_N}{4\pi r} e^{-m_a r} \,, \tag{2.37}$$

$$V_{MD}(r) = -\frac{g^P_N g^S_N}{8\pi m_N} \boldsymbol{\sigma}\cdot\hat{\mathbf{r}} \left(\frac{m_a}{r} + \frac{1}{r^2}\right) e^{-m_a r} \,, \tag{2.38}$$

$$V_{DD}(r) = -\frac{g^P_N g^P_N}{16\pi m_N m_{N'}} \left[\boldsymbol{\sigma}\cdot\boldsymbol{\sigma}' \left(\frac{m_a}{r^2} + \frac{1}{r^3} + \frac{4\pi}{3}\delta^3(\mathbf{x})\right) - (\boldsymbol{\sigma}\cdot\hat{\mathbf{r}})(\boldsymbol{\sigma}'\cdot\hat{\mathbf{r}}) \left(\frac{m_a^2}{r} + \frac{3m_a}{r^2} + \frac{3}{r^3}\right)\right] e^{-m_a r} \,, \tag{2.39}$$

where $m_{N,N'} \sim$ GeV are the nucleon masses while $\boldsymbol{\sigma}, \boldsymbol{\sigma}'$ are the spin vectors of the interacting particles. The Yukawa potential in eq. (2.37) leads to departures from Newton's inverse-square law and the weak equivalence principle, hence searches in this direction are important in the exploration of possible modifications of gravity. The parameter space probed by these experiments allows to estimate a bound for the magnitude the nucleon scalar coupling of

$$|g^S_N| \lesssim 10^{-20} \tag{2.40}$$

around the centimeter scale, improving the astrophysical limits.
Difficulties in handling large quantities of polarized atoms make in general spin-dependent forces less sensitive. Nevertheless, they can still be tested by searching for the spin depolarization of nucleons when exposed to surrounding bulk matter. Laboratory and astrophysical tests already probed a large region of the parameter space, as shown in fig.(2.2), for the mixed interaction in eq. (5.27). A fundamental improvement will be achieved by the experiment ARIADNE [42], for which the projections in the figure seem to indicate that this could be the first experiment to overcome the limitations posed by astrophysical considerations and current laboratory bounds [43]. The strategy for its possible detection consist in rewriting the spin-dependent interaction energies using an axion potential as

$$-\boldsymbol{\nabla} V_a \cdot \boldsymbol{\sigma}' \tag{2.41}$$

where $\boldsymbol{\nabla} V_a$ is the gradient of eq. (4.10, 4.14) if an axion can be exchanged between two spins. Hence, the axion potential by polarized or unpolarized objects acts on nearby fermions just like an effective magnetic field such as

$$\mathbf{B}_{eff} = \frac{2}{\hbar \gamma_f} \boldsymbol{\nabla} V_a \tag{2.42}$$

in which γ_f is the fermion gyromagnetic ratio. Notice that this field is couples differently from a classical magnetic field since interacts to the spin of the particle, is independent from the fermion magnetic moment and distinguish between neutrons and electrons.

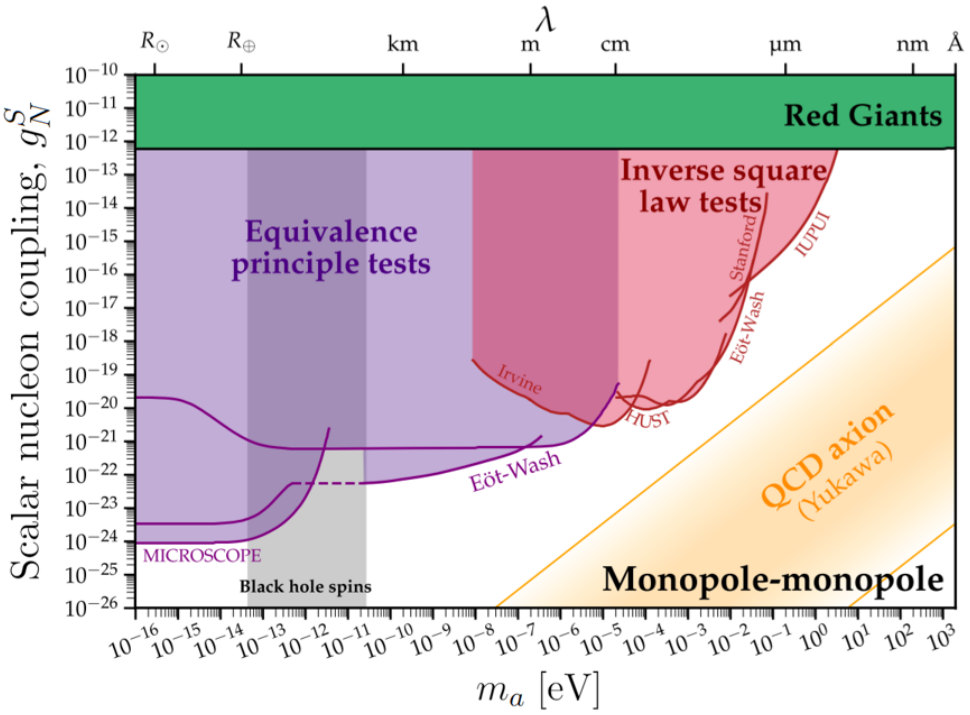

Figure 2.1: Figure from [41]. Experimental searches for the axion-nucleon scalar coupling. The literature on these tests usually shown constraints between the axion mass m_a, or its Compton wavelength λ, and the scalar coupling g_N^S. The astrophysical bound is represented by the upper green band, in red are tests of the inverse-square law whereas those in purple are tests of the weak equivalence principle. The excluded region from black hole spin arguments is depicted in gray and, lastly, the diagonal yellow band shows the expected range for the QCD axion scalar coupling.

A similar search strategy is pursued the QUAX-$g_s g_p$ experiment [44] (located at the INFN Labs of Legnaro), axion-mediated force in between unpolarized nucleons and polarized electrons. The most stringent limit so far can be derived for $|g_N^S g_{e,N}^P|$ from the combination of astrophysical and laboratory bounds shown e.g. in fig. (2.2,2.3). Remaining on the macroscopic centimeters scales, the upper limit for these couplings are around

$$|g_N^S g_e^P| \lesssim 10^{-33} \quad , \quad |g_N^S g_N^P| \lesssim 10^{-30}. \tag{2.43}$$

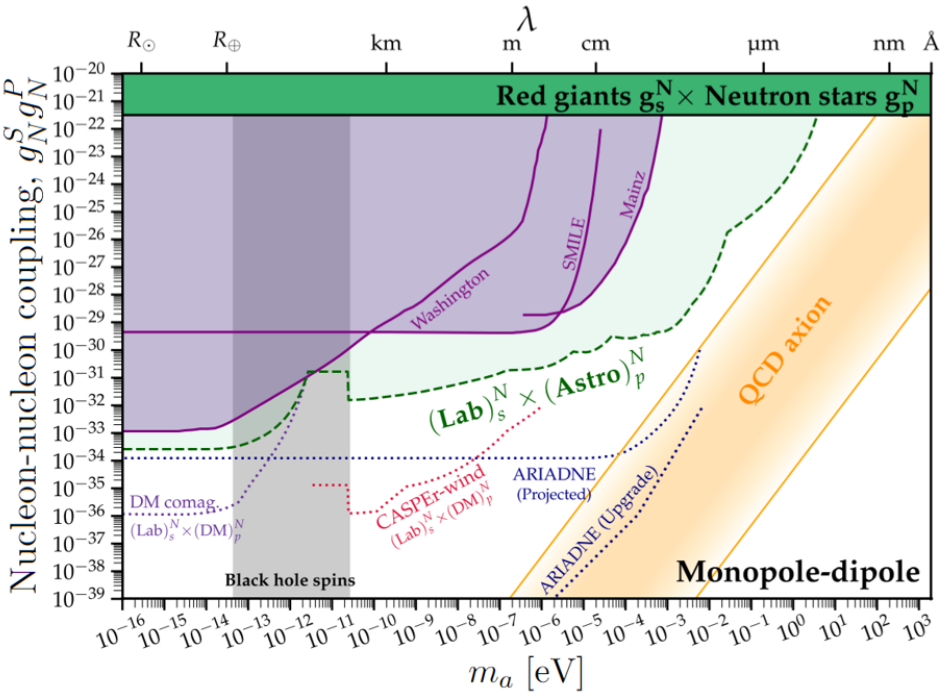

Figure 2.2: Figure from [41]. Bounds for the mixed scalar pseudo-scalar couplings between nucleons. The solid lines are all existing limits on this parameter space, the dashed lines correspond to a combination of laboratory scalar searches and astrophysical pseudoscalar bounds, and the dotted lines are all projections. In green the astrophsical limits while the QCD band is depicted in yellow.

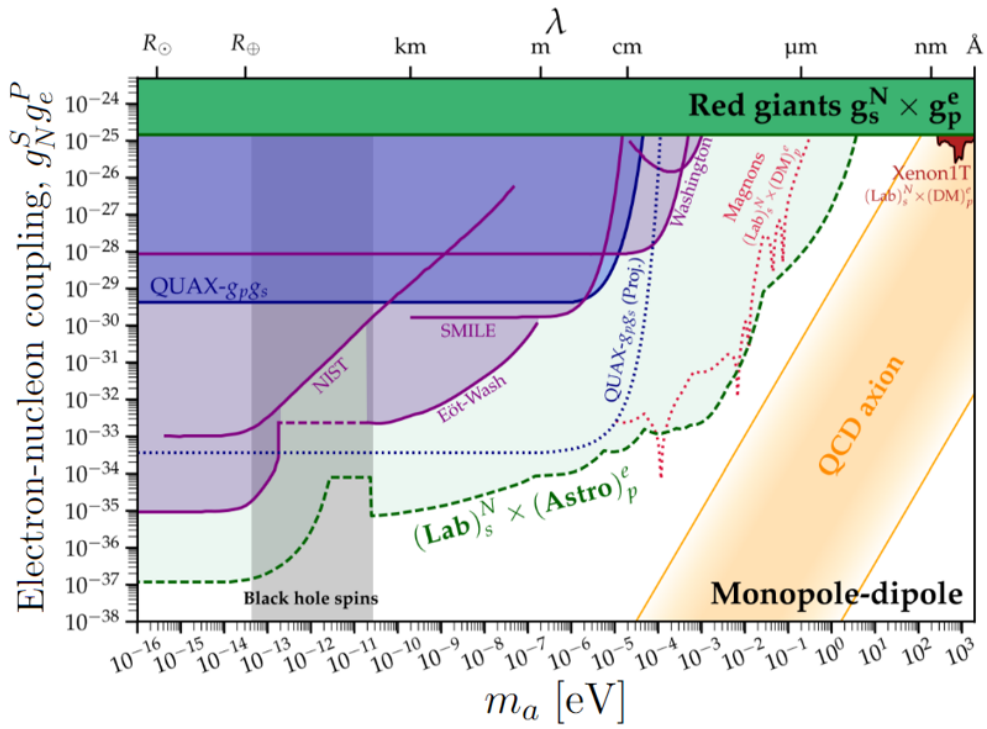

Figure 2.3: Figure from [41]. Experimental searches for the scalar pseudo-scalar mixed coupling of electrons and nucleons. The solid lines corresponds to existing laboratory bounds, the dotted lines are the future projections while the dashed lines represents the combination of laboratory and astrophysical bounds. In blue are reported the results of QUAX-$g_p g_s$ whereas in purple are other searches for monopole-dipole forces. The green band corresponds to the astrophysical bound and the axion QCD band is shown in yellow.

Dipole-dipole forces, in eq. (5.29), can also be searched for in laboratory experiments, but their results are much less restrictive than the corresponding astrophysical limits. It should be mentioned that other types of experiments [45] are usually employed to hunt for the axion, such as helioscopes, which rely on the additional assumptions that the axion comprises dark matter.

2.3.2 Dark Photon Phenomenology

The parameter space of dark photons has been probed by a plethora of experiments, from cosmological to laboratory searches. In fig. (2.4) is reported the landscape of bounds on dark photons lighter than 0.1 MeV and the kinetic mixing parameter with photons. Similar techniques can be borrowed from ARIADNE experiment, for light massive gauge boson searches, yielding a projected sensitivity [41] for the mixing parameter of $\epsilon \lesssim 10^{-12}$. Many model-independent bounds on dark photon have been obtained also through tests of the Coulomb force law and the photon mass. Direct cosmological searches set bounds on the hidden photon as dark matter candidate, while astrophysical limits at higher masses are those based on stellar cooling arguments applied to the Sun, horizontal branch stars, and red giant stars. Purely laboratory bounds come from atomic spectroscopy and microscopy. Outside the sphere of dark photons, precision molecular spectroscopy experiments are used to test new physics below the angstrom scale using the transition frequencies of simple molecular systems. Indeed, the presence of dark forces shift the energy levels of quantum. The most relevant ones are the hydrogen molecule, the molecular hydrogen-deuterium ion and the exotic muonic molecular deuterium ion. Certain of these results have recently been used to bound short-distance modifications of gravity. The same types of bounds can be obtained also from the scattering of cold neutrons on nuclei measured via optical and transition methods and Bragg diffraction.

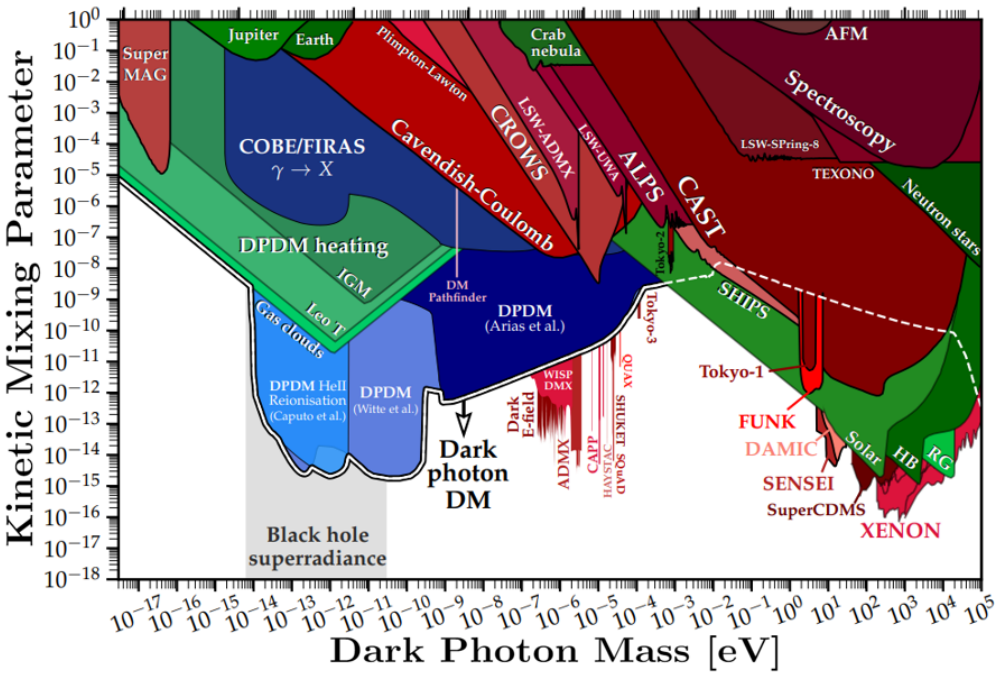

Figure 2.4: Figure from [46]. Bounds on dark photon mass and the kinetic mixing parameter. In blue are cosmological limits, experimental bounds in red and astrophysical searches in green. The grey region is excluded from arguments about the superradiance effects in black holes. The white line corresponds to dark photon limits as dark matter candidate.

2.4 Thesis Goals and Direction

The main goal of this thesis work is to revise the calculation of non-relativistic potentials mediated by new light particles, going beyond the simplified scenarios offered by axion-like particles and dark photons. To this end, we will first introduce in Chapter (3) the formalism of scattering theory and the

tools in order to compute the non-relativistic potentials. In Chapter (4) we will revise the calculations of tree-level mediated potentials within simplified models. Next, we will relax the exact elasticity hypothesis and consider in Chapter (5) novel contributions arising at the next-to-leading order (NLO) in the non-relativistic expansion. Chapter (6) deals instead with loop-mediated potentials, while in (7) we aim at a general model-independent approach.

CHAPTER 3

NON-RELATIVISTIC POTENTIALS

In this Chapter we provide the theoretical tools needed to derive the non-relativistic potentials mediated by new light particles coupled to the SM fields. At the leading-order these are obtained by taking the Fourier transform of the elastic scattering amplitude in QFT expanded in the non-relativistic limit. An alternative formulation based on dispersion theory, that is well-suited for the calculation of non-relativistic potentials beyond tree level, will be also introduced.

3.1 Scattering Theory and Lippmann-Schwinger Equation

Scattering Theory (see e.g. [47, 48]) is a framework for studying the scattering of particles that interact under the influence of a potential V. For our purposes it is sufficient to treat only quantities that do not change in time, so let us suppose to have a time-independent scattering described by

$$H = H_0 + V \ , \quad H_0 = \frac{p^2}{2m} \tag{3.1}$$

with H_0 the free-Hamiltonian whose eigenstates are plane waves of momentum $\mathbf{p}$. If the scattering is elastic, the energies of the particles are the same before and after the process and, requiring to obtain the free case as $V \to 0$, we look for a solution of the Schrödinger equation with the same energy eigenvalue, i.e.

$$H_0|\phi\rangle = E|\phi\rangle \xrightarrow[\text{Scattering}]{\text{Elastic}} (H_0 + V)|\psi\rangle = E|\psi\rangle \, . \tag{3.2}$$

In both cases the energy spectrum is continuos and the well-known solution is provided by the Lippmann-Schwinger equation

$$|\psi^{(\pm)}\rangle = |\phi\rangle + \frac{V|\psi^{(\pm)}\rangle}{E - H_0 \pm i\epsilon} \tag{3.3}$$

making E slightly complex to avoid singularity problems. Projecting on the coordinate space, this results into the integral equation

$$\langle \mathbf{x}|\psi^{\pm}\rangle = \langle \mathbf{x}|\phi\rangle + \int d^3x' \langle \mathbf{x}| \frac{1}{E - H_0 \pm i\epsilon} |\mathbf{x}'\rangle \langle \mathbf{x}'|V|\psi^{\pm}\rangle \, , \tag{3.4}$$

while in momentum space

$$\langle \mathbf{p}|\psi^{\pm}\rangle = \langle \mathbf{p}|\phi\rangle + \frac{1}{E - p^2/2m \pm i\epsilon} \langle \mathbf{p}|V|\psi^{\pm}\rangle \, , \tag{3.5}$$

recalling that

$$\begin{aligned} \langle \mathbf{x}|\phi\rangle &= \frac{e^{i\mathbf{p}\cdot\mathbf{x}}}{(2\pi)^{3/2}}\,, \\ \int d^3x \langle \mathbf{p}'|\mathbf{x}\rangle\langle \mathbf{x}|\mathbf{p}\rangle &= \delta^3(\mathbf{p}-\mathbf{p}')\,. \end{aligned} \tag{3.6}$$

Working in the position representation, the expectation value of the energy operator has to be evaluated [47]. Starting from eq. (3.4) and inserting a completeness relation

$$\begin{aligned} \langle \mathbf{x}|\frac{1}{E-H_0\pm i\epsilon}|\mathbf{x}'\rangle &= \int d^3p' d^3p'' \langle \mathbf{x}|\mathbf{p}'\rangle\langle \mathbf{p}'|\frac{1}{E-|\mathbf{p}'|^2/2m\pm i\epsilon}|\mathbf{p}''\rangle\langle \mathbf{p}''|\mathbf{x}'\rangle = \\ &= \int \frac{d^3p'}{(2\pi)^3}\frac{e^{i\mathbf{p}'\cdot(\mathbf{x}-\mathbf{x}')}}{E-|\mathbf{p}'|^2/2m\pm i\epsilon}\,. \end{aligned} \tag{3.7}$$

Then, setting $E\equiv k^2/2m$, via the Residue Theorem the integral reads

$$\begin{aligned} &\frac{2m}{(2\pi)^2}\int_0^\infty p'^2 dp' \int_{-1}^1 d(\cos\theta)\frac{e^{ip'|\mathbf{x}-\mathbf{x}'|\cos\theta}}{k^2-p'^2\pm i\epsilon} = \\ &= \frac{2m}{8\pi^2 i|\mathbf{x}-\mathbf{x}'|}\int_{-\infty}^\infty dp' p' \frac{(e^{ip'|\mathbf{x}-\mathbf{x}'|}-e^{-ip'|\mathbf{x}-\mathbf{x}'|})}{k^2-p'^2\pm i\epsilon} = -\frac{2m}{4\pi}\frac{e^{\pm ik|\mathbf{x}-\mathbf{x}'|}}{|\mathbf{x}-\mathbf{x}'|}\,. \end{aligned} \tag{3.8}$$

After substituting into eq. (3.4) we obtain

$$\langle \mathbf{x}|\psi^\pm\rangle = \langle \mathbf{x}|\phi\rangle - \frac{m}{2\pi}\int d^3x' \frac{e^{\pm ik|\mathbf{x}-\mathbf{x}'|}}{|\mathbf{x}-\mathbf{x}'|}\langle \mathbf{x}'|V|\psi^\pm\rangle\,, \tag{3.9}$$

which shows that the wave function $\langle \mathbf{x}|\psi^\pm\rangle$ in the presence of the scatterer is written as the sum of he wave function of the incident wave $\langle \mathbf{x}|\phi^\pm\rangle$ and a term that represents the effects of the scattering.
To extract an explicit behaviour for $\langle \mathbf{x}|\psi^\pm\rangle$ let us consider the specific case where V is a local potential, i.e.

$$\langle \mathbf{x}|V|\mathbf{x}'\rangle = V(\mathbf{x})\delta^3(\mathbf{x}-\mathbf{x}')\,, \tag{3.10}$$

in this way the matrix element returns

$$\langle \mathbf{x}'|V|\psi^\pm\rangle = V(\mathbf{x}')\langle \mathbf{x}'|V|\psi^\pm\rangle\,. \tag{3.11}$$

The integral Lippmann-Schwinger equation now becomes

$$\langle \mathbf{x}|\psi^\pm\rangle = \langle \mathbf{x}|\phi\rangle - \frac{m}{2\pi}\int d^3x' \frac{e^{\pm ik|\mathbf{x}-\mathbf{x}'|}}{|\mathbf{x}-\mathbf{x}'|}V(\mathbf{x}')\langle \mathbf{x}'|\psi^\pm\rangle \tag{3.12}$$

and to proceed further it is necessary to approximate this expression. To do so, notice that $\mathbf{x}$ is the position of the detector at which the wave function is evaluated, while the integrated coordinate $\mathbf{x}'$ represent the region of space where is active the potential. In scattering processes we are interested in studying the effect of the scatterer at a point far outside the range of the potential, since we cannot put a detector at short distance near the scattering center. As consequence, the region in fig. (3.1) described by the position $\mathbf{x}'$ is reasonably smaller respect to the detector position, $\mathbf{x}$, so we can safely set

$$|\mathbf{x}| \gg |\mathbf{x}'| \tag{3.13}$$

and expand the difference as

$$|\mathbf{x}-\mathbf{x}'| = \sqrt{|\mathbf{x}|^2 - 2|\mathbf{x}||\mathbf{x}'|\cos\alpha + |\mathbf{x}'|^2} \simeq |\mathbf{x}| - \hat{\mathbf{r}}\cdot\mathbf{x}'\,, \tag{3.14}$$

where $\hat{\mathbf{r}}$ is the unit vector pointing at $\mathbf{x}$, while α is the angle subtended by the two positions. Thus, the plane wave becomes

$$e^{\pm ik|\mathbf{x}-\mathbf{x}'|} \simeq e^{\pm ik|\mathbf{x}|}\, e^{\mp i\mathbf{k}'\cdot\mathbf{x}'} \quad , \quad \mathbf{k}' \equiv k\hat{\mathbf{r}}\,. \tag{3.15}$$

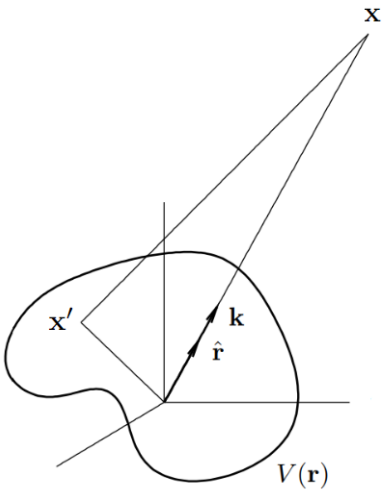

Figure 3.1: The region where the potential is active, covered by $\mathbf{x}'$, is much smaller than the position $\mathbf{x}$ in which the wave function $\langle \mathbf{x}|\psi^{\pm}\rangle$ is evaluated.

defining $\mathbf{k}'$ as the propagation vector for waves reaching the observation point.
In the long-distance limit then

$$\langle \mathbf{x}|\psi^{\pm}\rangle \xrightarrow[\text{Range}]{\text{Long}} \langle \mathbf{x}|\phi\rangle - \frac{me^{\pm ik|\mathbf{x}|}}{2\pi|\mathbf{x}|}\int d^3x' e^{\mp i\mathbf{k}'\cdot\mathbf{x}'}V(\mathbf{x}')\langle \mathbf{x}'|\psi^{\pm}\rangle \tag{3.16}$$

and by renaming $\mathbf{x} \equiv r$ we arrive at the known equation in scattering theory in which, after the scattering, we have the original wave propagating along $\mathbf{k}$ plus an outgoing spherical wave with amplitude $f(\mathbf{k},\mathbf{k}')$, called scattering amplitude, given by

$$f(\mathbf{k},\mathbf{k}') \equiv -\frac{m}{2\pi}\int d^3x' e^{-i\mathbf{k}'\cdot\mathbf{x}'}V(\mathbf{x}')\langle \mathbf{x}'|\psi^{\pm}\rangle\,, \tag{3.17}$$

$$\langle \mathbf{x}|\psi^{+}\rangle \xrightarrow[\text{Range}]{\text{Long}} \frac{1}{(2\pi)^{3/2}}\left(e^{i\mathbf{k}\cdot\mathbf{x}} + \frac{e^{ikr}}{r}f(\mathbf{k},\mathbf{k}')\right)\,, \tag{3.18}$$

where the positive solution was taken because it is difficult to prepare a system satisfying the boundary condition appropriate for the negative one. At the end, the scattering amplitude is directly related to the differential cross-section, indeed the ratio between the number of particles scattered into the solid angle $d\Omega$ and the number of incident particles crossing the unit area, per unit time, is

$$\frac{d\sigma}{d\Omega}d\Omega = \frac{r^2|\mathbf{j}_{scat.}|}{|\mathbf{j}_{inc.}|}d\Omega = |f(\mathbf{p},\mathbf{p}')|^2 d\Omega\,, \tag{3.19}$$

where $\mathbf{j}_{inc.}$ and $\mathbf{j}_{scat.}$ are the flux densities of incoming and scattered particles.
Having a direct connection to an experimental quantity is good for our purposes. However, the expression of the scattering amplitude is still too formal to be used directly in calculations, due to the lack of knowledge of $\psi^{+}(\mathbf{x})$. If the effect of the scatterer is not very strong, we may assume a plane wave approximation for the behaviour of the scattered wave, replacing

$$\langle \mathbf{x}'|\psi^{+}\rangle \longrightarrow \langle \mathbf{x}'|\phi\rangle = \frac{e^{i\mathbf{p}\cdot\mathbf{x}'}}{(2\pi)^{3/2}} \tag{3.20}$$

inside the integral. This method, known as Born Approximation, allows us to re-express the scattering amplitude as follows

$$f(\mathbf{p},\mathbf{p}') = -\frac{m}{2\pi}\int d^3x\, e^{-i\mathbf{q}\cdot\mathbf{x}}V(\mathbf{x})\ , \quad \mathbf{q} = \mathbf{p}' - \mathbf{p}\,, \tag{3.21}$$

or, apart for a multiplicative factor, to connect the amplitude and the potential via a Fourier transformation.

All that is left is to connect this last formula to the Feynman amplitude of the QFT formalism [49, 50] by building a bridge between a more fundamental QFT and the non-relativistic potentials to be measured in the laboratory.
Recalling the covariant normalization for quantum states in the relativistic mechanics

$$\langle \mathbf{p}|\mathbf{p}'\rangle = (2\pi)^3 2E_{\mathbf{p}}\delta^3(\mathbf{p}-\mathbf{p}')\,, \tag{3.22}$$

from the scattering matrix relation to the canonically normalized transition amplitude

$$S_{fi} = \mathbb{1} + i(2\pi)^4\delta^4(P_f - P_i)\mathcal{M}_{fi}^{CN} \tag{3.23}$$

the Feynman amplitude $\mathcal{M}$ is recovered by multiplying $\mathcal{M}_{fi}^{CN}$ by the normalization of the states. Now, defining classical quantum mechanical amplitude as

$$\frac{2\pi}{m} f(\mathbf{p},\mathbf{p}') \tag{3.24}$$

the matching in the non-relativistic limit makes it possible to identify

$$f(\mathbf{p},\mathbf{p}') = \frac{m}{(2\pi)^4}\mathcal{M}_{NR}(\mathbf{q}) \tag{3.25}$$

thus, the final expression for the potential, after inverting the transformation of eq. (3.21), is

$$V(\mathbf{x}) = -\int \frac{d^3q}{(2\pi)^3}\, e^{i\mathbf{q}\cdot\mathbf{x}}\mathcal{M}_{NR}(\mathbf{q})\,. \tag{3.26}$$

The result obtained above is only the first-order of a series that better interpolates the real solution. To extract the series, let us define the transition operator such that

$$V|\psi^{(\pm)}\rangle \equiv T|\phi\rangle \tag{3.27}$$

and substitute it into eq. (3.3)

$$T|\phi\rangle = V|\phi\rangle + V\frac{1}{E - H_0 \pm i\epsilon}T|\phi\rangle\,. \tag{3.28}$$

Since it holds for any ket, at the operatorial level we have

$$T = V + V\frac{1}{E - H_0 \pm i\epsilon}T\,. \tag{3.29}$$

This equation can be solved iteratively, resulting in

$$T = V + V\frac{1}{E - H_0 \pm i\epsilon}V + V\frac{1}{E - H_0 \pm i\epsilon}V\frac{1}{E - H_0 \pm i\epsilon}V + \dots \tag{3.30}$$

and from that, it is straightforward to deduce that also the scattering amplitude must come into an expansion

$$f(\mathbf{p}',\mathbf{p}) = \sum_{n=1}^{\infty} f^n(\mathbf{p}',\mathbf{p})\,. \tag{3.31}$$

In particular, in the long-distance limit and in the momentum basis

$$\begin{aligned} f^1(\mathbf{p}',\mathbf{p}) &= -\frac{m}{2\pi}(2\pi)^3\langle \mathbf{p}'|V|\mathbf{p}\rangle \\ f^2(\mathbf{p}',\mathbf{p}) &= -\frac{m}{2\pi}(2\pi)^3\langle \mathbf{p}'|V\frac{1}{E - H_0 \pm i\epsilon}V|\mathbf{p}\rangle \\ &\vdots \end{aligned} \tag{3.32}$$

which correspond to higher orders in the Born approximation.

3.2 Dispersion Theory for Non-relativistic Potentials

A different approach for the calculation of the non-relativistic potentials relies on a Dispersion Theory [51, 52], in which the analytic properties of the Feynman amplitude are explicitly taken into account for the manipulation of non-trivial loop integrals. Indeed, the presence of one-particle intermediate states leads to simple poles in the Fourier transforms of the matrix elements, while multi-particle intermediate states produce more complicated singularities.
Important properties of an interacting QFT emerge from the so-called spectral representation of the vacuum expectation values of suitable quantities, e.g. propagators. For the sake of simplicity, let us consider a complex scalar operator $\Phi(x)$ in the Heisenberg picture, which may or may not be an elementary particle field. Its 2-point function

$$\langle 0|\Phi(x)\Phi^\dagger(y)|0\rangle \tag{3.33}$$

may be written in a different way via a completeness insertion of any complete sets of states, as

$$\sum_\alpha \langle 0|\Phi(x)|\alpha\rangle\langle\alpha|\Phi^\dagger(y)|0\rangle \tag{3.34}$$

where α can be taken as discrete or continuous index. Choosing the eigenstates of p^μ, translational invariance tells us how $\Phi(x)$ transforms under the unitary representation $U(a) = e^{ip\cdot a}$ of the restriced Poincarè cover group $\mathcal{P}_+^\uparrow$, i.e.

$$U(a)\Phi(x)U(a)^\dagger = \Phi(x-a)\,. \tag{3.35}$$

As consequence

$$\begin{aligned}\sum_\alpha \langle 0|U(x)\Phi(0)U(x)^\dagger|\alpha\rangle\langle\alpha|U(y)\Phi(0)U(y)^\dagger|0\rangle &= \sum_\alpha e^{-ip_\alpha\cdot(x-y)}|\langle 0|\Phi(0)|\alpha\rangle|^2 = \\ &= \int \frac{d^4q}{(2\pi)^3}\sigma_+(q)e^{-iq\cdot(x-y)}\,,\end{aligned} \tag{3.36}$$

where the Fourier transform of the 2-point function has been defined as

$$\sigma_+(q) \equiv (2\pi)^3 \sum_\alpha \delta(q-p_\alpha)|\langle 0|\Phi(0)|\alpha\rangle|^2\,. \tag{3.37}$$

It is straightforward to then derive the following properties of $\sigma_+(q)$:

- it is a real and semi-definite positive function;
- $\sigma_+(q) \neq 0$ only inside the future lightcone which contains the spectrum of p^μ;
- it is a Lorentz-scalar, i.e. $\sigma_+(\Lambda q) = \sigma_+(q)$ for $\Lambda \in \mathcal{P}_+^\uparrow$.

The above properties ensure to $\sigma_+(q)$ all the credentials of a probability density distribution, such that its most general form is

$$\sigma_+(q) = \rho(q^2)\theta(q^0) + (2\pi)^3|\langle 0|\Phi(0)|0\rangle|^2\delta(q)\,, \tag{3.38}$$

where $\sigma(q^2) = 0$ for $q^2 < 0$ and $\delta(q)$ takes into account possible non vanishing VEV. In fact, it is easy to show that, when the canonical commutation relations are satisfied for $\Phi(x)$, then

$$\int_{-\infty}^{+\infty} dq^0\, q^0\big(\sigma_+(q) - \sigma_+(-q)\big) = 1 \implies \int_0^\infty d\mu^2\,\rho(\mu^2) = 1\,, \tag{3.39}$$

as expected by a probability density.
We can finally rewrite eq. (3.36) as

$$\begin{aligned}\langle 0|\Phi(x)\Phi^\dagger(y)|0\rangle &= \int_0^\infty d\mu^2\rho(\mu^2)\int \frac{d^4q}{(2\pi)^3}\delta(q^2-\mu^2)\theta(q^0)e^{-iq\cdot(x-y)} + |\langle 0|\Phi(0)|0\rangle|^2 = \\ &= \int_0^\infty d\mu^2\rho(\mu^2)\Delta_+(x-y;\mu) + |\langle 0|\Phi(0)|0\rangle|^2\,,\end{aligned} \tag{3.40}$$

with $\Delta_+(x-y;\mu)$ the positive frequency 2-point function of the free-theory. The last term can be formally removed just by shifting $\Phi(x)$. Eq. (3.40) tells us that in the interacting theory we can write the 2-points functions as an integral of 2-points functions of the free-fields with varying mass. This fact is a purely relativistic effect due to Lorentz invariance. A similar treatment can be performed with time ordered operators inside the matrix element, such that the same relation holds for the effective propagator

$$\langle 0|\mathrm{T}[\Phi(x)\Phi^\dagger(y)]|0\rangle \equiv i\Delta(x-y) = \int_0^\infty d\mu^2 \rho(\mu^2) i\Delta_F(x-y;\mu)\,, \tag{3.41}$$

where now the momentum space propagator of the free-field is

$$\Delta_F(q;\mu) = \frac{1}{q^2-\mu^2+i\epsilon}\,. \tag{3.42}$$

In the most general case beyond the tree-level, the Källén-Lehmann spectral representation reads

$$\Delta(q) = \int_0^\infty d\mu^2\, \frac{\rho(\mu^2)}{q^2-\mu^2+i\epsilon} \tag{3.43}$$

and it can be easily extended to the other cases of spin-1/2 and -1 with few cautions.
Apart from the coupling constants, inserting the non-relativistic limit of eq. (3.43) into eq. (3.26) allows to recast the functional form of the potential into

$$V(\mathbf{x}) \sim \frac{1}{4\pi r}\int_0^\infty d\mu^2\, \rho(\mu^2)\, e^{-\mu r}\,. \tag{3.44}$$

It is clear that at tree-level $\rho(\mu^2) = \delta(\mu^2 - M^2)$, hence the scalar Yukawa interaction $g_i^y \bar{\psi}_i \psi_i \phi$ results into

$$V(\mathbf{x}) = -\frac{g_1^y g_2^y}{4\pi r} e^{-Mr}\,. \tag{3.45}$$

In general, finding $\rho(q)$ for a specific interaction is provided by immediately recognising eq. (3.43) as a dispersion relation [51] with spectral density

$$\rho(\mu^2) = -\frac{1}{\pi}\mathrm{Im}\{\Delta(q)\}\,. \tag{3.46}$$

The final tool necessary to calculate the imaginary parts is the optical theorem for forward scattering, which states that

$$2\mathrm{Im}\{\Delta(q)\} = \sum_X \int d\Pi_X (2\pi)^4 \delta(p_A - p_X) |\mathcal{M}(q\to X)|^2\,, \tag{3.47}$$

where $d\Pi_X$ is the Lorentz-invariant phase space measure for the intermediate state X. $\mathcal{M}(q\to X)$, instead, corresponds to the tree-level cut of the loop diagram, and it is natural to interpret it as the decay of an external source of momentum q to a final state of two hidden particles.
As we shall see, the dispersion techniques allow to tackle quantum processes from a different angle, avoiding conventional loop calculations and obtaining the same results in a simple manner.

CHAPTER 4

TREE-LEVEL POTENTIALS

Long-range potentials acting between SM matter fields can be derived using basic tools of QFT such as interacting Lagrangians and Feynman diagrams [50]. New light particles, as mediator of a new Fifth Force, are generally added to the SM through simple extensions. For later convenience, we split the Lagrangian in

$$\mathcal{L} = \mathcal{L}_{kin} + \mathcal{L}_{int}\,, \tag{4.1}$$

where the kinetic part describes the free fields of the model, and the interacting sector is responsible for the new phenomena that could be observed.
Scattering between two different SM fermions are described at tree-level by t-channel diagrams, as in fig. (**??**). The masses of the external states are denoted as m_1 and m_2, while the interaction occurs through the exchange of a new light boson of mass M.

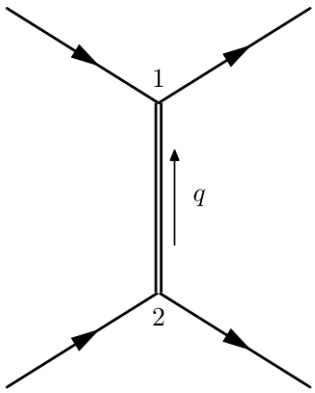

Figure 4.1: Representative Feynman diagram responsible for tree-level potentials mediated by a new light boson.

According to the laws of non-relativistic quantum mechanics, in particular the inverse Born approximation [47], the LO form of the non-relativistic potentials is directly connected to the Fourier transform of the scattering amplitude $\mathcal{M}(\mathbf{q})$ expanded in the non-relativistic limit, as given by eq. (3.26).

4.1 Non-relativistic Potentials in the Elastic Limit

The first step of our treatment focuses on the calculation of the LO of non-relativistic potentials to consolidate and correct some results present in literature, as in [37, 12, 11]. The path we follow goes from the simplest interactions, mediated by axion-like particles, to the more complicated ones, always compatible to the exchange of a new boson at tree-level. A natural classification emerges via the contraction with all possible Lorentz forms of spinor matrices

$$\Gamma = \{\mathbb{1}, \gamma^5, \gamma^\mu, \gamma^\mu\gamma^5, \sigma^{\mu\nu}\}\,. \tag{4.2}$$

The elastic scattering hypothesis impose the conservation of the energy between the external particles, in this way the transferred energy vanishes and the only quantity to be integrated is the transferred momentum $\mathbf{q}$.
The analysis is held within the formalism we have discussed so far, while other technical details can be found in the Appendices (A,B).

4.1.1 Axion-Like Particles

Interactions mediated by an axion-like particle between SM fermions are described via

$$\mathcal{L}_{kin} = \frac{1}{2}\partial_\mu a \partial^\mu a - \frac{1}{2}M^2 a^2 + \sum_{i=1}^{2} \bar{\psi}_i \left(i\partial\!\!\!/ - m_i\right)\psi_i\,, \tag{4.3}$$

$$\mathcal{L}_{int} = -\sum_{i=1}^{2} \bar{\psi}_i (g_i^S + g_i^P i\gamma^5)\psi_i\, a\,, \tag{4.4}$$

where both the scalar and pseudoscalar vertices are present in the Lagrangian, so that three types of interactions are possible, all of them expressed by the following t-channel diagram.

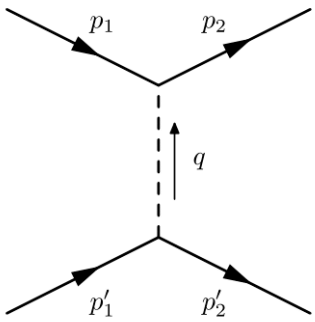

Figure 4.2: Feynman diagram for a tree-level scalar exchange.

Scalar Scalar Interaction

The Feynman rules in momentum space allow us to write the relativistic amplitude

$$i\mathcal{M} = (-ig_1^S)(-ig_2^S)\bar{u}_r(p_2)u_s(p_1)\frac{i}{q^2 - M^2}\bar{u}_{r'}(p_2')u_{s'}(p_1')\,, \tag{4.5}$$

and taking the non-relativistic limit, see A.1 for details, it becomes

$$\mathcal{M} = \frac{g_1^S g_2^S}{|\mathbf{q}|^2 + M^2}\,. \tag{4.6}$$

The associated Yukawa potential is proportional to the Fourier transform of $\mathcal{M}$, hence

$$V(r) = -g_1^S g_2^S \int \frac{d^3q}{(2\pi)^3} \frac{e^{i\mathbf{q}\cdot\mathbf{x}}}{|\mathbf{q}|^2 + M^2} = -\frac{g_1^S g_2^S}{4\pi r} e^{-Mr}\,, \tag{4.7}$$

where the integral is given in B.2.

Scalar Pseudo-scalar Interaction

A diagram with a scalar and a pseudo-scalar vertex produces the amplitude

$$\begin{aligned} i\mathcal{M} &= (-ig_1^P)(-ig_2^S)\bar{u}_r(p_2)i\gamma^5 u_s(p_1)\frac{i}{q^2 - M^2}\bar{u}_{r'}(p_2')u_{s'}(p_1') = \\ &= g_1^P g_2^S \bar{u}_r(p_2)\gamma^5 u_s(p_1)\frac{i^2}{|\mathbf{q}|^2 + M^2}\bar{u}_{r'}(p_2')u_{s'}(p_1') \end{aligned} \tag{4.8}$$

and since the pseudoscalar bilinear is exact in the elastic limit, see A.1,

$$\mathcal{M} = -i\frac{g_1^P g_2^S}{|\mathbf{q}|^2 + M^2}\frac{\mathbf{q}\cdot\boldsymbol{\sigma}}{2m_1}\,. \tag{4.9}$$

The resulting spin-dependent potential is

$$\begin{aligned} V(r) &= \frac{g_1^P g_2^S}{2m_1}(\boldsymbol{\sigma}\cdot\boldsymbol{\nabla})\left(\frac{e^{-Mr}}{4\pi r}\right) = \\ &= -\frac{g_1^P g_2^S}{8\pi m_1}\boldsymbol{\sigma}\cdot\hat{\mathbf{r}}\left(\frac{M}{r} + \frac{1}{r^2}\right)e^{-Mr}\,. \end{aligned} \tag{4.10}$$

Pseudo-scalar Pseudo-scalar Interaction

In this case the amplitude is

$$\begin{aligned} i\mathcal{M} &= (-ig_1^P)(-ig_2^P)\bar{u}_r(p_2)i\gamma^5 u_s(p_1)\frac{i}{q^2 - M^2}\bar{u}_{r'}(p_2')i\gamma^5 u_{s'}(p_1') = \\ &= g_1^P g_2^P \bar{u}_r(p_2)\gamma^5 u_s(p_1)\frac{i^3}{|\mathbf{q}|^2 + M^2}\bar{u}_{r'}(p_2')\gamma^5 u_{s'}(p_1')\,, \end{aligned} \tag{4.11}$$

taking the exact expression of the bilinears, A.1, and paying attention to the negative sign arising from the second bilinear, one obtains

$$\mathcal{M} = -g_1^P g_2^P \frac{(-\mathbf{q}\cdot\boldsymbol{\sigma})(\mathbf{q}\cdot\boldsymbol{\sigma}')}{4m_1 m_2}\frac{1}{|\mathbf{q}|^2 + M^2}\,. \tag{4.12}$$

Employing Einstein's convention on repeated indices, the potential reads

$$\begin{aligned} V(r) &= \frac{g_1^P g_2^P}{4m_1 m_2}(\boldsymbol{\sigma}\cdot\boldsymbol{\nabla})(\boldsymbol{\sigma}'\cdot\boldsymbol{\nabla})\int \frac{d^3q}{(2\pi)^3}\ \frac{e^{i\mathbf{q}\cdot\mathbf{x}}}{|\mathbf{q}|^2 + M^2} = \\ &= \frac{g_1^P g_2^P}{4m_1 m_2}\sigma^i\sigma'^j\partial_i\partial_j\left(\frac{e^{-Mr}}{4\pi r}\right)\,. \end{aligned} \tag{4.13}$$

which, according to the results in B.2, yields

$$V(r) = -\frac{g_1^P g_2^P}{16\pi m_1 m_2}\left[\boldsymbol{\sigma}\cdot\boldsymbol{\sigma}'\left(\frac{M}{r^2} + \frac{1}{r^3} + \frac{4\pi}{3}\delta^3(\mathbf{x})\right) - (\boldsymbol{\sigma}\cdot\hat{\mathbf{r}})(\boldsymbol{\sigma}'\cdot\hat{\mathbf{r}})\left(\frac{M^2}{r} + \frac{3M}{r^2} + \frac{3}{r^3}\right)\right]e^{-Mr}\,. \tag{4.14}$$

Note the presence of a Dirac delta function, which arise from the singular part of the second derivatives of $1/r$. Apart from the other terms, a contact interaction represented by $\delta^3(\mathbf{x})$ belong to the microscopic world and cannot be probed at classical scales. However, it is a new effect that may cause shifts on the energies of quantum systems, as explained later in Chapter (5).

4.1.2 Vector bosons

The next category of interactions concern spin-1 massive mediators, whose interacting vertices with SM fermions are described by

$$\mathcal{L}_{kin} = -\frac{1}{4}X^{\mu\nu}X_{\mu\nu} + \frac{1}{2}M^2X^\mu X_\mu + \sum_{i=1}^{2}\bar{\psi}_i\left(i\partial\!\!\!/ - m_i\right)\psi_i\,, \tag{4.15}$$

$$\mathcal{L}_{int} = -\sum_{i=1}^{2}\bar{\psi}_i\gamma^\mu(g_i^V + g_i^A\gamma^5)\psi_i X_\mu\,, \tag{4.16}$$

coupling the vector boson with vector and axial currents, as shown in the figure below.

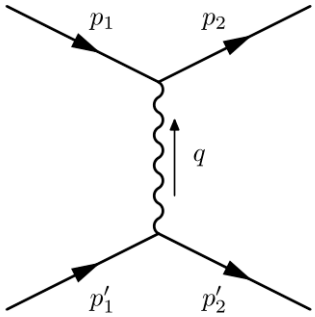

Figure 4.3: Feynman diagram for a tree-level vector boson exchange.

Vector Vector Interaction

The vector interaction involve a contraction between two vector currents and the propagator of a massive gauge boson. Since the vector current is conserved, then all the quantities contracted to $q^\mu q^\nu$ vanishes, and what remains in the Feynman amplitude is the following

$$i\mathcal{M} = (-ig_1^V)(-ig_2^V)\bar{u}_r(p_2)\gamma^\mu u_s(p_1)\frac{-i}{q^2-M^2}\left(\eta_{\mu\nu} - \frac{q_\mu q_\nu}{M^2}\right)\bar{u}_{r'}(p_2')\gamma^\nu u_{s'}(p_1') \tag{4.17}$$

and in the non-relativistic limit

$$\mathcal{M} = -\frac{g_1^V g_2^V}{|\mathbf{q}|^2 + M^2}\left(1 - \frac{(\mathbf{q}\times\boldsymbol{\sigma})\cdot(\mathbf{q}\times\boldsymbol{\sigma}')}{4m_1m_2}\right)\,, \tag{4.18}$$

where the contraction with $q_\mu q_\nu$ vanished due to the conservation of the vector current. Thus, the potential is

$$\begin{aligned} V(r) &= g_1^V g_2^V\left(1 + \frac{(\boldsymbol{\sigma}\times\boldsymbol{\nabla})\cdot(\boldsymbol{\sigma}'\times\boldsymbol{\nabla})}{4m_1m_2}\right)\left(\frac{e^{-Mr}}{4\pi r}\right) = \\ &= g_1^V g_2^V\frac{e^{-Mr}}{4\pi r} + \frac{g_1^V g_2^V}{16\pi m_1 m_2}\Bigg[(\boldsymbol{\sigma}\cdot\boldsymbol{\sigma}')\left(\frac{M^2}{r} + \frac{M}{r^2} + \frac{1}{r^3} - \frac{8\pi}{3}\delta^3(\mathbf{x})\right) + \\ &- (\boldsymbol{\sigma}\cdot\hat{\mathbf{r}})(\boldsymbol{\sigma}'\cdot\hat{\mathbf{r}})\left(\frac{M^2}{r} + 3\frac{M}{r^2} + \frac{3}{r^3}\right)\Bigg]e^{-Mr}\,. \end{aligned} \tag{4.19}$$

In particular, in the limit for $M \to 0$ the above expression recovers [53] the Coulomb potential with fine structure correction

$$V(r) = \frac{g_1^V g_2^V}{4\pi r} - \frac{g_1^V g_2^V}{16\pi m_1 m_2\, r^3}\Big[3(\boldsymbol{\sigma}\cdot\hat{\mathbf{r}})(\boldsymbol{\sigma}'\cdot\hat{\mathbf{r}}) - \boldsymbol{\sigma}\cdot\boldsymbol{\sigma}'\Big] - \frac{g_1^V g_2^V}{6m_1m_2}\boldsymbol{\sigma}\cdot\boldsymbol{\sigma}'\delta^3(\mathbf{x})\,, \tag{4.20}$$

where the second term represents the interaction between the magnetic dipoles associated to the spins $\boldsymbol{\sigma}$ and $\boldsymbol{\sigma}'$, and the last one is the Fermi contact term.
Recalling the classical spin vector

$$\mathbf{S} = \frac{\boldsymbol{\sigma}}{2}\,, \tag{4.21}$$

and its relation with the dipole magnetic moment

$$\boldsymbol{\mu} = g\frac{e}{2m_e}\mathbf{S}\,, \tag{4.22}$$

where g is the spin-gyromagnetic factor, the classical potential between two magnetic dipoles [54] is

$$V(r)_{\boldsymbol{\mu},\boldsymbol{\mu}'} = -\frac{1}{4\pi r^3}\big(3(\boldsymbol{\mu}\cdot\hat{\mathbf{r}})(\boldsymbol{\mu}'\cdot\hat{\mathbf{r}}) - \boldsymbol{\mu}\cdot\boldsymbol{\mu}'\big) - \frac{2}{3}\boldsymbol{\mu}\cdot\boldsymbol{\mu}'\delta^3(\mathbf{x})\,. \tag{4.23}$$

A direct comparison with eq. (4.20) allows us to determine the spin-gyromagnetic factors of the two fermions at the classical level, i.e.

$$g = 2\,. \tag{4.24}$$

Vector Axial Interaction

The mixed interaction involve a contraction between the axial and the vector current with the propagator of a gauge field. The Feynman amplitude is then

$$i\mathcal{M} = g_1^A g_2^V \bar{u}_s(p_2)\gamma^\mu\gamma^5 u_r(p_1)\frac{i}{q^2 - M^2}\bar{u}_{s'}(p_2')\gamma_\mu u_{r'}(p_1') \tag{4.25}$$

which, in the non-relativistic expansion, becomes

$$\mathcal{M} = -\frac{g_1^A g_2^V}{|\mathbf{q}|^2 + M^2}\left[\left(\frac{\mathbf{P}}{m_1} - \frac{\mathbf{P}'}{m_2}\right)\cdot\boldsymbol{\sigma} + \frac{1}{2m_2}(\boldsymbol{\sigma}\times\boldsymbol{\sigma}')\cdot i\mathbf{q}\right]. \tag{4.26}$$

The associated potential in the Born approximation reads

$$\begin{aligned} V(r) &= g_1^A g_2^V\left[\left(\frac{\mathbf{P}}{m_1} - \frac{\mathbf{P}'}{m_2}\right)\cdot\boldsymbol{\sigma} + \frac{1}{2m_2}(\boldsymbol{\sigma}\times\boldsymbol{\sigma}')\cdot\boldsymbol{\nabla}\right]\left(\frac{e^{-Mr}}{4\pi r}\right) = \\ &= \frac{g_1^A g_2^V}{4\pi r}\left[\boldsymbol{\sigma}\cdot\left(\frac{\mathbf{P}}{m_1} - \frac{\mathbf{P}'}{m_2}\right) - \frac{1}{2}(\boldsymbol{\sigma}\times\boldsymbol{\sigma}')\cdot\hat{\mathbf{r}}\left(\frac{M}{m_2} + \frac{1}{m_2 r}\right)\right]e^{-Mr}\,. \end{aligned} \tag{4.27}$$

Axial Axial Interaction

The case of two axial vertices involves two axial currents which are not conserved, so the contraction with $q^\mu q^\nu$ cannot be neglected, thus

$$\begin{aligned} i\mathcal{M} &= -g_1^A g_2^A \bar{u}_s(p_2)\gamma^\mu\gamma^5 u_r(p_1)\frac{-i}{q^2 - M^2}\left(\eta_{\mu\nu} - \frac{q_\mu q_\nu}{M^2}\right)\bar{u}_{s'}(p_2')\gamma^\nu\gamma^5 u_{r'}(p_1') = \\ &= g_1^A g_2^A \frac{-i}{|\mathbf{q}|^2 + M^2}\Big[\bar{u}_s(p_2)\gamma^\mu\gamma^5 u_r(p_1)\bar{u}_{s'}(p_2')\gamma_\mu\gamma^5 u_{r'}(p_1') + \\ &\qquad - \frac{1}{M^2}\bar{u}_s(p_2)\not{q}\gamma^5 u_r(p_1)\bar{u}_{s'}(p_2')\not{q}\gamma^5 u_{r'}(p_1')\Big]\,. \end{aligned} \tag{4.28}$$

Substituting the non-relativistic expansions at the leading order gives us

$$\mathcal{M} = \frac{g_1^A g_2^A}{|\mathbf{q}|^2 + M^2}\left[\boldsymbol{\sigma}\cdot\boldsymbol{\sigma}' + \frac{1}{M^2}(\boldsymbol{\sigma}\cdot\mathbf{q})(\boldsymbol{\sigma}'\cdot\mathbf{q})\right], \tag{4.29}$$

where the NLO term must be kept since it is amplified by the M^2 factor at denominator. The integration leads to

$$\begin{aligned} V(r) &= -g_1^A g_2^A\left[\boldsymbol{\sigma}\cdot\boldsymbol{\sigma}' - \frac{1}{M^2}(\boldsymbol{\sigma}\cdot\boldsymbol{\nabla})(\boldsymbol{\sigma}'\cdot\boldsymbol{\nabla})\right]\left(\frac{e^{-Mr}}{4\pi r}\right) = \\ &= -g_1^A g_2^A(\boldsymbol{\sigma}\cdot\boldsymbol{\sigma}')\frac{e^{-Mr}}{4\pi r} - \frac{g_1^A g_2^A}{4\pi M^2}\Big[(\boldsymbol{\sigma}\cdot\boldsymbol{\sigma}')\left(\frac{1}{r^3} + \frac{M^2}{r} + \frac{4\pi}{3}\delta^3(\mathbf{x})\right) + \\ &\quad - (\boldsymbol{\sigma}\cdot\hat{\mathbf{r}})(\boldsymbol{\sigma}'\cdot\hat{\mathbf{r}})\left(\frac{M^2}{r} + 3\frac{M}{r^2} + \frac{3}{r^3}\right)\Big]e^{-Mr}\,. \end{aligned} \tag{4.30}$$

4.1.3 Field Strength Interactions

The last type of tree-level interaction involving a the field strength of a massive vector boson is given by

$$\mathcal{L}_{int} = -\sum_{i=1}^{2} \bar{\psi}_i \sigma^{\mu\nu} (g_i^T + g_i^{\tilde{T}} i\gamma^5) \psi_i F_{\mu\nu} \,, \tag{4.31}$$

in which the coupling coefficients have mass dimension $[g_i^T] = [g_i^{\tilde{T}}] = -1$ and

$$\sigma^{\mu\nu} = \frac{i}{2} [\gamma^\mu, \gamma^\nu] \quad , \quad F^{\mu\nu} = \partial^\mu A^\nu - \partial^\nu A^\mu \,, \tag{4.32}$$

with $F^{\mu\nu}$ the field strength of the vector boson. Despite the form of eq. (4.31), exploiting the antisymmetric property of $\sigma^{\mu\nu}$ and integrating by parts, the interaction term can be recast into

$$\mathcal{L}_{Int} = 2 \sum_{i=1}^{2} \partial_\mu [\bar{\psi}_i \sigma^{\mu\nu} (g_i^T + g_i^{\tilde{T}} i\gamma^5) \psi_i] A_\nu \,. \tag{4.33}$$

Tensor Tensor Interaction

The derivative interaction of the t-channel scattering gives

$$\mathcal{M} = -4 g_1^T g_2^T \bar{u}_s(p_2) q_i \sigma^{i\nu} u_r(p_1) \frac{i\eta_{\nu\beta}}{|\mathbf{q}|^2 + M^2} \bar{u}_{s'}(p_2') q^j \sigma_{j\beta} u_{r'}(p_1') \,, \tag{4.34}$$

where the $q^\mu q^\nu$ term inside the propagator vanishes from the contraction with $\sigma^{\mu\nu}$. Using the non-relativistic expansion of the bilinear forms, see A.1, the amplitude becomes

$$\mathcal{M} = \frac{4 g_1^T g_2^T}{|\mathbf{q}|^2 + M^2} \left[(\boldsymbol{\sigma} \cdot \boldsymbol{\sigma}') |\mathbf{q}|^2 - (\boldsymbol{\sigma} \cdot \mathbf{q})(\boldsymbol{\sigma}' \cdot \mathbf{q}) \right] \tag{4.35}$$

and the related potential in the Born approximation reads

$$\begin{aligned} V(r) &= 4 g_1^T g_2^T \left[(\boldsymbol{\sigma} \cdot \boldsymbol{\sigma}') \nabla^2 - (\boldsymbol{\sigma} \cdot \boldsymbol{\nabla})(\boldsymbol{\sigma}' \cdot \boldsymbol{\nabla}) \right] \left(\frac{e^{-Mr}}{4\pi r} \right) = \\ &= \frac{g_1^T g_2^T}{\pi} \left[(\boldsymbol{\sigma} \cdot \boldsymbol{\sigma}') \left(\frac{M^2}{r} + \frac{M}{r^2} + \frac{1}{r^3} - \frac{8\pi}{3} \delta^3(\mathbf{x}) \right) - (\boldsymbol{\sigma} \cdot \hat{\mathbf{r}})(\boldsymbol{\sigma}' \cdot \hat{\mathbf{r}}) \left(\frac{M^2}{r} + 3\frac{M}{r^2} + \frac{3}{r^3} \right) \right] e^{-Mr} \,. \end{aligned} \tag{4.36}$$

Pseudo-tensor Pseudo-tensor Interaction

The Feynman amplitude for a mix of tensor and pseudo-tensor currents is

$$\begin{aligned} i\mathcal{M} &= (2ig_1^{\tilde{T}})(2ig_2^{\tilde{T}})(iq)_\mu \bar{u}_s(p_2) \sigma^{\mu\nu} i\gamma^5 u_r(p_1) \frac{-i\eta_{\nu\beta}}{q^2 - M^2} (-iq)_\alpha \bar{u}_{s'}(p_2') \sigma^{\alpha\beta} i\gamma^5 u_{r'}(p_1') = \\ &= 4i g_1^{\tilde{T}} g_2^{\tilde{T}} q_i \bar{u}_s(p_2) \sigma^{i\nu} \gamma^5 u_r(p_1) \frac{\eta_{\nu\beta}}{|\mathbf{q}|^2 + M^2} q_j \bar{u}_{s'}(p_2') \sigma^{j\beta} \gamma^5 u_{r'}(p_1') \,. \end{aligned} \tag{4.37}$$

The non-relativistic expansion yields

$$\mathcal{M} \simeq \frac{4 g_1^{\tilde{T}} g_2^{\tilde{T}}}{|\mathbf{q}|^2 + M^2} q^i q^j \left((i\sigma^i)(i\sigma^j) \right) = -\frac{4 g_1^{\tilde{T}} g_2^{\tilde{T}}}{|\mathbf{q}|^2 + M^2} (\boldsymbol{\sigma} \cdot \mathbf{q})(\boldsymbol{\sigma}' \cdot \mathbf{q}) \,. \tag{4.38}$$

and produces the potential

$$\begin{aligned} V(r) &= -4 g_1^{\tilde{T}} g_2^{\tilde{T}} (\boldsymbol{\sigma} \cdot \boldsymbol{\nabla})(\boldsymbol{\sigma}' \cdot \boldsymbol{\nabla}) \left(\frac{e^{-Mr}}{4\pi r} \right) = \\ &= \frac{g_1^{\tilde{T}} g_2^{\tilde{T}}}{\pi} \left[(\boldsymbol{\sigma} \cdot \boldsymbol{\sigma}') \left(\frac{M}{r^2} + \frac{1}{r^3} + \frac{4\pi}{3} \delta^3(\mathbf{x}) \right) - (\boldsymbol{\sigma} \cdot \hat{\mathbf{r}})(\boldsymbol{\sigma}' \cdot \hat{\mathbf{r}}) \left(\frac{M^2}{r} + 3\frac{M}{r^2} + \frac{3}{r^3} \right) \right] e^{-Mr} \,. \end{aligned} \tag{4.39}$$

Tensor Pseudo-tensor Interaction

The last Feynman amplitude to examine for the elastic scattering is

$$\begin{aligned} i\mathcal{M} &= (2ig_1^{\tilde{T}})(2ig_2^T)(iq)_\mu \bar{u}_s(p_2)\sigma^{\mu\nu} i\gamma^5 u_r(p_1)\frac{-i\eta_{\nu\beta}}{q^2}(-iq)_\alpha \bar{u}_{s'}(p_2')\sigma^{\alpha\beta}u_{r'}(p_1') = \\ &= 4g_1^{\tilde{T}} g_2^T \frac{q^i q^j}{|\mathbf{q}|^2}\bar{u}_s(p_2)\sigma^{i\nu}\gamma^5 u_r(p_1)\,\eta_{\nu\beta}\,\bar{u}_{s'}(p_2')\sigma^{j\beta}u_{r'}(p_1') \end{aligned} . \tag{4.40}$$

Expanding in the non-relativistic limit leads to

$$\bar{u}_s(p_2)q^i\sigma^{i0}\gamma^5 u_r(p_1)\bar{u}_{s'}(p_2')q^j\sigma^{j0}u_{r'}(p_1') = -(\mathbf{q}\cdot\boldsymbol{\sigma})\left[\frac{|\mathbf{q}|^2}{2m_2} + \frac{\mathbf{P}'}{m_2}\cdot\left(\boldsymbol{\sigma}'\times i\mathbf{q}\right)\right], \tag{4.41}$$

$$\bar{u}_s(p_2)q^i\sigma^{ik}\gamma^5 u_r(p_1)\bar{u}_{s'}(p_2')q^j\sigma^{jk}u_{r'}(p_1') = i\left[|\mathbf{q}|^2\left(\boldsymbol{\sigma}\times\boldsymbol{\sigma}'\right) - \left(\boldsymbol{\sigma}'\cdot\mathbf{q}\right)\left(\boldsymbol{\sigma}\times\mathbf{q}\right)\right]\cdot\frac{\mathbf{P}}{m_1}, \tag{4.42}$$

and so

$$\mathcal{M} = 4\frac{g_1^{\tilde{T}}g_2^T}{|\mathbf{q}|^2+M^2}\left[\frac{|\mathbf{q}|^2}{2m_2}(\boldsymbol{\sigma}\cdot i\mathbf{q}) - (\boldsymbol{\sigma}\cdot\mathbf{q})\frac{\mathbf{P}'}{m_2}\cdot(\boldsymbol{\sigma}'\times\mathbf{q}) - |\mathbf{q}|^2\frac{\mathbf{P}}{m_1}\cdot(\boldsymbol{\sigma}\times\boldsymbol{\sigma}') + (\boldsymbol{\sigma}'\cdot\mathbf{q})\frac{\mathbf{P}}{m_1}\cdot(\boldsymbol{\sigma}\times\mathbf{q})\right]. \tag{4.43}$$

The derivatives of the Yukawa potential, see B.1, results in

$$\begin{aligned} V(r) &= -4g_1^{\tilde{T}}g_2^T\left\{(\boldsymbol{\sigma}\cdot\boldsymbol{\nabla})\left[-\frac{\nabla^2}{2m_2} + \frac{\mathbf{P}'}{m_2}\cdot\left(\boldsymbol{\sigma}'\times\boldsymbol{\nabla}\right)\right] + \left[\nabla^2\left(\boldsymbol{\sigma}\times\boldsymbol{\sigma}'\right) - \left(\boldsymbol{\sigma}'\cdot\boldsymbol{\nabla}\right)\left(\boldsymbol{\sigma}\times\boldsymbol{\nabla}\right)\right]\cdot\frac{\mathbf{P}}{m_1}\right\}\left(\frac{e^{-Mr}}{4\pi r}\right) \\ &= \frac{4g_1^{\tilde{T}}g_2^T}{4\pi}\left\{-\frac{4\pi}{2m_2}\boldsymbol{\sigma}\cdot\boldsymbol{\nabla}\delta^3(\mathbf{x}) - \left(\frac{M^3}{r} + \frac{M^2}{r^2} - 4\pi M\delta^3(\mathbf{x})\right)\frac{\boldsymbol{\sigma}\cdot\hat{\mathbf{r}}}{2m_2} + \right. \\ &- \left(\frac{M}{r^2} + \frac{1}{r^3} + \frac{4\pi}{3}\delta^3(\mathbf{x})\right)(\boldsymbol{\sigma}\times\boldsymbol{\sigma}')\cdot\left(\frac{\mathbf{P}}{m_1} + \frac{\mathbf{P}'}{m_2}\right) - \left(\frac{M^2}{r} - 4\pi\delta^3(\mathbf{x})\right)\frac{\mathbf{P}}{m_1}\cdot(\boldsymbol{\sigma}\times\boldsymbol{\sigma}') + \\ &\left. + \left(\frac{M^2}{r} + \frac{3M}{r^2} + \frac{3}{r^3}\right)\left[(\boldsymbol{\sigma}'\cdot\hat{\mathbf{r}})\frac{\mathbf{P}}{m_1}\cdot(\boldsymbol{\sigma}\times\hat{\mathbf{r}}) - (\boldsymbol{\sigma}\cdot\hat{\mathbf{r}})\frac{\mathbf{P}'}{m_2}\cdot(\boldsymbol{\sigma}'\times\hat{\mathbf{r}})\right]\right\}e^{-Mr}. \end{aligned} \tag{4.44}$$

4.2 Comparison with Results in the Literature

We here highlight a list of discrepancies with respect to the previous literature about the calculation of the non-relativistic potentials. The calculations were also checked with little programs in Mathematica, to avoid possible errors given the length of the formulae.

- Scalar Pseudo-scalar Potential (eq. (4.10))

  We find an overall minus sign with respect to the result of Refs. [37, 12] arising from an inconsistency of the conventions. As reported in A.2, the Feynman diagram used in the thesis are compatible the positive exponent of the Fourier transforms. Eq. (4.10) is derived from a t-channel diagram in which the momentum q is transferred from the scalar to the pseudo-scalar current. We note that this disagreement was also previously realized in Ref. [55].

- Pseudo-scalar Pseudo-scalar Potential (eq. (4.14))

  We find an overall minus sign with respect to the result of Refs. [37, 12]. This probably originates from a missing sign in the derivation of the non-relativistic limit of the pseudo-scalar bilinears. Recalling the expression $q = p_2 - p_1 = p_1' - p_2'$, the explicit expressions of the fermion bilinears differ by

$$\bar{u}_r(p_2)\gamma^5 u_s(p_1) = -\frac{\mathbf{q}\cdot\boldsymbol{\sigma}}{2m_1}, \tag{4.45}$$

$$\bar{u}_{r'}(p_2')\gamma^5 u_{s'}(p_1') = \frac{\mathbf{q}\cdot\boldsymbol{\sigma}'}{2m_2}. \tag{4.46}$$

The difference may not have been taken into account in the reference, resulting in a disagreement between the calculations.

- Tensor Pseudo-tensor Potential (eq. (4.48))

  Working in the $M \to 0$ limit, Ref. [11] finds

$$V(r) = \frac{4g_1^{\tilde{T}} g_2^T}{4\pi}\Bigg[-\frac{4\pi}{2m_2}\boldsymbol{\sigma}\cdot\boldsymbol{\nabla}\delta^3(\mathbf{x}) + \left(\frac{1}{r^3}+\frac{4\pi}{3}\delta^3(\mathbf{x})\right)(\boldsymbol{\sigma}\times\boldsymbol{\sigma}')\cdot\left(\frac{\mathbf{P}}{m_1}-\frac{\mathbf{P}'}{m_2}\right)+ \\ + \frac{3}{r^3}(\boldsymbol{\sigma}\cdot\hat{\mathbf{r}})\left(\frac{\mathbf{P}}{m_1}-\frac{\mathbf{P}'}{m_2}\right)\cdot(\boldsymbol{\sigma}'\times\hat{\mathbf{r}})\Bigg], \tag{4.47}$$

  while we obtained instead

$$V(r) = \frac{4g_1^{\tilde{T}} g_2^T}{4\pi}\Bigg\{ -\frac{4\pi}{2m_2}\boldsymbol{\sigma}\cdot\boldsymbol{\nabla}\delta^3(\mathbf{x}) - \left(\frac{1}{r^3}+\frac{4\pi}{3}\delta^3(\mathbf{x})\right)(\boldsymbol{\sigma}\times\boldsymbol{\sigma}')\cdot\left(\frac{\mathbf{P}}{m_1}+\frac{\mathbf{P}'}{m_2}\right)+ \\ + 4\pi\delta^3(\mathbf{x})(\boldsymbol{\sigma}\times\boldsymbol{\sigma}')\cdot\frac{\mathbf{P}}{m_1}+\frac{3}{r^3}\left[(\boldsymbol{\sigma}'\cdot\hat{\mathbf{r}})\frac{\mathbf{P}}{m_1}\cdot(\boldsymbol{\sigma}\times\hat{\mathbf{r}})-(\boldsymbol{\sigma}\cdot\hat{\mathbf{r}})\frac{\mathbf{P}'}{m_2}\cdot(\boldsymbol{\sigma}'\times\hat{\mathbf{r}})\right]\Bigg\}. \tag{4.48}$$

  that has been also confirmed by performing the non-relativistic expansion by means of a Mathematica code.

CHAPTER 5

TREE-LEVEL POTENTIALS BEYOND LEADING ORDER

Until now we have been concerned with reproducing the calculation of the tree-level potentials discussed in the literature, limiting ourselves to LO contributions in the non-relativistic expansion and elastic scattering. In this Chapter we consider instead higher-order corrections in the non-relativistic expansion and relax as well the hypothesis of elastic scattering. This latter point is actually required in order to provide a consistent non-relativistic expansion, since the elasticity condition is automatically enforced by taking the leading order in the non-relativistic expansion. As discussed below, this analysis will reveal the presence of new sizeable contact interactions in the non-relativistic potentials that have been previously compute at the LO and which might play an important phenomenological role.

5.1 Exact Bilinears and Anelastic Corrections

In the the previous calculation of the non-relativistic potentials, we encountered some cases where certain bilinear forms seem not to have non-relativistic correction. An investigation of the simpler case of the pseudo-scalar bilinear is useful, before venturing into more complicated expansions.
First of all, the form of the Dirac spinor, see A.1,

$$u_r(p) = \frac{\not{p} + m}{\sqrt{2m(E_{\mathbf{p}} + m)}} u_r(0) \ , \quad u_r(0) \equiv \varphi_r \, , \tag{5.1}$$

is a covariant expression valid in every inertial frame. The reference frame we have considered so far is the center of mass frame, where the dynamics is completely determined by the two independent momenta

$$\begin{cases} q = p_2 - p_1 \\ P = \dfrac{p_1 + p_2}{2} \end{cases} \Longrightarrow \begin{cases} p_1 = P - \dfrac{q}{2} \\ p_2 = P + \dfrac{q}{2} \end{cases} . \tag{5.2}$$

The last important assumption that we have made is the elastic limit of the scattering, meaning that in the CoM frame

$$q^0 = 0 \ \longrightarrow \ E_{\mathbf{p}_2} = E_{\mathbf{p}_1} \, , \quad |\mathbf{p}_1| = |\mathbf{p}_2| \tag{5.3}$$

All these assumptions provide a strong constraint on the non-relativistic expansion. Taking, for example, the pseudo-scalar bilinear given by

$$\begin{aligned}\bar{u}_s(p_2)\gamma^5 u_r(p_1) &= \frac{1}{2m_1}\left(\sqrt{E_{\mathbf{p}_2}+m_1}\,\varphi_s^T\,,\quad \varphi_s^T\frac{\mathbf{p}_2\cdot\boldsymbol{\sigma}}{\sqrt{E_{\mathbf{p}_2}+m_1}}\right)\gamma^0\gamma^5\begin{pmatrix}\sqrt{E_{\mathbf{p}_1}+m_1}\,\varphi_r\\ \frac{\mathbf{p}_1\cdot\boldsymbol{\sigma}}{\sqrt{E_{\mathbf{p}_1}+m_1}}\varphi_r\end{pmatrix} = \\ &= \frac{1}{2m_1}\varphi_s^T\left(\mathbf{p}_1\cdot\boldsymbol{\sigma}-\mathbf{p}_2\cdot\boldsymbol{\sigma}\right)\varphi_r = -\frac{\mathbf{q}\cdot\boldsymbol{\sigma}}{2m_1}\,.\end{aligned} \tag{5.4}$$

In this case, the two main quantities to expanded in the non-relativistic limit are

$$\frac{\sqrt{E_{\mathbf{p}_2}+m_1}}{\sqrt{E_{\mathbf{p}_1}+m_1}} = 1\ ,\quad \sqrt{E_{\mathbf{p}_2}+m_1}\sqrt{E_{\mathbf{p}_1}+m_1} \simeq 2m_1\left(1+\frac{|\mathbf{p}_1|^2}{4m_1^2}+\mathcal{O}\left(\frac{|\mathbf{p}_1|^2}{m_1^2}\right)\right)\,, \tag{5.5}$$

where only the second one gives an infinite series in terms of $|\mathbf{p}_1|^2/m_1^2$. The first ratio, instead, will always be exact as long as the elastic assumption persists.
Therefore the elastic hypothesis plays a crucial role in the non-relativistic expansion of the tree-level potentials. When relaxing the latter, we need to keep track of the terms $q^0 \neq 0$ in the amplitude. So, for instance, a common factor among Feynman propagators is

$$\frac{i}{q^2-M^2} \tag{5.6}$$

with q the transferred 4-momentum. In the elastic limit, the energy conservation in the CoM reference frame implies that initial and final momenta of the external particles have the same magnitudes, i.e.

$$q^0 = 0 \longrightarrow |\mathbf{p}_1| = |\mathbf{p}_3|\,, \tag{5.7}$$

and as a consequence the following relation holds

$$\mathbf{P}\cdot\mathbf{q} = \frac{1}{2}\left(|\mathbf{p}_3|^2-|\mathbf{p}_1|^2\right) = 0 \tag{5.8}$$

leading to cancellations in the expansions, while the propagator reduces to

$$\frac{-i}{|\mathbf{q}|^2+M^2}\,. \tag{5.9}$$

It is worth to relax our hypothesis in order to study scattering processes where the transferred energy slightly differs from zero and a mass gap exists, in such a way that the anelastic behaviour emerges without the creation of different particles. Taking

$$q^0 \neq 0 \longrightarrow |\mathbf{p}_1| \neq |\mathbf{p}_3|\ ,\ \ \mathbf{P}\cdot\mathbf{q} \neq 0 \tag{5.10}$$

the propagator now reads

$$\frac{i}{(q^0)^2-|\mathbf{q}|^2-M^2} \tag{5.11}$$

where the time-like component can be expanded as

$$(q^0)^2 \simeq \frac{(\mathbf{P}\cdot\mathbf{q})^2}{2m^2}+\dots \tag{5.12}$$

leading to the expression

$$\frac{i}{\frac{(\mathbf{P}\cdot\mathbf{q})^2}{2m^2}-|\mathbf{q}|^2-M^2+\dots}\,. \tag{5.13}$$

Knowing the non-relativistic nature of the external momenta and the heaviness of the scattered particles, the last equation can be expanded as

$$\frac{-i}{|\mathbf{q}|^2+M^2}\left(1-\frac{(\mathbf{P}\cdot\mathbf{q})^2}{2m^2}\frac{1}{|\mathbf{q}|^2+M^2}+\dots\right)^{-1} \simeq \frac{-i}{|\mathbf{q}|^2+M^2}\left(1+\frac{(\mathbf{P}\cdot\mathbf{q})^2}{2m^2}\frac{1}{|\mathbf{q}|^2+M^2}+\dots\right) \tag{5.14}$$

entering as a correction into all the scattering amplitudes, including those naively looking exact in the non-relativistic expansion, as the pseudo-scalar pseudo-scalar one in eq. (4.9).

5.2 Non-relativistic Potentials at Next to Leading Order

We now proceed with the calculation of the non-relativistic corrections to the tree-level potentials, taking into account for consistency both the non-relativistic expansion of the Dirac spinors and the anelastic corrections to the propagators, which imply new terms proportional to $|\mathbf{p}_i|/m_i^2$ (see eq. (5.14)). In fact, depending on the mass ratios generated from the non-relativistic expansion, there may be present suppression or enhancement factors stemming from the hierarchies $|\mathbf{p}_i| \ll m_i$ and $M \ll m_i$. For this reason it is useful to introduce two adimensional parameters

$$\begin{cases} \epsilon_i \equiv M/m_i \\ \boldsymbol{v}_i \equiv \mathbf{P}_i/m_i \end{cases}, \tag{5.15}$$

where i is the index of the external fermion. In general, we have $\epsilon_i \ll |\boldsymbol{v}_i| \ll 1$.

Scalar Scalar Corrections

Considering the NLO terms in the elastic amplitude

$$\begin{aligned} \mathcal{M}_{el}(\mathbf{q}) &= \frac{g_1^S g_2^S}{|\mathbf{q}|^2+M^2}\left(1+\frac{|\mathbf{q}|^2}{8m_1^2}+\frac{i}{4m_1^2}(\mathbf{P}\times\mathbf{q})\cdot\boldsymbol{\sigma}+\dots\right)\left([1+\frac{|\mathbf{q}|^2}{8m_2^2}-\frac{i}{4m_2^2}(\mathbf{P}'\times\mathbf{q})\cdot\boldsymbol{\sigma}'+\dots\right)= \\ &\equiv \frac{g_1^S g_2^S}{|\mathbf{q}|^2+M^2}\left(1+\frac{|\mathbf{q}|^2}{8\mu^2}+\frac{1}{4}\mathbf{K}\cdot\, i\mathbf{q}+\dots\right), \end{aligned} \tag{5.16}$$

where we have employed the definitions

$$\frac{1}{\mu^2} \equiv \frac{m_1^2+m_2^2}{m_1^2 m_2^2}\ , \quad \mathbf{K} \equiv \frac{\boldsymbol{\sigma}\times\mathbf{P}}{m_1^2}-\frac{\boldsymbol{\sigma}'\times\mathbf{P}'}{m_2^2}\,. \tag{5.17}$$

The potential can now be written as

$$V_{el}(\mathbf{x}) = -g_1^S g_2^S\left(1-\frac{\nabla^2}{8\mu^2}+\frac{\mathbf{K}}{4}\cdot\nabla\right)\int\frac{d^3q}{(2\pi)^3}\frac{e^{i\mathbf{q}\cdot\mathbf{x}}}{|\mathbf{q}|^2+M^2}\,, \tag{5.18}$$

resulting in

$$V_{el}(r) = -\frac{g_1^S g_2^S}{4\pi r}\left[1-\frac{m_1^2+m_2^2}{8m_1^2m_2^2}\left(M^2-4\pi r\delta^3(\mathbf{x})\right)+\frac{1}{4}\left(M+\frac{1}{r}\right)\left(\frac{\mathbf{P}\times\boldsymbol{\sigma}}{m_1^2}-\frac{\mathbf{P}'\times\boldsymbol{\sigma}'}{m_2^2}\right)\cdot\hat{\mathbf{r}}\right]e^{-Mr} \tag{5.19}$$

or, by means of the adimensional parameters of eq. (5.15),

$$\begin{aligned} V_{el}(r) = -\frac{g_1^S g_2^S}{4\pi r}\Bigg\{1-\frac{1}{8}\left[\left(1+\frac{m_1^2}{m_2^2}\right)\epsilon_1^2-\frac{4\pi r\delta^3(\mathbf{x})}{\mu^2}\right]+ \\ +\frac{1}{4}\left(\epsilon_1+\frac{1}{m_1 r}\right)\boldsymbol{v}_1\times\boldsymbol{\sigma}\cdot\hat{\mathbf{r}}-\frac{1}{4}\left(\epsilon_2+\frac{1}{m_2 r}\right)\boldsymbol{v}_2\times\boldsymbol{\sigma}'\cdot\hat{\mathbf{r}}\Bigg\}e^{-Mr}\,. \end{aligned} \tag{5.20}$$

Contributions of the same order arise also from anelastic corrections of the propagator that involve a different integral, analyzed in appendix B.2. In this case, the amplitude can be written as

$$\begin{aligned} \mathcal{M} &= \frac{g_1^S g_2^S}{|\mathbf{q}|^2+M^2}\left(1+\frac{(\mathbf{P}\cdot\mathbf{q})^2}{2m_1^2}\frac{1}{|\mathbf{q}|^2+M^2}\right)\left[1+\frac{|\mathbf{q}|^2}{8\mu^2}+\frac{1}{4}\mathbf{K}\cdot\, i\mathbf{q}+\dots\right] \\ &= \mathcal{M}_{el}+\frac{(\mathbf{P}\cdot\mathbf{q})^2}{2m_1^2}\frac{g_1^S g_2^S}{(|\mathbf{q}|^2+M^2)^2}+\dots\,, \end{aligned} \tag{5.21}$$

and the total correction to the Yukawa potential at NLO reads

$$\begin{aligned} V(r) &= V_{el}+\frac{g_1^S g_2^S}{2m_1^2}(\mathbf{P}\cdot\boldsymbol{\nabla})^2\int\frac{d^3q}{(2\pi)^3}\frac{e^{i\mathbf{q}\cdot\mathbf{x}}}{(|\mathbf{q}|^2+M^2)^2} \\ &= V_{el}+\frac{g_1^S g_2^S}{16\pi r}\left[(1+Mr)\,(\boldsymbol{v}_1\cdot\hat{\mathbf{r}})^2-|\boldsymbol{v}_1|^2\right]e^{-Mr}\,, \end{aligned} \tag{5.22}$$

where V_{el} is given by eq. (5.20).

Scalar Pseudo-scalar Corrections

The elastic amplitude expanded up to NLO is given by

$$\mathcal{M}_{el} = i\frac{g_1^P g_2^S}{|\mathbf{q}|^2+M^2}\left(-\frac{\mathbf{q}\cdot\boldsymbol{\sigma}}{2m_1}\right)\left(1+\frac{|\mathbf{q}|^2}{8m_2^2}-\frac{i}{4m_2^2}(\mathbf{P}'\times\mathbf{q})\cdot\boldsymbol{\sigma}'+\dots\right), \tag{5.23}$$

thus the potential reads

$$\begin{aligned} V_{el}(r) &= \frac{g_1^P g_2^S}{2m_1}\left(\boldsymbol{\sigma}\cdot\boldsymbol{\nabla}-\frac{1}{8m_2^2}(\boldsymbol{\sigma}\cdot\boldsymbol{\nabla})\nabla^2-\frac{(\boldsymbol{\sigma}\cdot\boldsymbol{\nabla})}{4m_2^2}(\mathbf{P}'\times\boldsymbol{\nabla})\cdot\boldsymbol{\sigma}'\right)\left(\frac{e^{-Mr}}{4\pi r}\right)= \\ &= -\frac{g_1^P g_2^S}{8\pi m_1}\Bigg\{\boldsymbol{\sigma}\cdot\hat{\mathbf{r}}\left(\frac{M}{r}+\frac{1}{r^2}\right)-\frac{1}{8m_2^2}(\boldsymbol{\sigma}\cdot\hat{\mathbf{r}})\left(\frac{M^3}{r}+\frac{M^2}{r^2}-4\pi M\delta^3(\mathbf{x})\right)-\frac{\pi}{2m_2^2}\boldsymbol{\sigma}\cdot\boldsymbol{\nabla}\delta^3(\mathbf{x})+ \\ &- \frac{1}{4m_2^2}\left[\left(\frac{M}{r^2}+\frac{1}{r^3}+\frac{4\pi}{3}\delta^3(\mathbf{x})\right)\boldsymbol{\sigma}\cdot(\boldsymbol{\sigma}'\times\mathbf{P}')-\left(\frac{M^2}{r}+3\frac{M}{r^2}+\frac{3}{r^3}\right)(\boldsymbol{\sigma}\cdot\hat{\mathbf{r}})(\boldsymbol{\sigma}'\times\mathbf{P}')\cdot\hat{\mathbf{r}}\right]\Bigg\}e^{-Mr} \end{aligned} \tag{5.24}$$

and in terms of adimensional variables

$$\begin{aligned} V_{el}(r) = -\frac{g_1^P g_2^S}{8\pi m_1}\Bigg[&\boldsymbol{\sigma}\cdot\hat{\mathbf{r}}\left(\frac{M}{r}+\frac{1}{r^2}-\frac{M\epsilon_2^2}{r}-\frac{\epsilon_2^2}{r^2}+\frac{4\pi\epsilon_2\delta^3(\mathbf{x})}{m_2}\right)-\frac{\pi}{2m_2^2}\boldsymbol{\sigma}\cdot\boldsymbol{\nabla}\delta^3(\mathbf{x})+ \\ &-\frac{1}{4}\left(\frac{\epsilon_2}{r^2}+\frac{1}{m_2 r^3}+\frac{4\pi}{3m_2}\delta^3(\mathbf{x})\right)\boldsymbol{\sigma}\cdot(\boldsymbol{\sigma}'\times\boldsymbol{v}_2)+\frac{1}{4}\left(\frac{M}{r}\epsilon_2+3\frac{\epsilon_2}{r^2}+\frac{3}{m_2 r^3}\right)(\boldsymbol{\sigma}\cdot\hat{\mathbf{r}})(\boldsymbol{\sigma}'\times\boldsymbol{v}_2)\cdot\hat{\mathbf{r}}\Bigg]e^{-Mr}. \end{aligned} \tag{5.25}$$

The next step is to consider anelastic corrections, leading to

$$\begin{aligned} \mathcal{M} &= i\frac{g_1^P g_2^S}{|\mathbf{q}|^2+M^2}\left(1+\frac{(\mathbf{P}\cdot\mathbf{q})^2}{2m_1^2}\frac{1}{|\mathbf{q}|^2+M^2}\right)\left(-\frac{\mathbf{q}\cdot\boldsymbol{\sigma}}{2m_1}\right)\left[1+\frac{|\mathbf{q}|^2}{8m_2^2}-\frac{i}{4m_2^2}(\mathbf{P}'\times\mathbf{q})\cdot\boldsymbol{\sigma}'\right] \\ &= \mathcal{M}_{el}-i\frac{g_1^P g_2^S}{(|\mathbf{q}|^2+M^2)^2}\frac{(\mathbf{P}\cdot\mathbf{q})^2\mathbf{q}\cdot\boldsymbol{\sigma}}{4m_1^3} \end{aligned} \tag{5.26}$$

and the associated potential is corrected by

$$\begin{aligned} V(r) &= V_{el}-\frac{g_1^P g_2^S}{4m_1^3}(\mathbf{P}\cdot\boldsymbol{\nabla})^2\boldsymbol{\sigma}\cdot\boldsymbol{\nabla}\int\frac{d^3q}{(2\pi)^3}\frac{e^{i\mathbf{q}\cdot\mathbf{x}}}{(|\mathbf{q}|^2+M^2)^2}= \\ &= V_{el}-\frac{g_1^P g_2^S}{32\pi m_1}\Bigg[\left(\frac{M}{r}+\frac{1}{r^2}\right)\left(|\boldsymbol{v}_1|^2\boldsymbol{\sigma}\cdot\hat{\mathbf{r}}+2(\boldsymbol{v}_1\cdot\boldsymbol{\sigma})(\boldsymbol{v}_1\cdot\hat{\mathbf{r}})\right)+ \\ &- \left(\frac{3M}{r}+M^2+\frac{3}{r^2}\right)(\boldsymbol{v}_1\cdot\hat{\mathbf{r}})^2(\boldsymbol{\sigma}\cdot\hat{\mathbf{r}})\Bigg]e^{-Mr}, \end{aligned} \tag{5.27}$$

where V_{el} is given by eq. (5.25).

Pseudo-scalar Pseudo-scalar Corrections

Dealing with only pseudo-scalar vertices, the only type of non-relativistic correction arises from the propagator in the anelastic case. The NLO amplitude reads then

$$\begin{aligned} \mathcal{M} &= \frac{g_1^P g_2^P}{|\mathbf{q}|^2+M^2}\left(1+\frac{(\mathbf{P}\cdot\mathbf{q})^2}{2m_1^2}\frac{1}{|\mathbf{q}|^2+M^2}+\dots\right)\frac{(\mathbf{q}\cdot\boldsymbol{\sigma})(\mathbf{q}\cdot\boldsymbol{\sigma}')}{4m_1 m_2} \\ &= \mathcal{M}_{el}+\frac{g_1^P g_2^P}{(|\mathbf{q}|^2+M^2)^2}\frac{(\mathbf{q}\cdot\boldsymbol{\sigma})(\mathbf{q}\cdot\boldsymbol{\sigma}')(\mathbf{P}\cdot\mathbf{q})^2}{8m_1^3 m_2}, \end{aligned} \tag{5.28}$$

so the potential is extended in

$$\begin{aligned}V(r) &= V_{el} - \frac{g_1^P g_2^P}{8m_1^3 m_2}\left(\boldsymbol{\nabla}\cdot\boldsymbol{\sigma}\right)\left(\boldsymbol{\nabla}\cdot\boldsymbol{\sigma}'\right)\left(\mathbf{P}\cdot\boldsymbol{\nabla}\right)^2\left(\frac{e^{-Mr}}{8\pi M}\right)\\ &= V_{el} - \frac{g_1^p g_2^P}{64\pi m_1 m_2}\Bigg[\left(M^3+\frac{6M^2}{r}+\frac{15M}{r^2}+\frac{15}{r^3}\right)(\boldsymbol{v}_1\cdot\hat{\mathbf{r}})^2(\boldsymbol{\sigma}\cdot\hat{\mathbf{r}})(\boldsymbol{\sigma}'\cdot\hat{\mathbf{r}})+\\ &-\left(\frac{M^2}{r}+\frac{3M}{r^2}+\frac{3}{r^3}\right)(\boldsymbol{\sigma}\cdot\boldsymbol{\sigma}')(\boldsymbol{v}_1\cdot\hat{\mathbf{r}})^2-\left(\frac{2M^2}{r}+\frac{6M}{r^2}+\frac{6}{r^3}\right)\big((\boldsymbol{\sigma}\cdot\boldsymbol{v}_1)(\boldsymbol{\sigma}'\cdot\hat{\mathbf{r}})(\boldsymbol{v}_1\cdot\hat{\mathbf{r}})+\\ &+(\boldsymbol{\sigma}'\cdot\boldsymbol{v}_1)(\boldsymbol{\sigma}\cdot\hat{\mathbf{r}})(\boldsymbol{v}_1\cdot\hat{\mathbf{r}})\big)-\left(\frac{M^2}{r}+\frac{3M}{r^2}+\frac{3}{r^3}\right)|\boldsymbol{v}_1|^2(\boldsymbol{\sigma}\cdot\hat{\mathbf{r}})(\boldsymbol{\sigma}'\cdot\hat{\mathbf{r}})+\\ &+\left(\frac{M}{r^2}+\frac{1}{r^3}\right)\big((\boldsymbol{\sigma}\cdot\boldsymbol{\sigma}')|\boldsymbol{v}_1|^2+2(\boldsymbol{v}_1\cdot\boldsymbol{\sigma})(\boldsymbol{v}_1\cdot\boldsymbol{\sigma}')\big)\Bigg]e^{-Mr}\,,\end{aligned} \tag{5.29}$$

where V_{el} is given by eq. (4.10).

Vector Vector Corrections

The NLO amplitude in the elastic limit is

$$\begin{aligned}\mathcal{M}_{el} = &-\frac{g_1^V g_2^V}{|\mathbf{q}|^2+M^2}\left(1-\frac{(\mathbf{q}\times\boldsymbol{\sigma})\cdot(\mathbf{q}\times\boldsymbol{\sigma}')}{4m_1m_2}\right)-\frac{g_1^V g_2^V}{|\mathbf{q}|^2+M^2}\Bigg[\frac{|\mathbf{P}|^2}{2m_1^2}-\frac{\mathbf{P}\cdot\mathbf{P}'}{m_1m_2}+\frac{|\mathbf{P}|^2}{2m_1^2}+\\ &+i\mathbf{q}\cdot\left(\frac{\boldsymbol{\sigma}'\times\mathbf{P}'}{4m_2^2}-\frac{\boldsymbol{\sigma}\times\mathbf{P}}{4m_1^2}-\frac{\boldsymbol{\sigma}'\times\mathbf{P}}{2m_1m_2}+\frac{\boldsymbol{\sigma}\times\mathbf{P}'}{2m_1m_2}\right)\Bigg]\,.\end{aligned} \tag{5.30}$$

After the integration and in terms of adimensional parameters, the NLO potential results in

$$\begin{aligned}V_{el}(r) = &\frac{g_1^V g_2^V}{4\pi r}\Bigg[\left(1+\frac{1}{2}|\boldsymbol{v}_1-\boldsymbol{v}_2|^2\right)+\left(\frac{1}{m_1r}+\epsilon_1\right)\frac{\boldsymbol{\sigma}}{8}\times(\boldsymbol{v}_1-2\boldsymbol{v}_2)\cdot\hat{\mathbf{r}}+\\ &-\left(\frac{1}{m_2r}+\epsilon_2\right)\frac{\boldsymbol{\sigma}'}{8}\times(\boldsymbol{v}_2-2\boldsymbol{v}_1)\cdot\hat{\mathbf{r}}+\frac{(\boldsymbol{\sigma}\cdot\boldsymbol{\sigma}')}{4}\left(\epsilon_1\epsilon_2+\frac{\epsilon_1}{m_2r}+\frac{1}{m_1m_2r^2}-\frac{8\pi r}{3m_1m_2}\delta^3(\mathbf{x})\right)+\\ &-\frac{(\boldsymbol{\sigma}\cdot\hat{\mathbf{r}})(\boldsymbol{\sigma}'\cdot\hat{\mathbf{r}})}{4}\left(\epsilon_1\epsilon_2+\frac{3\epsilon_1}{m_2r}+\frac{3}{m_1m_2r^2}\right)\Bigg]e^{-Mr}\,.\end{aligned} \tag{5.31}$$

Including the anelastic correction from the propagator, we obtain

$$\begin{aligned}\mathcal{M} &= -\frac{g_1^V g_2^V}{|\mathbf{q}|^2+M^2}\left(1+\frac{(\mathbf{P}\cdot\mathbf{q})^2}{2m_1^2}\frac{1}{|\mathbf{q}|^2+M^2}+\dots\right)\left(1-\frac{(\mathbf{q}\times\boldsymbol{\sigma})\cdot(\mathbf{q}\times\boldsymbol{\sigma}')}{4m_1m_2}+\dots\right)=\\ &= \mathcal{M}_{el}-\frac{(\mathbf{P}\cdot\mathbf{q})^2}{2m_1^2}\frac{g_1^V g_2^V}{(|\mathbf{q}|^2+M^2)^2}\,,\end{aligned} \tag{5.32}$$

and the associate potential at NLO is

$$\begin{aligned}V(r) &= V_{el}-\frac{g_1^V g_2^V}{16\pi m_1^2 M}(\mathbf{P}\cdot\boldsymbol{\nabla})^2 e^{-Mr}=\\ &= V_{el}-\frac{g_1^V g_2^V}{16\pi r}\left[(1+Mr)(\boldsymbol{v}_1\cdot\hat{\mathbf{r}})^2-|\boldsymbol{v}_1|^2\right]e^{-Mr}\,,\end{aligned} \tag{5.33}$$

where V_{el} is given by eq. (5.31).

Axial Vector Corrections

At NLO the elastic amplitude is found to be the amplitude can be rewritten in a convenient way as

$$\mathcal{M}_{el} = \mathcal{M}_{\rm LO} - \frac{g_1^A g_2^V}{|\mathbf{q}|^2+M^2}\left[A+\mathbf{B}\cdot i\mathbf{q}+q^iq^jC^{ij}+D|\mathbf{q}|^2+\mathbf{E}\cdot i\mathbf{q}|\mathbf{q}|^2\right]\,, \tag{5.34}$$

where we have introduced the coefficients

$$\begin{aligned}
A &\equiv \frac{\left(|\boldsymbol{v}_2|^2 - \boldsymbol{v}_1\cdot\boldsymbol{v}_2\right)}{2}\,\boldsymbol{v}_1\cdot\boldsymbol{\sigma}\,,\\
\mathbf{B} &\equiv \frac{1}{4}\left(\frac{\boldsymbol{v}_1\times\boldsymbol{v}_2}{m_1} - (\boldsymbol{v}_1\cdot\boldsymbol{\sigma})\frac{(\boldsymbol{v}_2-\boldsymbol{v}_1)}{m_2}\times\boldsymbol{\sigma}'\right),\\
C^{ij} &\equiv \frac{1}{8m_1}\left(\frac{v_1^i\sigma'^j}{m_2} + \frac{v_2^i\sigma^j}{m_1}\right),\\
D &\equiv -\frac{1}{8m_1}\left(\frac{\boldsymbol{v}_1\cdot\boldsymbol{\sigma}'}{m_2} + \frac{\boldsymbol{v}_2\cdot\boldsymbol{\sigma}}{m_1}\right),\\
\mathbf{E} &\equiv \frac{\boldsymbol{\sigma}\times\boldsymbol{\sigma}'}{16m_1^2m_2}\,.
\end{aligned} \tag{5.35}$$

Hence, the potential at the NLO is

$$\begin{aligned}
V_{el}(r) &= V_{\rm LO}(\mathbf{x}) + g_1^A g_2^V\left[A + \mathbf{B}\cdot\boldsymbol{\nabla} - C^{ij}\partial_i\partial_j - D\nabla^2 - (\mathbf{E}\cdot\boldsymbol{\nabla})\nabla^2\right]\left(\frac{e^{-Mr}}{4\pi r}\right) =\\
&= V_{\rm LO}(\mathbf{x}) + \frac{g_1^A g_2^V}{4\pi r}\left[\frac{\left(|\boldsymbol{v}_2|^2 - \boldsymbol{v}_1\cdot\boldsymbol{v}_2\right)}{2}\,\boldsymbol{v}_1\cdot\boldsymbol{\sigma} - (1+Mr)\left(\frac{\boldsymbol{v}_1\times\boldsymbol{v}_2}{m_1 r} - \frac{(\boldsymbol{v}_1\cdot\boldsymbol{\sigma})}{m_2 r}\,(\boldsymbol{v}_2-\boldsymbol{v}_1)\times\boldsymbol{\sigma}'\right)\cdot\frac{\hat{\mathbf{r}}}{4} +\right.\\
&+ \frac{1}{16m_1^2m_2r^3}\left(M^2r^2 + M^3r^3 - 4\pi r^4 M\delta^3(\mathbf{x})\right)(\boldsymbol{\sigma}\times\boldsymbol{\sigma}')\cdot\hat{\mathbf{r}} + \frac{\pi r}{4m_1^2m_2}(\boldsymbol{\sigma}\times\boldsymbol{\sigma}')\cdot\boldsymbol{\nabla}\delta^3(\mathbf{x}) +\\
&- \frac{1}{8m_1 r}\left(M^2r^2 + 3Mr + 3\right)\left(\frac{(\boldsymbol{v}_1\cdot\hat{\mathbf{r}})(\boldsymbol{\sigma}'\cdot\hat{\mathbf{r}})}{m_2 r} + \frac{(\boldsymbol{v}_2\cdot\hat{\mathbf{r}})(\boldsymbol{\sigma}\cdot\hat{\mathbf{r}})}{m_1 r}\right) + \frac{1}{8m_1 r}\left(\frac{\boldsymbol{v}_1\cdot\boldsymbol{\sigma}'}{m_2 r} + \frac{\boldsymbol{v}_2\cdot\boldsymbol{\sigma}}{m_1 r}\right)\cdot\\
&\left.\cdot\left(1 + Mr + M^2r^2 - \frac{8\pi r^3}{3}\delta^3(\mathbf{x})\right)\right]e^{-Mr}\,,
\end{aligned} \tag{5.36}$$

where $V_{\rm LO}$ is given by eq. (4.27). Including the anelastic corrections we obtain

$$\mathcal{M} = \mathcal{M}_{el} - \frac{(\mathbf{P}\cdot\mathbf{q})^2}{2m_1^2}\left[\left(\frac{\mathbf{P}}{m_1} - \frac{\mathbf{P}'}{m_2}\right)\cdot\boldsymbol{\sigma} + \frac{1}{2m_2}(\boldsymbol{\sigma}\times\boldsymbol{\sigma}')\cdot i\mathbf{q}\right]\frac{g_1^A g_2^V}{(|\mathbf{q}|^2 + M^2)^2} \tag{5.37}$$

that modifies the potential into

$$\begin{aligned}
V(r) &= V_{el} - \frac{g_1^A g_2^V}{16\pi m_1^2 M}(\mathbf{P}\cdot\boldsymbol{\nabla})^2\left[\boldsymbol{\sigma}\cdot\left(\frac{\mathbf{P}}{m_1} - \frac{\mathbf{P}'}{m_2}\right) + (\boldsymbol{\sigma}\times\boldsymbol{\sigma}')\cdot\frac{\boldsymbol{\nabla}}{2m_2}\right]e^{-Mr}\\
&= V_{el} - \frac{g_1^A g_2^V}{16\pi r}\boldsymbol{\sigma}\cdot(\boldsymbol{v}_1 - \boldsymbol{v}_2)\left[(1+Mr)(\boldsymbol{v}_1\cdot\hat{\mathbf{r}})^2 - |\boldsymbol{v}_1|^2\right]e^{-Mr} - \frac{g_1^A g_2^V}{32\pi m_2 r^2}(\boldsymbol{\sigma}\times\boldsymbol{\sigma}')\cdot\\
&\left[(1+Mr)\left(|\boldsymbol{v}_1|^2\hat{\mathbf{r}} + 2(\boldsymbol{v}_1\cdot\hat{\mathbf{r}})\boldsymbol{v}_1\right) - \left(3 + 3Mr + M^2r^2\right)(\boldsymbol{v}_1\cdot\hat{\mathbf{r}})^2\hat{\mathbf{r}}\right]e^{-Mr}\,,
\end{aligned} \tag{5.38}$$

where V_{el} is given by eq. (5.36).

Axial Axial Corrections

The elastic amplitude with two axial vertices is described at NLO by

$$\begin{aligned}
\mathcal{M}_{el} =& \frac{g_1^A g_2^A}{|\mathbf{q}|^2 + M^2}\left[\boldsymbol{\sigma}\cdot\boldsymbol{\sigma}' + \left(\frac{1}{M^2} - \frac{1}{8m_1^2} - \frac{1}{8m_2^2}\right)(\boldsymbol{\sigma}\cdot\mathbf{q})(\boldsymbol{\sigma}'\cdot\mathbf{q}) - i\mathbf{q}\left(\frac{\mathbf{P}\times\boldsymbol{\sigma}'}{4m_1^2} - \frac{\mathbf{P}'\times\boldsymbol{\sigma}}{4m_2^2}\right) +\right.\\
&+ \frac{(\mathbf{P}\cdot\boldsymbol{\sigma})(\mathbf{P}\cdot\mathbf{q})(\boldsymbol{\sigma}'\cdot\mathbf{q})}{2M^2m_1^2} + \frac{(\mathbf{P}'\cdot\boldsymbol{\sigma}')(\mathbf{P}'\cdot\mathbf{q})(\boldsymbol{\sigma}\cdot\mathbf{q})}{2M^2m_2^2} - \frac{\boldsymbol{\sigma}\cdot\boldsymbol{\sigma}'}{8}\left(\frac{1}{m_1^2} - \frac{1}{m_2^2}\right)|\mathbf{q}|^2 +\\
&\left.+ (\mathbf{P}\cdot\boldsymbol{\sigma})(\mathbf{P}'\cdot\boldsymbol{\sigma}')\left(\frac{1}{2m_1^2} + \frac{1}{2m_1^2} - \frac{1}{m_1m_2}\right)\right]
\end{aligned} \tag{5.39}$$

and the associated potential results in

$$\begin{aligned}V(r)_{el} = \frac{g_1^A g_2^A}{4\pi r}\Bigg[&- \boldsymbol{\sigma}\cdot\boldsymbol{\sigma}' + (\boldsymbol{v}_1\cdot\boldsymbol{\sigma})(\boldsymbol{v}_2\cdot\boldsymbol{\sigma}')\left(\frac{m_2}{2m_1}+\frac{m_1}{2m_2}-1\right)+\\ &-(1+Mr)\left(\frac{\boldsymbol{v}_1\times\boldsymbol{\sigma}'}{4m_1 r}-\frac{\boldsymbol{v}_2\times\boldsymbol{\sigma}}{4m_2 r}\right)\cdot\hat{\mathbf{r}}-\left(1+Mr+\frac{4\pi r^3\delta^3(\mathbf{x})}{3}\right)\cdot\\ &\cdot\left((\boldsymbol{\sigma}\cdot\boldsymbol{\sigma}')\left(\frac{1}{M^2r^2}-\frac{1}{8m_1^2r^2}-\frac{1}{8m_2^2r^2}\right)+\frac{(\boldsymbol{v}_1\cdot\boldsymbol{\sigma})(\boldsymbol{v}_1\cdot\boldsymbol{\sigma}')}{2M^2r^2}+\frac{(\boldsymbol{v}_2\cdot\boldsymbol{\sigma}')(\boldsymbol{v}_2\cdot\boldsymbol{\sigma})}{2M^2r^2}\right)+\\ &+\left(M^2r^2+3Mr+3\right)\left((\boldsymbol{\sigma}\cdot\hat{\mathbf{r}})(\boldsymbol{\sigma}'\cdot\hat{\mathbf{r}})\left(\frac{1}{M^2r^2}-\frac{1}{8m_1^2r^2}-\frac{1}{8m_2^2r^2}\right)+\frac{(\boldsymbol{v}_1\cdot\boldsymbol{\sigma})(\boldsymbol{v}_1\cdot\hat{\mathbf{r}})(\boldsymbol{\sigma}'\cdot\hat{\mathbf{r}})}{2M^2r^2}+\right.\\ &\left.+\frac{(\boldsymbol{v}_2\cdot\boldsymbol{\sigma}')(\boldsymbol{v}_2\cdot\hat{\mathbf{r}})(\boldsymbol{\sigma}\cdot\hat{\mathbf{r}})}{2M^2r^2}\right)+(\boldsymbol{\sigma}\cdot\boldsymbol{\sigma}')\left(M^2r^2-4\pi r^3\delta^3(\mathbf{x})\right)\left(\frac{1}{8m_2^2r^2}-\frac{1}{8m_1^2r^2}\right)\Bigg]e^{-Mr}\,.\end{aligned} \tag{5.40}$$

Relaxing the elastic hypothesis implies the correction

$$\mathcal{M} = \mathcal{M}_{el} + \frac{g_1^A g_2^A}{(|\mathbf{q}|^2+M^2)^2}\frac{(\mathbf{P}\cdot\mathbf{q})^2}{2m_1^2}\left[\boldsymbol{\sigma}\cdot\boldsymbol{\sigma}'+\frac{1}{M^2}(\boldsymbol{\sigma}\cdot\mathbf{q})(\boldsymbol{\sigma}'\cdot\mathbf{q})\right] \tag{5.41}$$

and the associated NLO potential is found to be

$$\begin{aligned}V(r) &= V_{el} + \frac{g_1^A g_2^A}{16\pi m_1^2 M}(\mathbf{P}\cdot\boldsymbol{\nabla})^2\left[\boldsymbol{\sigma}\cdot\boldsymbol{\sigma}'-\frac{1}{M^2}(\boldsymbol{\sigma}\cdot\boldsymbol{\nabla})(\boldsymbol{\sigma}'\cdot\boldsymbol{\nabla})\right]e^{-Mr} =\\ &= V_{el}+\frac{g_1^A g_2^A}{16\pi r}(\boldsymbol{\sigma}\cdot\boldsymbol{\sigma}')\left[(1+Mr)(\boldsymbol{v}_1\cdot\hat{\mathbf{r}})^2-|\boldsymbol{v}_1|^2\right]e^{-Mr}-\frac{g_1^A g_2^A}{16\pi r}\cdot\\ &\left[\left(6+Mr+\frac{15}{Mr}+\frac{15}{M^2r^2}\right)(\boldsymbol{v}_1\cdot\hat{\mathbf{r}})^2(\boldsymbol{\sigma}\cdot\hat{\mathbf{r}})(\boldsymbol{\sigma}'\cdot\hat{\mathbf{r}})+\right.\\ &-\left(1+\frac{3}{Mr}+\frac{3}{M^2r^2}\right)(\boldsymbol{\sigma}\cdot\boldsymbol{\sigma}')(\boldsymbol{v}_1\cdot\hat{\mathbf{r}})^2-\left(2+\frac{6}{Mr}+\frac{6}{M^2r^2}\right)\big((\boldsymbol{\sigma}\cdot\boldsymbol{v}_1)(\boldsymbol{\sigma}'\cdot\hat{\mathbf{r}})(\boldsymbol{v}_1\cdot\hat{\mathbf{r}})+\\ &+(\boldsymbol{\sigma}'\cdot\boldsymbol{v}_1)(\boldsymbol{\sigma}\cdot\hat{\mathbf{r}})(\boldsymbol{v}_1\cdot\hat{\mathbf{r}})\big)-\left(1+\frac{3}{Mr}+\frac{3}{M^2r^2}\right)|\boldsymbol{v}_1|^2(\boldsymbol{\sigma}\cdot\hat{\mathbf{r}})(\boldsymbol{\sigma}'\cdot\hat{\mathbf{r}})+\\ &\left.+\left(\frac{1}{Mr}+\frac{1}{M^2r^2}\right)\big((\boldsymbol{\sigma}\cdot\boldsymbol{\sigma}')|\boldsymbol{v}_1|^2+2(\boldsymbol{v}_1\cdot\boldsymbol{\sigma})(\boldsymbol{v}_1\cdot\boldsymbol{\sigma}')\big)\right]e^{-Mr}\,,\end{aligned} \tag{5.42}$$

where V_{el} is given by eq. (5.40).

Correction to the Tensor Structures

The NLO correction to the remaining tensor and pseudo-tensor interactions turn out to be more cumbersome. In general, the amplitudes expanded upo to NLO have the following structure

$$\mathcal{M}_{TT} = \frac{4g_1^T g_2^T}{|\mathbf{q}|^2+M^2}\left[(\boldsymbol{\sigma}\cdot\boldsymbol{\sigma}')|\mathbf{q}|^2-(\boldsymbol{\sigma}\cdot\mathbf{q})(\boldsymbol{\sigma}'\cdot\mathbf{q})+i|\mathbf{q}|^2\mathbf{q}\cdot\mathbf{A}+q^iq^jB^{ij}+|\mathbf{q}|^2C+|\mathbf{q}|^4D+E^{ij}q^iq^j|\mathbf{q}|^2\right]\,, \tag{5.43}$$

$$\mathcal{M}_{\tilde{T}\tilde{T}} = \frac{4g_1^{\tilde{T}} g_2^{\tilde{T}}}{|\mathbf{q}|^2+M^2}\left(q^iq^jA^{ij}+B|\mathbf{q}|^2+C^{ij}q^iq^j|\mathbf{q}|^2\right)\,, \tag{5.44}$$

$$\mathcal{M}_{\tilde{T}T} = 4\frac{g_1^{\tilde{T}} g_2^{T}}{|\mathbf{q}|^2+M^2}\left[A^{ij}q^iq^j|\mathbf{q}|^2+B|\mathbf{q}|^2+C^{ij}q^iq^j+\mathbf{D}\cdot i\mathbf{q}|\mathbf{q}|^2+E|\mathbf{q}|^4+\mathbf{F}\cdot i\mathbf{q}|\mathbf{q}|^4\right] \tag{5.45}$$

where the functions $A, B, C, \ldots$ are defined for each cases in appendix C.1, together with the expressions of the associated potentials.

5.3 Physical Interpretation of the Next to Leading Order Corrections

The formulae obtained in the previous section require a numerical examination in order to understand the relative importance of their individual terms. Dealing with long-range forces, we expect suppression or enhancement factors based on the scaling with M, m_i and $|\mathbf{p}_i|$.
A boson with a sufficiently small mass, e.g. of the order of $M \sim 10^{-4}$ eV, has a macroscopic Compton wavelength of $r \sim 1\,\text{cm}$, and hence mediate a force on the laboratory scales. On the other hand, for the external fermions we have in mind nucleons with mass $m_i \sim \text{GeV}$. A similar discussion would apply when dealing with electrons ad external states, in that case $m_i \sim \text{MeV}$. Another scale stems from the non-relativistic nature of the external momenta, requiring $|\boldsymbol{v}_i| \ll 1$, that is satisfied e.g. for $|\mathbf{p}_i| \lesssim \text{MeV}$.
These orders of magnitude suggests the following size for the dimensionless parameters defined in eq. (5.15)

$$\begin{cases} \epsilon_i \sim 10^{-13} \\ |\boldsymbol{v}_i| \sim 10^{-3} \end{cases} \longrightarrow \quad \epsilon_i \ll |\boldsymbol{v}_i| \ll 1\,, \tag{5.46}$$

which can be used to understand the relative importance of the individual pieces in the NLO potentials computed in the previous Section, for which we are going to employ the following numerical benchmark:

$$\begin{aligned} &M \sim 10^{-4}\text{eV}\,, \;\; m_i \sim \mu \sim \text{GeV}\,, \;\; |\mathbf{p}| \sim \text{MeV}\,, \\ &r \sim 10^{10}\,\text{MeV}^{-1}\,, \;\; \frac{r}{\mu^2} \sim 10^{4}\,\text{MeV}^{-3}\,, \;\; \frac{r^2}{m_i} \sim 10^{-1}\text{eV}^{-3}\,, \\ &\frac{1}{m_i r} \sim 10^{-13}\,, \;\; Mr \sim 1\,, \;\; |\boldsymbol{v}_i| \sim 10^{-3}\,, \;\; \frac{m_1}{m_2} \sim 1\,. \end{aligned} \tag{5.47}$$

In the NLO potentials we also notice the appearance of contact terms proportional to delta functions. An analogy with atomic physics is helpful in order to understand its physical consequences. To give a concrete example, relativistic effects play an important role in the hyperfine structure of the hydrogen atom. Among them, the Darwin term affects the s-state of the wave function from its proportionality with $\delta^3(\mathbf{x})$. In the quantum formalism, operators like this must be evaluated inside the matrix elements between the normalized states $|n,l,m\rangle$ of the hydrogen atom [53], in order to extract the expectation values. Apart from constant terms, it turns out that

$$H_D \sim \delta^3(\mathbf{x}) \implies \langle 1,0,0|H_D|1,0,0\rangle \sim \frac{1}{a_0^3}\,, \tag{5.48}$$

where a_0 is the Bohr radius. Knowing its expression

$$a_0 = \frac{1}{m_e e^2} \simeq 20\ \text{MeV}^{-1}\,, \tag{5.49}$$

we can associate, at least formally, a scaling to the Dirac delta like

$$\delta^3(\mathbf{x}) \sim 10^{-4}\text{MeV}^3\,. \tag{5.50}$$

For later purposes, it is worth to calculate also the matrix element of $\boldsymbol{\nabla}\delta^3(\mathbf{x})$ via the coordinate representation of the hydrogen wave functions

$$\varphi_{n,l,m}(\mathbf{x}) = R_{n,l}(r) Y^l_m(\theta,\phi)\,, \tag{5.51}$$

leading to

$$\begin{aligned} \langle 1,0,0|\boldsymbol{\nabla}\delta^3(\mathbf{x})|1,0,0\rangle &= \int d^3x\, \varphi^*_{1,0,0}(\mathbf{x})\boldsymbol{\nabla}\delta^3(\mathbf{x})\varphi_{1,0,0}(\mathbf{x}) = \\ &= -\int d^3x \frac{d}{dr}\left(\frac{e^{-2r/a_0}}{\pi a_0^3}\right)\hat{\mathbf{r}}\delta(r) = \frac{2\hat{\mathbf{r}}}{\pi a_0^4}\,. \end{aligned} \tag{5.52}$$

This implies that, formally,

$$\partial^{(n)}_{\mathbf{x}}\delta^3(\mathbf{x}) \sim \frac{1}{a_0^{3+n}}\,, \tag{5.53}$$

giving us a scaling also for derivatives of contact interactions.
In the light of this example, we can extend the discussion to approach the Dirac deltas emerging in the non-relativistic potentials between nucleons. To this end, we introduce a length scale along the lines of the Bohr radius, but that is associated to the mass of the nucleon as

$$a_N \sim \frac{1}{m_N} \simeq \text{GeV}^{-1}\,, \tag{5.54}$$

such that in the case of nucleons the formal scaling of the contact terms becomes

$$\delta^3(\mathbf{x}) \sim \frac{1}{a_N^3} \simeq \text{GeV}^3 \quad , \quad \boldsymbol{\nabla}\delta^3(\mathbf{x}) \sim \frac{1}{a_N^4} \simeq \text{GeV}^4\,. \tag{5.55}$$

These numerical benchmarks allow us to gauge the relative importance of the NLO corrections, and rewrite the first six potentials keeping only the dominant terms (a similar discussion applies to the tensor structures, given in appendix C.1)

$$V(\mathbf{x})^{SS}_{tot} = -\frac{g_1^S g_2^S}{4\pi}\left[\frac{1}{r} + \frac{\pi}{2}\frac{\delta^3(\mathbf{x})}{\mu^2}\right] e^{-Mr}\,; \tag{5.56}$$

$$\begin{aligned} V(\mathbf{x})^{PS}_{tot} = -\frac{g_1^P g_2^S}{8\pi m_1 r^2}\Big[&\boldsymbol{\sigma}\cdot\hat{\mathbf{r}}\,(Mr+1) + \frac{\pi r^2\epsilon_2}{2m_2}(\boldsymbol{\sigma}\cdot\hat{\mathbf{r}})\delta^3(\mathbf{x}) - \frac{\pi r^2}{2m_2^2}\boldsymbol{\sigma}\cdot\boldsymbol{\nabla}\delta^3(\mathbf{x}) + \\ &- \frac{\pi r^2}{3m_2}\delta^3(\mathbf{x})\boldsymbol{\sigma}\cdot(\boldsymbol{\sigma}'\times\boldsymbol{v}_2)\Big] e^{-Mr}\,; \end{aligned} \tag{5.57}$$

$$\begin{aligned} V(\mathbf{x})^{PP}_{tot} = -\frac{g_1^P g_2^P}{16\pi m_1 m_2 r^3}\Big[&\boldsymbol{\sigma}\cdot\boldsymbol{\sigma}'\left(Mr+1+\frac{4\pi r^3}{3}\delta^3\left(\mathbf{x}\right)\right) + \\ &- (\boldsymbol{\sigma}\cdot\hat{\mathbf{r}})(\boldsymbol{\sigma}'\cdot\hat{\mathbf{r}})\left(M^2r^2+3Mr+3\right)\Big] e^{-Mr}\,; \end{aligned} \tag{5.58}$$

$$V(\mathbf{x})^{VV}_{tot} = \frac{g_1^V g_2^V}{4\pi r}\left[1 - \frac{2\pi r(\boldsymbol{\sigma}\cdot\boldsymbol{\sigma}')}{3m_1m_2}\delta^3(\mathbf{x})\right] e^{-Mr}\,; \tag{5.59}$$

$$\begin{aligned} V(\mathbf{x})^{AV}_{tot} = \frac{g_1^A g_2^V}{4\pi r}\Big[&\boldsymbol{\sigma}\cdot(\boldsymbol{v}_1-\boldsymbol{v}_2) - \frac{(1+Mr)}{2m_2 r}(\boldsymbol{\sigma}\times\boldsymbol{\sigma}')\cdot\hat{\mathbf{r}} - \frac{\pi\epsilon_2 r}{4m_1^2}\delta^3(\mathbf{x})(\boldsymbol{\sigma}\times\boldsymbol{\sigma}')\cdot\hat{\mathbf{r}} + \\ &+ \frac{\pi r}{4m_1^2 m_2}(\boldsymbol{\sigma}\times\boldsymbol{\sigma}')\cdot\boldsymbol{\nabla}\delta^3(\mathbf{x}) - \frac{\pi r}{3m_1}\left(\frac{\boldsymbol{v}_1\cdot\boldsymbol{\sigma}'}{m_2} + \frac{\boldsymbol{v}_2\cdot\boldsymbol{\sigma}}{m_1}\right)\delta^3(\mathbf{x})\Big] e^{-Mr}\,; \end{aligned} \tag{5.60}$$

$$\begin{aligned} V(\mathbf{x})^{AA}_{tot} = -\frac{g_1^A g_2^A}{4\pi r}\Big[&\boldsymbol{\sigma}\cdot\boldsymbol{\sigma}' + \left(\frac{\boldsymbol{\sigma}\cdot\boldsymbol{\sigma}'}{M^2r^2}\right)\left(1+Mr+\frac{4\pi r^3}{3}\delta^3(\mathbf{x})\right) + \\ &- (\boldsymbol{\sigma}\cdot\hat{\mathbf{r}})(\boldsymbol{\sigma}'\cdot\hat{\mathbf{r}})\frac{\left(M^2r^2+3Mr+3\right)}{M^2r^2} + \frac{\pi r}{2}\left(\frac{1}{m_2^2}-\frac{1}{m_1^2}\right)(\boldsymbol{\sigma}\cdot\boldsymbol{\sigma}')\delta^3(\mathbf{x})\Big] e^{-Mr}\,. \end{aligned} \tag{5.61}$$

It should be noted that the contact terms proportional to the Dirac deltas arising from the NLO correction can be much more relevant than their LO counterparts. E.g. in the case of the scalar-scalar potential, one has that for $r \sim 1/M$, the two terms in the square bracket of eq. (5.56) are respectively of order: $M \ll \mu \sim$ GeV (with μ the reduced mass defined in eq. (5.17)), and $\delta^3(\mathbf{x})/\mu^2 \sim$ GeV. Hence, as long as the mass of the new boson mediator is $M \lesssim m_i \sim 1$ GeV, the contact term dominates with respect to the LO term. A similar discussion applies as well to the other type of potentials. On the other hand, it remains to be understood whether such contact terms can have a phenomenological impact. While we expect that they play no role in experimental tests of gravity, they may be relevant in nuclear or atomic physics, in analogy to the Darwin term which affects the ground state energy of the hydrogen atom.
The long-range forces derived so far also contain short-range parts, and both contribute to the interactions depending on the scale of the experiment. In fact, the exponential suppression e^{-Mr} is not active beneath the Compton wavelength of the new mediators. This means that both macroscopic and

microscopic experiments are useful for research, but a clear distinction must be made. In macroscopic-scale experiments the momentum and radial vectors may be treated as classical vectors. In atomic-scale experiments instead, they need to be treated as quantum operators, and explicit symmetrizations, such as $\{\mathbf{p}, f(r)\}$, must be introduced inside our expressions. In relation to spin-dependent potentials there is also the manifestation of parity or time reversal violation, e.g. dealing with $\boldsymbol{\sigma}\cdot\hat{\mathbf{r}}$. Classically $\hat{\mathbf{r}}$ is the radial vector connecting two macroscopic objects, so $\boldsymbol{\sigma}\cdot\hat{\mathbf{r}}$ causes the precession of the spin vector, reminiscent of a magnetic moment inside an external magnetic field. In the atomic regime, $\hat{\mathbf{r}}$ is the operator pointing between the atomic electrons and nucleons, therefore $\boldsymbol{\sigma}\cdot\hat{\mathbf{r}}$ mixes atomic states of opposite parity and give rise to atomic electric dipole moments. Both macroscopic and microscopic measurements involve spin precession about two different set of vectors: $\mathbf{B}$ and $\hat{\mathbf{r}}$ for macroscopic scales, $\mathbf{B}$ and $\mathbf{E}$ for atomic scales.

Convergence of the Non-relativistic Expansion

It is important to check whether the potentially large contributions arising from the contact terms in the NLO calculation might signal a convergence problem. What we are looking for is a possible trend that persists at higher orders. The simplest case for performing this check is provided by the scalar-scalar potential, in which NNLO has to be evaluated. Recalling eq. (5.16), the next term of the expansion returns the amplitude

$$\mathcal{M} = \frac{g_1^S g_2^S}{|\mathbf{q}|^2+M^2}\left[1+\frac{|\mathbf{q}|^2}{8\mu^2}+\frac{1}{4}\mathbf{K}\cdot\, i\mathbf{q}+|\mathbf{q}|^2\, i\mathbf{q}\cdot\mathbf{A}+B|\mathbf{q}|^4+q^iq^jC^{ij}+i\mathbf{q}\cdot\mathbf{D}+E|\mathbf{q}|^2\right], \tag{5.62}$$

where $\mathbf{A}, B, C^{ij}, \mathbf{D}, E, \mathbf{K}$ are specific tensors, functions of $\mathbf{P}_i, \boldsymbol{\sigma}_i, m_i, M$. Keeping only the leading terms in the non-relativistic expansion, following the rules established in the previous Section, we obtain

$$\begin{aligned} V(\mathbf{x}) = -g_1^S g_2^S\Bigg\{ & \frac{1}{4\pi r}+\left(\frac{1}{8m_1^2}+\frac{1}{8m_2^2}-\frac{|\mathbf{P}|^2}{32m_1^4}-\frac{|\mathbf{P}'|^2}{32m_2^4}\right)\delta^3(\mathbf{x})+ \\ & +\left[\frac{\mathbf{P}\times\boldsymbol{\sigma}}{32m_1^2}\left(\frac{1}{2m_1^2}-\frac{1}{m_2^2}\right)-\frac{\mathbf{P}'\times\boldsymbol{\sigma}'}{32m_2^2}\left(\frac{1}{2m_2^2}-\frac{1}{m_1^2}\right)\right]\cdot\boldsymbol{\nabla}\delta^3(\mathbf{x})+ \\ & -\left(\frac{1}{64m_1^2m_2^2}-\frac{1}{128m_1^4}-\frac{1}{128m_2^4}\right)\nabla^2\delta^3(\mathbf{x})+ \\ & +\left(\frac{(\mathbf{P}\times\boldsymbol{\sigma})\cdot(\mathbf{P}'\times\boldsymbol{\sigma}')}{16m_1^2m_2^2}-\frac{3|\mathbf{P}|^2}{32m_1^4}-\frac{3|\mathbf{P}'|^2}{32m_2^4}\right)\left(\frac{\delta^3(\mathbf{x})}{3}\right)\Bigg\}e^{-Mr}, \end{aligned} \tag{5.63}$$

while the NNLO terms in the anelastic propagator are highly suppressed by $|\boldsymbol{v}_1|^4\sim 10^{-12}$, thus safely negligible.

The final potential shows an overall convergence, since $|\mathbf{P}|/m_i \ll 1$ can be safely neglected, so one remains with the dominant contributions from NLO and NNLO given by

$$V(\mathbf{x}) = -\frac{g_1^S g_2^S}{4\pi r}\left(1|_{LO}+\frac{\pi r}{2}\frac{\delta^3(\mathbf{x})}{\mu^2}\bigg|_{NLO}+\alpha\frac{r\nabla^2\delta^3(\mathbf{x})}{m_i^2m_j^2}\bigg|_{NNLO}\right), \tag{5.64}$$

where α denotes a constant term that is zero for $m_1=m_2$. In particular, the ratio between the NNLO and NLO term is of order $\alpha\nabla^2\delta^3/\delta^3 m_N^2\sim\alpha a_N^2 m_N^2\lesssim\alpha$, that converges for $\alpha\ll 1$, corresponding to the case $m_1\simeq m_2$.

CHAPTER 6

NON-RELATIVISTIC POTENTIALS BEYOND TREE LEVEL

Until now, we have considered non-relativistic potentials generated by the tree-level exchange of any type of spin-0 or 1 particle. However, there are other possible structures for long-range potentials which may arise beyond tree level. A well-known possibility is given by the exchange of a loop of light neutrinos, stemming from effective 4-fermion neutral current interactions arising in the SM [56, 57, 58]. The first part of this Chapter is devoted to reviewing the formalism constructed by Feinberg and Sucher [13] in order to calculate the potential induced by the exchange of a pair of particles. Having examined the technicalities behind the specific case of neutrinos, we will then focus our attention on more general structures which can arise at one loop, in analogy to the approach discussed previously for tree-level potentials.

6.1 One-loop Neutrino Exchange

At the EFT level the interaction between a neutrinos ν and a generic SM particle χ is provided by the effective operator

$$\mathcal{L}_{\nu\nu} = G_{\nu\nu}\bar{\chi}\chi\bar{\nu}\nu \ , \quad [G_{\nu\nu}] = -2 \, , \tag{6.1}$$

from which the scattering is described by the loop diagram reported in fig. (6.1).

One might guess, based on dimensional analysis, that the potential for this interaction could scale like

$$U_{\nu\nu} \sim G_{\nu\nu}^2 \frac{m_\chi^2}{r^3} \, . \tag{6.2}$$

If this were the case the effects of such a force may be observable in laboratory tests. Unfortunately, the guessed form is incorrect and the right behaviour turns out to be

$$U_{\nu\nu} \sim \frac{G_{\nu\nu}^2}{r^5} \, , \tag{6.3}$$

that yields a much smaller effect.
Let us now derive this result. The loop amplitude can be easily solved using the standard methods of loop calculations, starting from

$$i\mathcal{M} = -(iG_{\nu\nu})^2 \bar{u}_r(p_2) u_s(p_1) \int \frac{d^4k}{(2\pi)^4} \mathrm{Tr}\left(\frac{i}{\not{k}} \frac{i}{\not{k} - \not{q}} \right) \bar{u}_{r'}(p_2') u_{s'}(p_1') \tag{6.4}$$

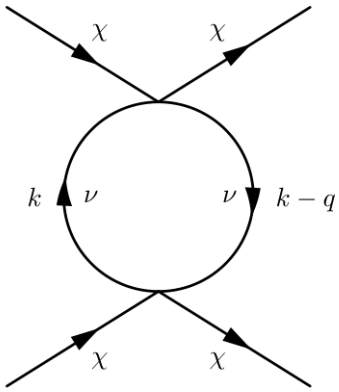

Figure 6.1: Scattering between SM particles via neutrino pair exchange.

that is quadratically divergent in the UV. The standard approach relies on dimensional regularization in which the regulator is taken as a complex small deviation from the ordinary 4-dimensional space-time, i.e.

$$d = 4 - \epsilon\,,\ \epsilon \in \mathbb{C} \quad \Rightarrow \quad G_{\nu\nu} \equiv \mu^{\epsilon} g\,. \tag{6.5}$$

Thus, substituting the bilinears with their non-relativistic expansion, we obtain

$$i\mathcal{M} = -\mu^{2\epsilon} g^2 \int \frac{d^d k}{(2\pi)^d} \frac{\mathrm{Tr}(\not{k}(\not{k} - \not{q}))}{k^2 (k-q)^2}\,. \tag{6.6}$$

Solving the trace and identifying the master integrals, in the limit $\epsilon \to 0$ the amplitude becomes

$$\mathcal{M}_{NR} = -\frac{G_{\nu\nu}^2}{8\pi^2} |\mathbf{q}|^2 \left(2 + \Delta_\epsilon + \log\left(\frac{\mu^2}{|\mathbf{q}|^2}\right)\right) \tag{6.7}$$

where Δ_ϵ is the divergent part, while μ is the renormalization scale.
The potential is obtained via its Fourier transform, but the logarithm in the integrand has to be treated with care, due to its analytic properties in the complex plane. It can be shown [56] that, for contact interactions, only the logarithm contributes, which has a branch cut on the imaginary axis. The UV part is responsible for the running of the coupling constant and does not play any role in the potential, hence the final result is

$$V(r) = -\frac{3 G_{\nu\nu}^2}{8\pi^3 r^5}\,. \tag{6.8}$$

However, the complex integration lacks a physical insight, so it is useful to re-derive the result above from the point of view of dispersion theory.

Dispersion Theory Approach

The dispersion theory approach, discussed in Chapter (3.2) , deals with the integration by rewriting the amplitude with the effective propagator $\Delta(q)$ as

$$i\mathcal{M} = -G_{\nu\nu}^2 \bar{u}_r(p_2) u_s(p_1) i\Delta(q) \bar{u}_{r'}(p_2') u_{s'}(p_1') \simeq -i G_{\nu\nu}^2 \Delta(q) \tag{6.9}$$

inside which lies the 1-loop structure and such that

$$V(r) = -\frac{G_{\nu\nu}^2}{4\pi r} \int_0^\infty d\mu^2\, \rho(\mu^2) e^{-\mu r}\,. \tag{6.10}$$

To extract the spectral function, recalling that

$$\rho(\mu^2) = -\frac{1}{\pi} \mathrm{Im}\{\Delta(q)\}\,, \tag{6.11}$$

it is sufficient to calculate the tree-level cutted amplitude $\mathcal{M}(q \to \nu\nu)$ of the decay of an external source of momentum q into a final state of intermediate neutrinos, i.e.

$$\mathcal{M}(q \to \nu\nu) = i\bar{u}_{\bar{\nu}} u_{\nu} \,, \tag{6.12}$$

where the coupling constants has already been taken into eq. (6.9). The modulus squared of the amplitude has to be summed over all possible spin and polarization states of the final state, so that the unpolarized amplitude is (taking the approximation of massless neutrinos)

$$|\bar{\mathcal{M}}(q \to \nu\nu)|^2 = \mathrm{Tr}[\not{k}\not{k}'] = 4(k \cdot k') \,. \tag{6.13}$$

The relativistic kinematics of the cut diagram is encoded into

$$t = q^2 = \mu^2 = (k - k')^2 \;\Rightarrow\; (k \cdot k') = -\frac{\mu^2}{2} \tag{6.14}$$

leading to

$$|\bar{\mathcal{M}}(q \to \nu\nu)|^2 = -2\mu^2 \,, \tag{6.15}$$

which does not depend on the integrated momenta k, k' of the phase space factor $d\Pi_{\nu\nu}$. Hence, from the optical theorem

$$\mathrm{Im}\{\Delta(q)\} = -\mu^2 \int d\Pi_{\nu\nu} (2\pi)^4 \delta(q - k - k') = -\frac{\mu^2}{8\pi} \tag{6.16}$$

yielding

$$\rho(\mu^2) = \frac{\mu^2}{8\pi^2} \Theta(\mu^2) \,, \tag{6.17}$$

that must be explicitly accompanied by the Heaviside Θ-function.
Eventually, the integration dictated by eq. (6.10) returns

$$V(r) = -\frac{G_{\nu\nu}^2}{32\pi^3 r} \int_0^{\infty} d\mu^2 \mu^2 e^{-\mu r} = -\frac{3G_{\nu\nu}^2}{8\pi^3 r^5} \tag{6.18}$$

in agreement with eq. (6.8). Having discussed this methodology, we can move on to the study of other loop potentials generated by new light particles coupled to SM fermions.

6.2 Loop Potentials Between Unpolarized Fermions

In the limit of unpolarized non-relativistic nucleons, only scalar and vector currents are relevant, inducing four-nucleon scattering when closing the DM loop. Their interactions with dark particles of spin-$0, 1/2, 1$ in principle depend on the UV completion of the theory. Indeed, the underlying nature of the new candidate, as completely new particle or pNGB of a spontaneously broken symmetry, is directly reflected into the type of Lagrangian taken into consideration. The main features of the final potentials, useful to check the rightness of the calculations, can be understood from dimensional analysis and the optical theorem [59]. The former shows the radial scaling in the long-range limit while the latter dictates the sign of the discontinuity over the branch cut and thus the sign of the potentials. The results presented in the first Section are in agreement with Ref. [60, 15], while the end of the Chapter extends some results present in Ref. [61].

6.2.1 Scalar Currents

The first type of interactions to be studied are between scalar currents of SM fermions. The dispersion theory treatment involves the analysis of the imaginary part of $\mathcal{M}$ across its branch cut. It turns out [59] that is already possible to establish some properties even before the computations. Indeed, dimensional analysis and the optical theorem impose an overall negative sign of the potentials (apart from those of the couplings), for the interaction between scalar currents mediated by any type of operators. Let us now verify it in the analysis.

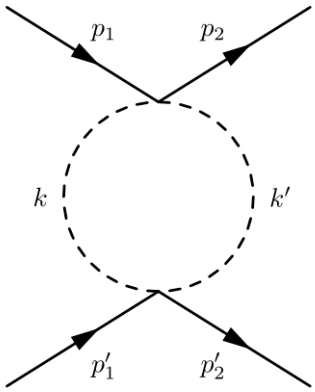

Figure 6.2: Loop diagram for a double scalar exchange.

Double Scalar Exchange

Consider the exchange of a scalar particle of mass M given by the operator

$$\mathcal{L}_{int} = -\sum_{i=1}^{2} \frac{G_i^\phi}{2} \bar{\psi}_i \psi_i \phi^2 \ , \quad [G_i^\phi] = -1 \tag{6.19}$$

described by the t-channel diagram in fig. (6.2).
The Feynman amplitude is

$$i\mathcal{M} = -\frac{G_1^\phi G_2^\phi}{4} \bar{u}_r(p_2) u_s(p_1) i\Delta(q) \bar{u}_{r'}(p_2') u_{s'}(p_1') \simeq -\frac{G_1^\phi G_2^\phi}{4} i\Delta(q) \,, \tag{6.20}$$

from which

$$V(r) = -\frac{G_1^\phi G_2^\phi}{16\pi r} \int_0^\infty d\mu^2 \rho(\mu^2)\, e^{-\mu r} \,. \tag{6.21}$$

Considering the cutted amplitude $\mathcal{M}(q \to \phi\phi)$ and taking into account the indistinguishability of the scalar mediators in the phase factor $d\Pi_{\phi\phi}$

$$|\bar{\mathcal{M}}(q \to \phi\phi)|^2 = 4 \implies \rho(\mu^2) = \frac{1}{8\pi^2} \sqrt{1 - \frac{4M^2}{\mu^2}} \Theta(\mu^2 - 4M^2) \,. \tag{6.22}$$

Thus, the potential is

$$\begin{aligned} V(r) &= -\frac{G_1^\phi G_2^\phi}{128\pi^3 r} \int_{4M^2}^\infty d\mu^2 \sqrt{1 - \frac{4M^2}{\mu^2}}\, e^{-\mu r} = \\ &= -\frac{G_1^\phi G_2^\phi}{64\pi^3 r^3} x K_1(x) \end{aligned} \tag{6.23}$$

where K_n are the modified Bessel functions of the second kind and index n, while $x \equiv 2Mr$ is an adimensional variable.

Double Spinor Exchange

The next step is to generalize the results from the neutrino exchange using massive spinor mediators with $m \neq 0$. From the interacting Lagrangian

$$\mathcal{L}_{int} = -\sum_{i=1}^{2} G_i^\chi \bar{\psi}_i \psi_i \bar{\chi}\chi \ , \quad [G_i^\chi] = -2 \,, \tag{6.24}$$

the t-channel amplitude is

$$i\mathcal{M} = G_1^\chi G_2^\chi \bar{u}_r(p_2) u_s(p_1) i\Delta(q) \bar{u}_{r'}(p_2') u_{s'}(p_1') \simeq G_1^\chi G_2^\chi i\Delta(q)\,, \tag{6.25}$$

leading to

$$V(r) = \frac{G_1^\chi G_2^\chi}{4\pi r} \int_0^\infty d\mu^2\, \rho(\mu^2)\, e^{-\mu r}\,. \tag{6.26}$$

The cutted amplitude of eq. (6.13) now generalizes to

$$|\bar{\mathcal{M}}(q \to \nu\nu)|^2 = 4[(k\cdot k') + M^2] = 2\left(4M^2 - \mu^2\right) \tag{6.27}$$

where $k\cdot k' = M^2 - \mu^2/2$. Hence the spectral function becomes

$$\rho(\mu^2) = \frac{M^2}{2\pi^2}\sqrt{1-\frac{4M^2}{\mu^2}}\left(1-\frac{\mu^2}{4M^2}\right)\Theta(\mu^2-4M^2)\,. \tag{6.28}$$

The generalized potential for an exchange of two fermions is then

$$\begin{aligned} V(r) &= \frac{G_1^\chi G_2^\chi M^2}{8\pi^3 r}\int_{4M^2}^\infty d\mu^2 \left(1-\frac{\mu^2}{4M^2}\right)\sqrt{1-\frac{4M^2}{\mu^2}}\, e^{-\mu r} = \\ &= -\frac{3G_1^\chi G_2^\chi}{16\pi^3 r^5} x^2 K_2(x)\,. \end{aligned} \tag{6.29}$$

Note that for $M \to 0$ the expression above coincides with eq. (6.8), since $x^2K_2(x) \xrightarrow{x\to 0} 2$.

Double Gauge Boson Exchange

The double gauge boson exchange is described by the effective operator

$$\mathcal{L}_{int} = -\sum_{i=1}^{2}\frac{G_i^X}{2}\bar{\psi}_i\psi_i X_\mu X^\mu \quad , \quad [G_i^X] = -1\,. \tag{6.30}$$

The associated amplitude is given by

$$i\mathcal{M} \simeq -iG_1^X G_2^X \Delta(q) \tag{6.31}$$

taking the general case of the gauge boson spectral representation. Denoting as $\varepsilon_\mu, \varepsilon_\nu^*$ the polarization vectors, the cutted amplitude is

$$\mathcal{M}(q \to XX) = i\eta^{\mu\alpha}\varepsilon_\mu(k)\varepsilon_\alpha^*(k')\,, \tag{6.32}$$

and thus

$$|\bar{\mathcal{M}}(q\to XX)|^2 = \eta^{\mu\alpha}\eta^{\nu\beta}\left(\eta_{\mu\nu}-\frac{k_\mu k_\nu}{M^2}\right)\left(\eta_{\alpha\beta}-\frac{k'_\alpha k'_\beta}{M^2}\right) = 2+\left(1-\frac{\mu^2}{2M^2}\right)^2\,. \tag{6.33}$$

With the same strategy of the previous cases, the spectral function

$$\rho(\mu^2) = \frac{1}{32\pi^2}\sqrt{1-\frac{4M^2}{\mu^2}}\left[2+\left(1-\frac{\mu^2}{2M^2}\right)^2\right]\Theta(\mu^2-4M^2) \tag{6.34}$$

produces the following potential

$$\begin{aligned} V(r) &= -\frac{G_1^X G_2^X}{32\pi^3 r}\int_{4M^2}^\infty d\mu^2\left[2+\left(1-\frac{\mu^2}{2M^2}\right)^2\right]\sqrt{1-\frac{4M^2}{\mu^2}}\, e^{-\mu r} = \\ &= -\frac{3G_1^X G_2^X}{4\pi^3 r^3}\left(\frac{5}{x}+\frac{x}{4}\right)K_3(x)\,. \end{aligned} \tag{6.35}$$

Scaling of the Potentials

Consider the general $n+4$-dimensional operators

$$\mathcal{L}_{int} \supset \frac{1}{\Lambda^n}\mathcal{O}_{2DS}\bar{\psi}\Gamma\psi \tag{6.36}$$

where ψ is the field associated to the SM external fermions and $\mathcal{O}_{2DS}$ are the operators describing the dark fields inside the loop.
Being interested in very light particles, e.g. $m_{DS} \simeq 10^{-5}$eV, the associated non-relativistic potential can be expanded for $r \ll 1/m_{DS}$. From the presence of two vertices in the scattering process, an estimate of the specific dependencies of the potential is derived from naive dimensional analysis as

$$V(r) \simeq \frac{1}{\Lambda^{2n}}\frac{1}{r^{2n+1}} \tag{6.37}$$

since $[U]=1$ and Λ is the UV cutoff. This behaviour is evident in the results obtained so far

$$\begin{aligned} V_{\phi\phi}(r) &= -\frac{G_1^\phi G_2^\phi}{64\pi^3}\frac{x}{r^3}K_1(x)\,, \\ V_{\chi\chi}(r) &= -\frac{3G_1^\chi G_2^\chi}{16\pi^3 r^5}x^2 K_2(x)\,, \\ V_{XX}(r) &= -\frac{3G_1^X G_2^X}{4\pi^3 r^3}\left(\frac{5}{x}+\frac{x^2}{4}\right)K_2(x)\,, \end{aligned} \tag{6.38}$$

with

$$x = 2m_{DS}r \;\;,\quad [G_i^\phi] = [G_i^X] = -1 \;\;,\quad [G_i^\chi] = -2\,, \tag{6.39}$$

and hence

$$x \sim \mathcal{O}(1) \;\;,\quad G_i^\phi \sim G_i^X \sim 1/\Lambda \;\;,\quad G_i^\chi \sim 1/\Lambda^2\,. \tag{6.40}$$

The potentials obtained so far scale as

- $V_{\phi\phi}(r), V_{XX}(r) \sim 1/r^3$ since the operators have dimension $4+1$;
- $V_{\chi\chi}(r) \sim 1/r^5$ since the operator has dimension $4+2$.

Double pNGB Exchange

Scalar fields can occur in the form of Goldstone bosons, interacting through derivative interaction as given by the operator

$$\mathcal{L}_{int} = -\sum_{i=1}^{2}\frac{G_i^D}{2}\bar{\psi}_i\psi_i\partial^\mu\phi\partial_\mu\phi \;\;,\quad [G_i^D] = -3 \tag{6.41}$$

giving the amplitude

$$i\mathcal{M} \simeq -\frac{G_1^D G_2^D}{4}i\Delta(q)\,. \tag{6.42}$$

The dispersion theory approach produces the following cut

$$\mathcal{M}(q\to\phi\phi) = 2(k\cdot k') \implies |\bar{\mathcal{M}}(q\to\phi\phi)|^2 = 4M^4\left(1-\frac{\mu^2}{2M^2}\right)^2 \tag{6.43}$$

so, the spectral function results in

$$\rho(\mu^2) = \frac{M^4}{4\pi^2}\left(1-\frac{\mu^2}{2M^2}\right)^2\sqrt{1-\frac{4M^2}{\mu^2}}\Theta\left(\mu^2-4M^2\right)\,. \tag{6.44}$$

The potential yields to

$$\begin{aligned} V(r) &= -\frac{G_1^D G_2^D M^4}{64\pi^3 r}\int_{4M^2}^{\infty}d\mu^2\,\left(1-\frac{\mu^2}{2M^2}\right)^2\sqrt{1-\frac{4M^2}{\mu^2}}e^{-\mu r} = \\ &= -\frac{G_1^D G_2^D x^2}{16\pi^3 r^7}\left[\frac{1}{8}x\left(15+\frac{1}{4}x^2\right)K_1(x)+\frac{1}{2}\left(15+\frac{3}{4}x^2\right)K_2(x)\right] \end{aligned} \tag{6.45}$$

Mixed Vector-pNGB Exchange

Another type of loop exchange comes from the union of two vertices in which the fermionic current interacts with a pNGB and a gauge field, as given by the following operator

$$\mathcal{L}_{int} = -\sum_{i=1}^{2} G_i^M \bar{\psi}_i \psi_i X^\mu \partial_\mu \pi \ , \quad [G_i^M] = -2 \tag{6.46}$$

giving back the amplitude

$$i\mathcal{M} \simeq -iG_1^M G_2^M \Delta(q) \, . \tag{6.47}$$

Solving within the optical theorem leads to

$$\mathcal{M}(q \to X\pi) = -\eta^{\mu\nu}\varepsilon_\mu(k)k'_\nu \implies |\bar{\mathcal{M}}(q \to X\pi)|^2 = M^2 \left(\frac{\mu^4}{4M^4} - \frac{\mu^2}{M^2} \right) \tag{6.48}$$

and to the spectral function

$$\rho(\mu^2) = \frac{M^2}{16\pi^2} \sqrt{1 - \frac{4M^2}{\mu^2}} \left(\frac{\mu^4}{4M^4} - \frac{\mu^2}{M^2} \right) \Theta\left(\mu^2 - 4M^2\right) \, . \tag{6.49}$$

The general case when $m_\pi \neq M$ yields to a difficult integral to deal with. However, under the assumption $m_\pi = M$, the potential can be obtained as

$$\begin{aligned} V(r) &= -\frac{G_1^M G_2^M M^2}{64\pi^3 r} \int_{4M^2}^{\infty} d\mu^2 \left(\frac{\mu^4}{4M^2} - \frac{\mu^2}{M^2} \right) \sqrt{1 - \frac{4M^2}{\mu^2}} \, e^{-\mu r} = \\ &= -\frac{G_1^M G_2^M}{32\pi^3 r^5} \left[\frac{15}{2} x K_1(x) + 2 \left(15 + \frac{3}{4} x^2 \right) 3K_2(x) \right] \, . \end{aligned} \tag{6.50}$$

6.2.2 Vector Currents

A second type of scattering involve two vector currents composed of SM fermions. The application of the optical theorem and dimensional analysis now imposes an overall positive sign.

4-Fermion Vector Interaction

In the case of vector-type interaction, let us consider the operator

$$\mathcal{L}_{int} = -\sum_{i=1}^{2} G_i^V \bar{\psi}_i \gamma^\mu \psi_i \bar{\chi} \gamma_\mu \chi \ , \quad [G_i^V] = -2 \, , \tag{6.51}$$

which yields

$$i\mathcal{M} = G_1^V G_2^V \bar{u}_r(p_2)\gamma_\mu u_s(p_1) i\Delta^{\mu\nu}(q) \bar{u}_{r'}(p'_2)\gamma_\nu u_{s'}(p'_1) \simeq iG_1^V G_2^V \Delta_{00}(q) \, . \tag{6.52}$$

The cut of $\mathcal{M}^{\mu\nu}(q \to \bar{\chi}\chi)$ produces the unpolarized squared amplitude

$$|\bar{\mathcal{M}}^{\mu\nu}(q \to \bar{\chi}\chi)|^2 = \mathrm{Tr}[(\not{k}' - M)\gamma^\mu(\not{k} + M)\gamma^\nu] \tag{6.53}$$

whose temporal component reads

$$|\bar{\mathcal{M}}^{00}(q \to \bar{\chi}\chi)|^2 = 8(k^0 k'^0 - M^2 + \frac{\mu^2}{4}) \, , \tag{6.54}$$

so it is required an integration of $k^0 k'^0$ into the 2-body phase space. The phase space integration yields

$$\int \frac{d^3k d^3k'}{(2\pi)^6 2k^0 2k'^0} (2\pi)^4 \delta^4(q - k - k') k^0 k'^0 = \frac{\mu^2}{32\pi} \sqrt{1 - \frac{4M^2}{\mu^2}} \, , \tag{6.55}$$

leading to the spectral function

$$\rho(\mu^2) = -\frac{M^2}{2\pi^2}\sqrt{1-\frac{4M^2}{\mu^2}}\left(1-\frac{2\mu^2}{4M^2}\right)\Theta(\mu^2-4M^2)\,. \tag{6.56}$$

This results into the following potential

$$\begin{aligned} V(r) &= -\frac{G_1^V G_2^V M^2}{8\pi^3 r}\int_{4M^2} d\mu^2\left(1-\frac{2\mu^2}{4M^2}\right)\sqrt{1-\frac{4M^2}{\mu^2}}\,e^{-\mu r} = \\ &= \frac{G_1^V G_2^V}{8\pi^3 r^5}\left(\frac{x^3}{2}K_1(x)+3x^2K_2(x)\right)\,. \end{aligned} \tag{6.57}$$

4-Fermion Vector-Axial Interaction

SM vector currents could also interact via dark axial currents in loop diagram originating from the operator

$$\mathcal{L}_{int} = -\sum_{i=1}^{2} G_i^A \bar{\psi}_i\gamma^\mu\psi_i\bar{\chi}\gamma_\mu\gamma^5\chi \tag{6.58}$$

giving the amplitude

$$i\mathcal{M} = iG_1^A G_2^A \bar{u}_r(p_2)\gamma_\mu u_s(p_1)\Delta^{\mu\nu}(q)\bar{u}_{r'}(p_2')\gamma_\nu u_{s'}(p_1') \simeq iG_1^A G_2^A\Delta^{00}(q)\,, \tag{6.59}$$

where now there are two insertion of γ^5 into $\mathcal{M}^{\mu\nu}(q\to\bar{\chi}\chi)$ which swaps the sign of the mass term inside the trace, so

$$|\mathcal{M}^{\mu\nu}(q\to\bar{\chi}\chi)|^2 = \mathrm{Tr}[\not{k}'\gamma^\mu\not{k}\gamma^\nu] + M^2\mathrm{Tr}[\gamma^\mu\gamma^\nu] \implies |\bar{\mathcal{M}}^{00}(q\to\bar{\chi}\chi)|^2 = 8\left(k^0k'^0+\frac{\mu^2}{4}\right)\,. \tag{6.60}$$

Following the same steps as in the previous Section, the spectral function is slightly modified into

$$\rho(\mu^2) = \frac{\mu^2}{4\pi^2}\sqrt{1-\frac{4M^2}{\mu^2}}\Theta(\mu^2-4M^2)\,. \tag{6.61}$$

which yields

$$\begin{aligned} V(r) &= \frac{G_1^A G_2^A}{16\pi^3 r}\int_{4M^2} d\mu^2\mu^2\sqrt{1-\frac{4M^2}{\mu^2}}\,e^{-\mu r} = \\ &= \frac{G_1^A G_2^A}{8\pi^3 r^5}\left(x^3K_1(x)+3x^2K_2(x)\right)\,. \end{aligned} \tag{6.62}$$

6.3 Loop Potentials Between Polarized Fermions

An additional class of potentials can be derived in a straightforward way from the previous analysis. To study the interactions with polarized currents, e.g. pseudo-scalar bilinears, the loop structure remains unaltered while what changes are the external currents. Indeed, all the amplitude involving scalar vertices are written as

$$\mathcal{M} \propto \bar{u}_r(p_2)u_s(p_1)\Delta(q)\bar{u}_{r'}(p_2')u_{s'}(p_1') \tag{6.63}$$

in which the loop behaviour is enconded inside the effective propagator $\Delta(q)$. To extend the treatment, it is sufficient to introduce the linear combination of currents

$$J_i^a \equiv \bar{\psi}_i(G_i^{a,S} + iG_i^{a,PS}\gamma^5)\psi_i\,, \tag{6.64}$$

where $i=1,2$ points to the external fermion and $a=\phi,\chi,X$ represents the type of light mediator. The amplitudes stemming from eq. (6.63) yields a non-relativistic potential proportional to

$$V(r) \propto \frac{1}{4\pi r}\int_0^\infty d\mu^2\,\rho(\mu^2)\,e^{-\mu r}\,, \tag{6.65}$$

since the LO non-relativistic expansion of the external scalar bilinear results in a Kronecker delta for the spin polarizations. If instead one wants to extract the potential with a mixture of scalar and pseudo-scalar currents, it is sufficient to replace a bilinear form and perform the calculation directly from the scalar results. With a pseudo-scalar current for the first fermion, the functional form of the potentials computed in the previous Section reads

$$V(r) \propto \frac{\boldsymbol{\sigma}\cdot\boldsymbol{\nabla}}{8\pi m_1 r}\int_0^\infty d\mu^2\,\rho(\mu^2)\,e^{-\mu r}\,, \tag{6.66}$$

apart for an overall factor. Following this observation, it is hence straightforward to derive the potentials below:

- Double scalar exchange

$$V(r) = -\frac{G_1^{\phi,PS}G_2^{\phi,S}}{256\pi^3 m_1 r^4}\left[4xK_1(x) + x^2(K_0(x)+K_2(x))\right](\boldsymbol{\sigma}\cdot\hat{\mathbf{r}})\,; \tag{6.67}$$

- Double spinor exchange

$$V(r) = -\frac{3G_1^{\chi,PS}G_2^{\chi,S}}{32\pi^3 m_1 r^6}\left[3x^2K_2(x) + \frac{1}{2}x^3(K_1(x)+K_3(x))\right](\boldsymbol{\sigma}\cdot\hat{\mathbf{r}})\,; \tag{6.68}$$

- Double vector boson exchange

$$V(r) = -\frac{3G_1^{X,PS}G_2^{X,S}}{8\pi^3 m_1 r^4}\left[\left(5+\frac{1}{4}x^3\right)K_1(x) + \frac{6}{x}\left(5+\frac{1}{8}x^3\right)K_2(x)\right](\boldsymbol{\sigma}\cdot\hat{\mathbf{r}})\,; \tag{6.69}$$

- Double Goldstone boson exchange

$$V(r) = -\frac{G_1^{D,PS}G_2^{D,S}}{32\pi^3 m_1 r^8}\left[\frac{x^2}{4}\left(105+\frac{15}{2}x^2+\frac{x^4}{16}\right)K_0(x) + \frac{15}{2}x\left(14+\frac{11}{4}x^2+\frac{x^4}{16}\right)K_1(x)\right](\boldsymbol{\sigma}\cdot\hat{\mathbf{r}})\,; \tag{6.70}$$

- Mixed Goldstone boson - vector boson exchange (with degenerate mass)

$$V(r) = -\frac{G_1^M G_2^M}{32\pi^3 m_1 r^6}\left[15\left(7+\frac{1}{2}x^2\right)K_0(x) - \frac{3}{x}\left(70+\frac{55}{4}x^2+\frac{1}{4}x^4\right)K_2(x)\right](\boldsymbol{\sigma}\cdot\hat{\mathbf{r}})\,. \tag{6.71}$$

CHAPTER 7

TOWARDS A MODEL-INDEPENDENT APPROACH

In the previous Chapters we always assumed a simplified model, with the exchange of a new light particle, in order to compute the non-relativistic potentials. A more model-independent approach exploits instead rotational invariance, that is the relevant symmetry in the non-relativistic case, in which the scattering amplitudes can be expressed in terms of scalar invariants formed out of the external spins $\boldsymbol{\sigma}$,$\boldsymbol{\sigma}'$ and momenta $\mathbf{p}_i$. Dealing with elastic scattering $q^0 = 0$, in the center of mass reference frame the only two independent momenta are

$$\begin{cases} \mathbf{q} = \mathbf{p}_2 - \mathbf{p}_1 \\ \mathbf{P} = \dfrac{\mathbf{p}_1 + \mathbf{p}_2}{2} \end{cases} , \tag{7.1}$$

which correspond respectively to the transferred momentum and the average momentum of the scattered fermion. Two spins and two momenta lead to 16 independent scalar combinations [12] that include all possible spin configurations:

$$\begin{aligned} &\mathcal{O}_1 = 1\,; \\ &\mathcal{O}_2 = \boldsymbol{\sigma}\cdot\boldsymbol{\sigma}'\,; \\ &\mathcal{O}_3 = \frac{1}{m_f^2}(\boldsymbol{\sigma}\cdot\mathbf{q})(\boldsymbol{\sigma}'\cdot\mathbf{q})\,; \\ &\mathcal{O}_{4,5} = \frac{i}{2m_f}(\boldsymbol{\sigma}\pm\boldsymbol{\sigma}')\cdot(\mathbf{P}\times\mathbf{q})\,; \\ &\mathcal{O}_{6,7} = \frac{i}{2m_f^2}\left[(\boldsymbol{\sigma}\cdot\mathbf{P})(\boldsymbol{\sigma}'\cdot\mathbf{q}) \pm (\boldsymbol{\sigma}'\cdot\mathbf{P})(\boldsymbol{\sigma}\cdot\mathbf{q})\right]\,; \\ &\mathcal{O}_8 = \frac{1}{m_f^2}(\boldsymbol{\sigma}\cdot\mathbf{P})(\boldsymbol{\sigma}'\cdot\mathbf{P})\,; \\ &\mathcal{O}_{9,10} = \frac{i}{2m_f}(\boldsymbol{\sigma}\pm\boldsymbol{\sigma}')\cdot\mathbf{q}\,; \\ &\mathcal{O}_{11} = \frac{i}{m_f}(\boldsymbol{\sigma}\times\boldsymbol{\sigma}')\cdot\mathbf{q}\,; \end{aligned} \tag{7.2}$$

$$\begin{aligned}
\mathcal{O}_{12,13} &= \frac{1}{2m_f}(\boldsymbol{\sigma} \pm \boldsymbol{\sigma}') \cdot \mathbf{P}\,; \\
\mathcal{O}_{14} &= \frac{1}{m_f}(\boldsymbol{\sigma} \times \boldsymbol{\sigma}') \cdot \mathbf{P}\,; \\
\mathcal{O}_{15} &= \frac{1}{2m_f^3}\Big\{(\boldsymbol{\sigma} \cdot \mathbf{q})\big[\boldsymbol{\sigma}' \cdot (\mathbf{P} \times \mathbf{q})\big] + (\boldsymbol{\sigma}' \cdot \mathbf{q})\big[\boldsymbol{\sigma} \cdot (\mathbf{P} \times \mathbf{q})\big]\Big\}\,; \\
\mathcal{O}_{16} &= \frac{1}{2m_f^3}\Big\{(\boldsymbol{\sigma} \cdot \mathbf{P})\big[\boldsymbol{\sigma}' \cdot (\mathbf{P} \times \mathbf{q})\big] + (\boldsymbol{\sigma}' \cdot \mathbf{P})\big[\boldsymbol{\sigma} \cdot (\mathbf{P} \times \mathbf{q})\big]\Big\}\,.
\end{aligned} \tag{7.3}$$

The above operators are divided into parity-even and parity-odd based on the powers of momenta, while the mass normalization guarantees the adimensionality. All possible operators that are generated by the non-relativistic expansion of a given scattering amplitude must therefore be a linear combination of $\mathcal{O}_i(\mathbf{q}, \mathbf{P})$, up to coefficients that may depend on the momenta only through $|\mathbf{q}|^2$ or $|\mathbf{P}|^2$.
Focusing on the form of amplitude, an important role is played by the type of exchanged boson. For instance, the long-range nature of the Coulomb law is a consequence of the specific structure of the photon propagator. More in general, within a Lorentz invariant QFT the common denominator among all propagators is denoted as

$$D(|\mathbf{q}^2|) \equiv -\frac{1}{\mathbf{q}^2 + M^2}\,, \tag{7.4}$$

and is responsible for the Yukawa-like behaviour of the potentials in Chapters (4,5), while powers of $\mathbf{q}$ at the numerator allows the extraction of its derivatives. It is then possible to write a complete general scattering amplitude in the momentum space as

$$\mathcal{M}(\mathbf{q}, \mathbf{P}_i) = D(\mathbf{q}^2) \sum_{i=1}^{16} \mathcal{O}_i(\mathbf{q}, \mathbf{P}) f_i\left(\frac{|\mathbf{q}|^2}{m_f^2}, \frac{|\mathbf{P}|^2}{m_f^2}\right)\,, \tag{7.5}$$

with f_i adimensional scalar polynomials of $|\mathbf{q}|^2, |\mathbf{P}|^2$ that contain also the various couplings. This is a general result based only on the assumption of rotational invariance.
The physical interpretation for $\mathcal{O}_i$ in the position space is given by the Fourier transform of the non-relativistic amplitude, as dictated in the Born approximation, in which the final potentials ultimately depend on both $r = |\mathbf{x}|$ and $\boldsymbol{v} = \mathbf{P}/m_f$. Powers of $|\mathbf{q}|^2/m_f^2$ in the polynomial lead to powers of M/m_f and $1/(m_f r)$ in the final results, denoted collectively for now as ε. At macroscopic scales $r \sim$ cm and $\varepsilon \sim 10^{-12}$, therefore it is customary to include only the $|\mathbf{q}|^2 = 0$ pieces of f_i at the LO. However, to keep the discussion as general as possible we include also these extremely small quantities which often multiply singular contact terms, as $\delta(r)$ and its derivatives. Regarding the operators $\mathcal{O}_i$, it is worth to notice that $\mathcal{O}_{1,2}$, $\mathcal{O}_i$ with $i = 9, 10, 11$ have effects of order ε, $i = 12, 13, 14$ of order $|\boldsymbol{v}|$ while the remaining ones have effects suppressed by higher powers of ε and $|\boldsymbol{v}|$.
The potentials between two fermions induced by a Lorentz-invariant boson exchange is then written as

$$V(r, \boldsymbol{v}) = \sum_{i=1}^{16} f_i(\varepsilon, |\boldsymbol{v}|^2)\mathcal{V}_i(\mathbf{x}, \boldsymbol{v}) \tag{7.6}$$

where the basis on which the expansion is made is given by

$$\mathcal{V}_i(\mathbf{x}, \boldsymbol{v}) = -\int \frac{d^3q}{(2\pi)^3} D(|\mathbf{q}|^2)\mathcal{O}_i(\mathbf{q}, \mathbf{P})\, e^{i\mathbf{q}\cdot\mathbf{x}}\,. \tag{7.7}$$

Defining the exponential suppression as the function

$$E(r) = \frac{e^{-Mr}}{4\pi}\,, \tag{7.8}$$

the resulting spin-dependent components $\mathcal{V}_i(r, \boldsymbol{v})$ are the following:

$$
\begin{aligned}
&\mathcal{V}_1 = \frac{E(r)}{r}\,;\\
&\mathcal{V}_2 = (\boldsymbol{\sigma}\cdot\boldsymbol{\sigma}')\frac{E(r)}{r}\,;\\
&\mathcal{V}_3 = \frac{1}{m_f^2 r^3}\left[(\boldsymbol{\sigma}\cdot\boldsymbol{\sigma}')\left(1 - r\frac{d}{dr} + \frac{4\pi r^3}{3}\delta^3(\mathbf{x})\right) - 3(\boldsymbol{\sigma}\cdot\hat{\mathbf{r}})(\boldsymbol{\sigma}'\cdot\hat{\mathbf{r}})\left(1 - r\frac{d}{dr} + \frac{r^2}{3}\frac{d^2}{dr^2}\right)\right]E(r)\,;\\
&\mathcal{V}_{4,5} = -\frac{1}{2m_f r^2}(\boldsymbol{\sigma}\pm\boldsymbol{\sigma}')\cdot(\boldsymbol{v}\times\hat{\mathbf{r}})\left(1 - r\frac{d}{dr}\right)E(r)\,;\\
&\mathcal{V}_{6,7} = -\frac{1}{2m_f r^2}\left[(\boldsymbol{\sigma}\cdot\boldsymbol{v})(\boldsymbol{\sigma}'\cdot\hat{\mathbf{r}}) \pm (\boldsymbol{\sigma}'\cdot\boldsymbol{v})(\boldsymbol{\sigma}\cdot\hat{\mathbf{r}})\right]\left(1 - r\frac{d}{dr}\right)E(r)\,;\\
&\mathcal{V}_8 = (\boldsymbol{\sigma}\cdot\boldsymbol{v})(\boldsymbol{\sigma}'\cdot\boldsymbol{v})\frac{E(r)}{r}\,;\\
&\mathcal{V}_{9,10} = -\frac{1}{2m_f r^2}(\boldsymbol{\sigma}\pm\boldsymbol{\sigma}')\cdot\hat{\mathbf{r}}\left(1 - r\frac{d}{dr}\right)E(r)\,;\\
&\mathcal{V}_{11} = -\frac{1}{m_f r^2}(\boldsymbol{\sigma}\times\boldsymbol{\sigma}')\cdot\boldsymbol{v}\,E(r)\,;\\
&\mathcal{V}_{12,13} = (\boldsymbol{\sigma}\pm\boldsymbol{\sigma}')\cdot\boldsymbol{v}\,\frac{E(r)}{2r}\,;\\
&\mathcal{V}_{14} = (\boldsymbol{\sigma}\times\boldsymbol{\sigma}')\cdot\boldsymbol{v}\,\frac{E(r)}{r}\,;\\
&\mathcal{V}_{15} = \frac{1}{2m_f r^3}\Bigg\{\Big[\boldsymbol{\sigma}\cdot(\boldsymbol{\sigma}'\times\boldsymbol{v}) + \boldsymbol{\sigma}'\cdot(\boldsymbol{\sigma}\times\boldsymbol{v})\Big]\left(1 - r\frac{d}{dr} + \frac{4\pi r^3}{3}\delta^3(\mathbf{x})\right) +\\
&\qquad\qquad - 3\Big[(\boldsymbol{\sigma}\cdot\hat{\mathbf{r}})(\boldsymbol{\sigma}'\times\boldsymbol{v})\cdot\hat{\mathbf{r}} + (\boldsymbol{\sigma}'\cdot\hat{\mathbf{r}})(\boldsymbol{\sigma}\times\boldsymbol{v})\cdot\hat{\mathbf{r}}\Big]\left(1 - r\frac{d}{dr} + \frac{r^2}{3}\frac{d^2}{dr^2}\right)\Bigg\}E(r)\,;\\
&\mathcal{V}_{16} = -\frac{1}{2m_f r^2}\Big\{\Big[\boldsymbol{\sigma}\cdot(\boldsymbol{v}\times\hat{\mathbf{r}})\Big](\boldsymbol{\sigma}'\cdot\boldsymbol{v}) + \Big[\boldsymbol{\sigma}'\cdot(\boldsymbol{v}\times\hat{\mathbf{r}})\Big](\boldsymbol{\sigma}\cdot\boldsymbol{v})\Big\}\left(1 - r\frac{d}{dr}\right)E(r)\,.
\end{aligned}
\tag{7.9}
$$

The basis found here is in agreement with Ref. [12], except for $\mathcal{V}_{15}$ which has a different functional form. In general, each of these potentials has an arbitrary coefficient, which can be constrained by the experimental search of new macroscopic forces.

7.1 Comparison with Simplified Models

In Chapter (4), the main potentials present in literature have been derived and corrected. From the rotational invariance, all the operator structures of eq. (7.2) appear inside the non-relativistic LO amplitudes.
Axion-like interactions give rise to:

- $\mathcal{V}_1$ for the scattering between scalar currents in eq. (4.7);
- $\mathcal{V}_{9,10}$ considering the mix of scalar and pseudo-scalar sources in eq. (4.10);
- $\mathcal{V}_3$ that describes entirely the dipole-dipole potential of eq. (4.14).

The vector boson exchange is responsible for the appearance of:

- $\mathcal{V}_{1,2,3}$ in the derivation of the Coulomb potential of eq. (4.19);
- $\mathcal{V}_{11,12,13}$ when a mixture of vector and axial sources interact via eq. (4.27);
- $\mathcal{V}_{2,3}$ in the potential between axial currents of eq. (4.30).

The derivative couplings of the field strength lead to:

- $\mathcal{V}_{2,3}$ for the potential between tensor currents in eq. (4.36);
- $\mathcal{V}_{9,10,14,15}$ considering a mixture of tensor and pseudo-tensor currents in eq. (4.39);
- $\mathcal{V}_3$ in eq. (4.48) for the potential acting between pseudo-tensor bilinears.

Note that not all possible model-independent structures emerged, in particular $\mathcal{V}_i$ with $i = 4, 5, 6, 7, 8, 16$. However, it is sufficient to go beyond the LO order in the non-relativistic expansion in order to find all of them. The following matching focuses only on the next order of the expansion of Chapter (5) within the elastic limit:

- $\mathcal{V}_{4,5}$, $\mathcal{V}_{15}$ and $\mathcal{V}_3$ arise for the scalar-mediated potentials respectively in eq. (5.19,5.25,4.14) (the last one remains unaltered due to the elastic exactness);
- $\mathcal{V}_{1,4,5}$, $\mathcal{V}_{1,11,12,13,16}$ and $\mathcal{V}_{2,3,4,5,8}$ are obtained respectively in the interactions of eq. (5.31,5.40,5.36);
- $\mathcal{V}_{1,\dots,8}$, $\mathcal{V}_{9,10,14,15,16}$ and $\mathcal{V}_{2,3,4,5,8}$ correspondingly to eq. (C.3,C.9,C.7).

Coming instead to the loop potentials of Chapter (6), operators with dimension greater than 4 can be added to describe scattering processes mediated by a pair of new particles. The simplest interactions are constructed through a vertex of four particles, two of them from the new sectors while the others are the scattered fermions. Among the external currents analyzed, we focused on

- unpolarized scalar sources that modify the Yukawa structure and proportional to $\mathcal{V}_1$;
- interactions with one polarized pseudo-scalar source written via $\mathcal{V}_{9,10}$;
- two polarized objects which, although not expicitly calculated, return $\mathcal{V}_3$.

CHAPTER 8

CONCLUSIONS

In this thesis we provided a critical re-examination of the calculation of non-relativistic potentials mediated by new light particles coupled to SM fermions. Within a general class of simplified models, we have reproduced and integrated some results present in the literature, also going beyond the conventional leading order Born approximation.

Key findings and contributions include:

1. In Chapter 4 we highlighted discrepancies in the current literature concerning the calculation of tree-level potentials, presenting a comparison with previous works in Section 4.2.
2. A significant outcome was the calculation in Chapter 5 of tree-level potentials that go beyond the leading order in the non-relativistic expansion. Notably, the presence of new contact terms, proportional to the Dirac's delta function, provides potential contributions that might be more dominant than previously considered long-range leading-order terms.
3. In Chapter 6 we computed loop-mediated potentials, extending some previous results, while Chapter 7 provided a comparison of our results, obtained within a general class of simplified models, with a more model-independent approach for the classification of non-relativistic potentials.

Undoubtedly, Point 2 represents the most relevant outcome of this thesis. Delving into the phenomenological implications of the new contact terms, that emerge in the next-to-leading order potentials, offers an interesting direction for future work.

Appendices

APPENDIX A

CONVENTIONS AND EXPANSIONS

A.1 Spinors and Bilinear Forms

The Dirac equations in momentum space [62] for the spinors with positive and negative energy, polarization r, mass m and 4-momentum p are

$$\begin{aligned}(\not{p} - m)u_r(p) = 0 \\ (\not{p} + m)v_r(p) = 0\end{aligned} \tag{A.1}$$

from which we can obtain the explicit expression of the spinors in terms of the unit vectors φ_r

$$\begin{aligned}u_r(p) &= \frac{\not{p} + m}{\sqrt{2m(E_{\mathbf{p}} + m)}} \begin{pmatrix}\varphi_r \\ \mathbf{0}\end{pmatrix} = \frac{1}{\sqrt{2m(E_{\mathbf{p}} + m)}} \begin{pmatrix}(E_{\mathbf{p}} + m)\varphi_r \\ \mathbf{p}\cdot\boldsymbol{\sigma}\,\varphi_r\end{pmatrix} \\ v_r(p) &= \frac{-\not{p} + m}{\sqrt{2m(E_{\mathbf{p}} + m)}} \begin{pmatrix}\mathbf{0} \\ \varphi_r\end{pmatrix} = \frac{1}{\sqrt{2m(E_{\mathbf{p}} + m)}} \begin{pmatrix}\mathbf{p}\cdot\boldsymbol{\sigma}\,\varphi_r \\ (E_{\mathbf{p}} + m)\varphi_r\end{pmatrix}\end{aligned} , \tag{A.2}$$

where

$$\varphi_r = \begin{pmatrix}1 \\ 0\end{pmatrix} \quad \text{if} \quad r = 1 \ , \quad \varphi_r = \begin{pmatrix}0 \\ 1\end{pmatrix} \quad \text{if} \quad r = 2 \tag{A.3}$$

and $\boldsymbol{\sigma} = (\sigma^1, \sigma^2, \sigma^3)$ is the vector composed by the Pauli matrices. This normalization is chosen in such a way to include the factor $1/2m$ within the explicit expression of the Dirac spinor, otherwise in every expression of Chapter (3) involving the Feynman amplitude a factor $1/4m_1m_2$ has to be inserted. In the limit $|\mathbf{p}|^2 \ll m^2$ then

$$\sqrt{E_{\mathbf{p}} + m} = \sqrt{2m}\left[1 + \frac{|\mathbf{p}|^2}{8m^2} - \frac{5}{128}\frac{|\mathbf{p}|^4}{m^4} + \mathcal{O}\left(\frac{|\mathbf{p}|^6}{m^6}\right)\right] . \tag{A.4}$$

It is then useful to identify the following vector

$$\varphi_r^T \boldsymbol{\sigma} \varphi_s \equiv \boldsymbol{\sigma} \tag{A.5}$$

as a classical unit vector representing the spin of a given fermion.
The explicit representation of the Dirac matrices is given in the Dirac basis, i.e.

$$\gamma^0 = \begin{pmatrix}\mathbb{1} & 0 \\ 0 & -\mathbb{1}\end{pmatrix} \ , \quad \gamma^i = \begin{pmatrix}0 & \sigma^i \\ -\sigma^i & 0\end{pmatrix} \ , \quad \gamma^5 = \begin{pmatrix}0 & \mathbb{1} \\ \mathbb{1} & 0\end{pmatrix}, \tag{A.6}$$

while the bilinear forms are calculated from the vertex in fig. (A.1).

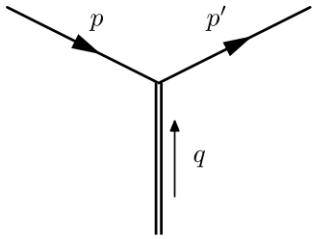

Figure A.1: Vertex of interaction.

Now we can proceed to calulate the non-relativistic expansion for various operators.
First, let us define the set of independent momenta that will be useful for the integrations

$$\begin{cases} q = p' - p \\ P = \dfrac{p + p'}{2} \end{cases} , \quad \begin{cases} p = P - \dfrac{q}{2} \\ p' = P + \dfrac{q}{2} \end{cases} . \tag{A.7}$$

The simplest type of bilinear form is given by the scalar current

$$\begin{aligned} \bar{u}_{r'}(p')u_r(p) &= \frac{1}{2m}\left[\sqrt{E_{\mathbf{p}'}+m}\sqrt{E_{\mathbf{p}}+m}\,\delta_{r,r'} - \varphi^T_{r'}\frac{(\mathbf{p}'\cdot\boldsymbol{\sigma})(\mathbf{p}\cdot\boldsymbol{\sigma})}{\sqrt{E_{\mathbf{p}}+m}\sqrt{E_{\mathbf{p}'}+m}}\varphi_r\right] = \\ &\simeq \left(1 + \frac{|\mathbf{p}|^2}{4m^2} - \frac{1}{4m^2}(\mathbf{p}\cdot\mathbf{p}')\right)\delta_{r,r'} + \frac{i}{4m^2}(\mathbf{p}\times\mathbf{p}')\cdot\boldsymbol{\sigma} + \mathcal{O}\left(\frac{|\mathbf{p}|^2}{m^2}\right) \\ &\simeq \left(1 + \frac{|\mathbf{q}|^2}{8m^2}\right)\delta_{r,r'} + \frac{i}{4m^2}(\mathbf{P}\times\mathbf{q})\cdot\boldsymbol{\sigma} + \mathcal{O}\left(\frac{|\mathbf{p}|^2}{m^2}\right) . \end{aligned} \tag{A.8}$$

The pseudoscalar one is exact at any order due to elastic scattering constraints

$$\begin{aligned} \bar{u}_{r'}(p')\gamma^5 u_r(p) &= \frac{1}{2m}\begin{pmatrix}\sqrt{E_{\mathbf{p}'}+m}\,\varphi^T_{r'} & \varphi^T_{r'}\frac{\mathbf{p}'\cdot\boldsymbol{\sigma}}{\sqrt{E_{\mathbf{p}'}+m}}\end{pmatrix}\gamma^0\gamma^5\begin{pmatrix}\sqrt{E_{\mathbf{p}}+m}\,\varphi_r \\ \frac{\mathbf{p}\cdot\boldsymbol{\sigma}}{\sqrt{E_{\mathbf{p}}+m}}\varphi_r\end{pmatrix} = \\ &= \frac{1}{2m}\varphi^T_{r'}\left(\mathbf{p}'\cdot\boldsymbol{\sigma} - \mathbf{p}\cdot\boldsymbol{\sigma}\right)\varphi_r \equiv -\frac{\mathbf{q}\cdot\boldsymbol{\sigma}}{2m} . \end{aligned} \tag{A.9}$$

Now for the vector bilinear we make separate calculations for the time and spatial components, also the latter is exact at any order

$$\begin{aligned} \bar{u}_{r'}(p')\gamma^0 u_r(p) = u^\dagger_{r'}(p')u_r(p) &\simeq \left(1 + \frac{|\mathbf{p}|^2}{4m^2} + \frac{1}{4m^2}(\mathbf{p}\cdot\mathbf{p}')\right)\delta_{r,r'} - \frac{i}{4m^2}(\mathbf{p}\times\mathbf{p}')\cdot\boldsymbol{\sigma} + \mathcal{O}\left(\frac{|\mathbf{p}|^2}{m^2}\right) \\ &\simeq \left(1 + \frac{|\mathbf{P}|^2}{2m^2}\right)\delta_{r,r'}\frac{i}{4m^2}(\mathbf{P}\times\mathbf{q})\cdot\boldsymbol{\sigma} + \mathcal{O}\left(\frac{|\mathbf{p}|^2}{m^2}\right) , \end{aligned} \tag{A.10}$$

$$\begin{aligned} \bar{u}_{r'}(p')\gamma^i u_r(p) &= \frac{1}{2m}\begin{pmatrix}\sqrt{E_{\mathbf{p}'}+m}\,\varphi^T_{r'} & -\varphi^T_{r'}\frac{\mathbf{p}'\cdot\boldsymbol{\sigma}}{\sqrt{E_{\mathbf{p}'}+m}}\end{pmatrix}\begin{pmatrix}\sigma^i\frac{\mathbf{p}\cdot\boldsymbol{\sigma}}{\sqrt{E_{\mathbf{p}}+m}}\varphi_r \\ -\sqrt{E_{\mathbf{p}}+m}\,\sigma^i\varphi_r\end{pmatrix} = \\ &= \frac{1}{2m}\varphi^T_{r'}\left(p^i + i(\mathbf{p}\times\boldsymbol{\sigma}) + p'^i - i(\mathbf{p}'\times\boldsymbol{\sigma})\right)\varphi_r = \\ &= \frac{1}{2m}\left(2\mathbf{P} - i(\mathbf{q}\times\boldsymbol{\sigma})\right)^i . \end{aligned} \tag{A.11}$$

It follows then the axial-vector bilinear, whose time component is now exact

$$\bar{u}_{r'}(p')\gamma^0\gamma^5 u_r(p) = \frac{1}{2m}\varphi^T_{r'}\left(\mathbf{p}'\cdot\boldsymbol{\sigma} + \mathbf{p}\cdot\boldsymbol{\sigma}\right)\varphi_r = \frac{\mathbf{P}}{m}\cdot\boldsymbol{\sigma} , \tag{A.12}$$

$$\bar{u}_{r'}(p')\gamma^i\gamma^5 u_r(p) \simeq \varphi^T_{r'}\left[\left(1+\frac{|\mathbf{p}|^2}{4m^2}\right)\sigma^i + \frac{1}{4m^2}(\mathbf{p}'\cdot\boldsymbol{\sigma})\sigma^i(\mathbf{p}\cdot\boldsymbol{\sigma}) + \mathcal{O}\left(\frac{|\mathbf{p}|^2}{m^2}\right)\right]\varphi_r = \\ \simeq \varphi^T_{r'}\Bigg[\left(1+\frac{|\mathbf{P}|^2}{4m^2}+\frac{|\mathbf{q}|^2}{16m^2}\right)\sigma^i + \frac{1}{4m^2}\left((\mathbf{P}+\frac{\mathbf{q}}{2})\cdot\boldsymbol{\sigma}\right)\sigma^i\left((\mathbf{P}-\frac{\mathbf{q}}{2})\cdot\boldsymbol{\sigma}\right) + \\ + \mathcal{O}\left(\frac{|\mathbf{p}|^2}{m^2}\right)\Bigg]\varphi_r\,. \tag{A.13}$$

The tensor current is constructed via the commutator between two Dirac matrices

$$\sigma^{\mu\nu} = \frac{i}{2}[\gamma^\mu,\gamma^\nu]\,, \tag{A.14}$$

in particular it is useful to calculate the following quantities

$$\sigma^{i0} = i\gamma^i\gamma^0 = -i\begin{pmatrix}0 & \sigma^i\\ \sigma^i & 0\end{pmatrix}\quad,\quad \sigma^{ij} = \epsilon^{ijk}\begin{pmatrix}\sigma^k & 0\\ 0 & \sigma^k\end{pmatrix} \tag{A.15}$$

$$\sigma^{i0}\gamma^5 = i\gamma^i\gamma^0\gamma^5 = -i\begin{pmatrix}\sigma^i & 0\\ 0 & \sigma^i\end{pmatrix}\quad,\quad \sigma^{ij}\gamma^5 = \epsilon^{ijk}\begin{pmatrix}0 & \sigma^k\\ \sigma^k & 0\end{pmatrix} \tag{A.16}$$

since in most cases the tensor current is contracted with $q_\mu q_\nu$, so the double temporal contraction vanishes by symmetry. The non-relativistic expansions of the tensor bilinear read

$$\bar{u}_{r'}(p')\sigma^{i0}u_r(p) = -\frac{i}{2m}\left(\sigma^i(\mathbf{p}\cdot\boldsymbol{\sigma}) - (\mathbf{p}'\cdot\boldsymbol{\sigma})\sigma^i\right) = -\frac{i}{2m}\left(-q^i + i(2\mathbf{P}\times\boldsymbol{\sigma})^i\right)\,, \tag{A.17}$$

$$\bar{u}_{r'}(p')\sigma^{ij}u_r(p) \simeq \epsilon^{ijk}\varphi^T_{r'}\Bigg[\left(1+\frac{|\mathbf{P}|^2}{4m^2}+\frac{|\mathbf{q}|^2}{16m^2}\right)\sigma^k - \frac{1}{4m^2}\left((\mathbf{P}+\frac{\mathbf{q}}{2})\cdot\boldsymbol{\sigma}\right)\sigma^k\left((\mathbf{P}-\frac{\mathbf{q}}{2})\cdot\boldsymbol{\sigma}\right) + \\ + \mathcal{O}\left(\frac{|\mathbf{p}|^2}{m^2}\right)\Bigg]\varphi_r\,. \tag{A.18}$$

Finally, the expansion of the bilinear components of the pseudo-tensor leads to

$$\bar{u}_{r'}(p')\sigma^{i0}\gamma^5 u_r(p) \simeq -i\,\varphi^T_{r'}\Bigg[\left(1+\frac{|\mathbf{P}|^2}{4m^2}+\frac{|\mathbf{q}|^2}{16m^2}\right)\sigma^i - \frac{1}{4m^2}\left((\mathbf{P}+\frac{\mathbf{q}}{2})\cdot\boldsymbol{\sigma}\right)\sigma^i\left((\mathbf{P}-\frac{\mathbf{q}}{2})\cdot\boldsymbol{\sigma}\right) + \\ + \mathcal{O}\left(\frac{|\mathbf{p}|^2}{m^2}\right)\Bigg]\varphi_r\,, \tag{A.19}$$

$$\bar{u}_{r'}(p')\sigma^{ij}\gamma^5 u_r(p) = \frac{\epsilon^{ijk}}{2m}\left(\sigma^k(\mathbf{p}\cdot\boldsymbol{\sigma}) - (\mathbf{p}'\cdot\boldsymbol{\sigma})\sigma^k\right) = \frac{\epsilon^{ijk}}{2m}\left(-q^k + i(2\mathbf{P}\times\boldsymbol{\sigma})^k\right)\,. \tag{A.20}$$

A.2 Convention on the Fourier Transform

The convention on the exponential factor of the Fourier transforms is directly connected to the direction of the transferred momentum inside a Feynman diagram. Considering all the incoming momenta in a vertex as positive the negative sign in the exponential for incoming momenta leads to the diagram in fig. (A.2), for which the Feynman propagator of the scalar field results in

$$i\Delta_F(x_1-x_2) = \int\frac{d^4q}{(2\pi)^4}\,\frac{i}{q^2-m^2+i\epsilon}\,e^{-iq\cdot(x_1-x_2)}\,; \tag{A.21}$$

The consistency of the chosen convention cannot be forgotten because it can lead to a mismatch of signs in the literature. Physical observables are not sensitive to convention as long as they are used consistently. All the analyses in the thesis adhere to the Fourier transform of the type

$$F(x) = \int\frac{d^4q}{(2\pi)^4}\tilde{F}(q)e^{-iq\cdot x} \tag{A.22}$$

for which the direction of the transferred momentum in a tree-level diagram is taken upwards. $F(x)$ denotes a general function in coordinate space damping to zero sufficiently fast, and $\tilde{F}(q)$ its Fourier counterpart in momentum space.

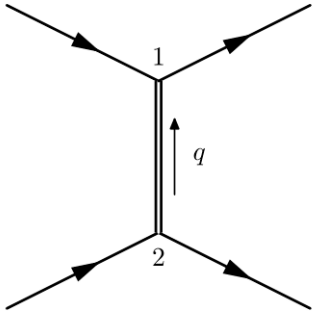

Figure A.2: Transferred momentum from 2 to 1.

A different convention can also be used considering a negative sign in the exponent of eq. (A.22), by appropriately reversing the sign of the moment transferred of the diagram in fig. (A.2).

APPENDIX B

USEFUL CALCULATIONS

B.1 Derivatives of the Yukawa potential

It is useful to calculate the various derivatives of

$$\frac{e^{-Mr}}{r}\,, \tag{B.1}$$

emerging from the Fourier transform of all non-relativistic potentials. First, let us take

$$\partial_i\partial_j\left(\frac{e^{-Mr}}{r}\right). \tag{B.2}$$

The second derivative must be considered in the two cases where:

- $r \neq 0$:

$$\partial_j\left(\frac{e^{-Mr}}{r}\right) = -x^j\left(\frac{M}{r^2}+\frac{1}{r^3}\right)e^{-Mr}\,, \tag{B.3}$$

$$\partial_i\partial_j\left(\frac{e^{-Mr}}{r}\right) = -\left[\delta^{ij}\left(\frac{M}{r^2}+\frac{1}{r^3}\right) - M\frac{x^ix^j}{r}\left(\frac{M}{r^2}+\frac{1}{r^3}\right) - \frac{x^ix^j}{r}\left(\frac{2M}{r^3}+\frac{3}{r^4}\right)\right]e^{-Mr}\,; \tag{B.4}$$

- $r = 0$:

$$\nabla^2\left(\frac{1}{r}\right) = -4\pi\delta^3(\mathbf{x}) \rightarrow \partial_i\partial_j\left(\frac{1}{r}\right) = -\frac{4\pi}{3}\delta^{ij}\delta^3(\mathbf{x}) \tag{B.5}$$

  due to the distributional nature of the Coulomb law, we must add this quantity within the term multiplying δ_{ij}.

At the end:

$$\boldsymbol{\nabla}\left(\frac{e^{-Mr}}{r}\right) = -\left(\frac{M}{r}+\frac{1}{r^2}\right)\hat{\mathbf{r}}e^{-Mr}\,, \tag{B.6}$$

$$\partial_i\partial_j\left(\frac{e^{-Mr}}{r}\right) = -\left[\delta^{ij}\left(\frac{M}{r^2}+\frac{1}{r^3}+\frac{4\pi}{3}\delta^3(\mathbf{x})\right) - \hat{r}^i\hat{r}^j\left(\frac{M^2}{r}+\frac{3M}{r^2}+\frac{3}{r^3}\right)\right]e^{-Mr}\,, \tag{B.7}$$

$$\nabla^2\left(\frac{e^{-Mr}}{r}\right) = \left(\frac{M^2}{r} - 4\pi\delta^3(\mathbf{x})\right)e^{-Mr}\,. \tag{B.8}$$

Moving forward with the differetiation

$$\boldsymbol{\nabla}\nabla^2\left(\frac{e^{-Mr}}{r}\right) = -\left(\frac{M^2}{r^2}\hat{\mathbf{r}} + \frac{M^3}{r}\hat{\mathbf{r}} + 4\pi\boldsymbol{\nabla}\delta^3(\mathbf{x}) - 4\pi M\delta^3(\mathbf{x})\hat{\mathbf{r}}\right)e^{-Mr}\,, \tag{B.9}$$

$$\nabla^4\left(\frac{e^{-Mr}}{r}\right)=\left(\frac{M^4}{r}-8\pi M^2\delta^3(\mathbf{x})-4\pi\nabla^2\delta^3(\mathbf{x})+8\pi M\boldsymbol{\nabla}\delta^3(\mathbf{x})\cdot\hat{\mathbf{r}}\right)e^{-Mr}\,, \tag{B.10}$$

$$\begin{aligned}\partial_i\partial_j\nabla^2\left(\frac{e^{-m_a r}}{r}\right)=&\left\{\left[\frac{M^4}{r}-4\pi\delta^3(\mathbf{x})\left(\frac{M}{r}+M^2\right)+\frac{4M^3}{r^2}+\frac{6M^2}{r^3}\right]\hat{r}^i\hat{r}^j-4\pi\partial_i\partial_j\delta^3(\mathbf{x})+\right.\\&\left.+4\pi M\big(\hat{r}^i\partial_j\delta^3(\mathbf{x})+\hat{r}^j\partial_i\delta^3(\mathbf{x})\big)-\left(\frac{M^3}{r}-4\pi M\delta^3(\mathbf{x})+\frac{2M^2}{r^2}\right)\delta^{ij}\right\}e^{-Mr}\,.\end{aligned} \tag{B.11}$$

B.2 Integrals

The main Fourier transforms appearing in the tree-level work are the following

$$\int\frac{d^3q}{(2\pi)^3}\frac{e^{i\mathbf{q}\cdot\mathbf{x}}}{|\mathbf{q}|^2+M^2}=\frac{1}{4\pi^2 ir}\int_{-\infty}^{+\infty}dq\frac{qe^{iqr}}{q^2+M^2}=\frac{e^{-Mr}}{4\pi r}\,, \tag{B.12}$$

$$\int\frac{d^3q}{(2\pi)^3}\frac{e^{i\mathbf{q}\cdot\mathbf{x}}}{(|\mathbf{q}|^2+M^2)^2}=\frac{1}{4\pi^2 ir}\int_{-\infty}^{+\infty}dq\frac{qe^{iqr}}{(q^2+M^2)^2}=\frac{e^{-Mr}}{8\pi M}\,, \tag{B.13}$$

$$\int\frac{d^3q}{(2\pi)^3}\frac{e^{i\mathbf{q}\cdot\mathbf{x}}}{(|\mathbf{q}|^2+M^2)^3}=\frac{1}{4\pi^2 ir}\int_{-\infty}^{+\infty}dq\frac{qe^{iqr}}{(q^2+M^2)^3}=\frac{1+Mr}{32\pi M^3}e^{-Mr}\,, \tag{B.14}$$

where $r\equiv|\mathbf{x}|$.
In Chapter (6), the Bessel functions are typical solutions of the following integrals

$$\int_1^\infty dx\,\sqrt{1-\frac{1}{x}}e^{-\alpha\sqrt{x}}=\frac{2}{\alpha}K_1(\alpha)\,, \tag{B.15}$$

$$\int_1^\infty dx\,x\sqrt{1-\frac{1}{x}}e^{-\alpha\sqrt{x}}=\frac{2}{\alpha}K_1(\alpha)+\frac{6}{\alpha^2}K_2(\alpha)\,, \tag{B.16}$$

$$\int_1^\infty dx\,x^2\sqrt{1-\frac{1}{x}}e^{-\alpha\sqrt{x}}=\frac{4}{\alpha^2}K_2(\alpha)+\frac{2}{\alpha^2}(15+\alpha^2)K_3(\alpha)\,, \tag{B.17}$$

$$\int_1^\infty dx\,x^3\sqrt{1-\frac{1}{x}}e^{-\alpha\sqrt{x}}=\frac{2}{\alpha^3}(15+\alpha^2)K_3(\alpha)+\frac{10}{\alpha^4}(21+\alpha^2)K_4(\alpha)\,. \tag{B.18}$$

It is also useful to know the relationship between the Bessel functions of a generic index n, i.e.

$$K_{n+1}(\alpha)=K_{n-1}(\alpha)+\frac{2n}{\alpha}K_n(\alpha)\,, \tag{B.19}$$

whereas their derivatives can be written as

$$\frac{dK_n(\alpha)}{d\alpha}=-\frac{1}{2}\left(K_{n-1}(\alpha)+K_{n+1}(\alpha)\right)\,. \tag{B.20}$$

APPENDIX C

FURTHER ANALYTICAL RESULTS

C.1 Tensor Corrections

Tensor Tensor

The NLO of the Feynman amplitude for a pair of tensor currents is

$$\mathcal{M}_{TT} = \frac{4g_1^T g_2^T}{|\mathbf{q}|^2 + M^2}\left[(\boldsymbol{\sigma}\cdot\boldsymbol{\sigma}')|\mathbf{q}|^2 - (\boldsymbol{\sigma}\cdot\mathbf{q})(\boldsymbol{\sigma}'\cdot\mathbf{q}) + i|\mathbf{q}|^2\mathbf{q}\cdot\mathbf{A} + q^i q^j B^{ij} + |\mathbf{q}|^2 C + |\mathbf{q}|^4 D + E^{ij}q^i q^j|\mathbf{q}|^2\right], \tag{C.1}$$

producing the potential

$$V(\mathbf{x}) = V_{LO} + 4g_1^T g_2^T\left[-\mathbf{A}\cdot\boldsymbol{\nabla}\nabla^2 - B^{ij}\partial_i\partial_j - C\nabla^2 + D\nabla^4 + E^{ij}\partial_i\partial_j\nabla^2\right]\left(\frac{e^{-Mr}}{4\pi r}\right) \tag{C.2}$$

and carring out the multiple derivatives becomes

$$\begin{aligned} V(\mathbf{x}) = V_{LO} + 4g_1^T g_2^T\Bigg\{ & \mathbf{A}\cdot\hat{\mathbf{r}}\left(\frac{M^2}{r^2} + \frac{M^3}{r} - 4\pi M\delta^3(\mathbf{x})\right) + 4\pi\mathbf{A}\cdot\boldsymbol{\nabla}\delta^3(\mathbf{x}) + B^{ii}\left(\frac{M}{r^2} + \frac{1}{r^3} + \frac{4\pi}{3}\delta^3(\mathbf{x})\right) + \\ & - B^{ij}\hat{r}^i\hat{r}^j\left(\frac{M^2}{r} + \frac{3M}{r^2} + \frac{3}{r^3}\right) - C\left(\frac{M^2}{r} - 4\pi\delta^3(\mathbf{x})\right) + D\Bigg(\frac{M^4}{r} - 8\pi M^2\delta^3(\mathbf{x}) - 4\pi\nabla^2\delta^3(\mathbf{x}) + \\ & + 8\pi M\boldsymbol{\nabla}\delta^3(\mathbf{x})\cdot\hat{\mathbf{r}}\Bigg) + E^{ij}\hat{r}^i\hat{r}^j\left[\frac{M^4}{r} - 4\pi\delta^3(\mathbf{x})\left(\frac{M}{r} + M^2\right) + \frac{4M^3}{r^2} + \frac{6M^2}{r^3}\right] - 4\pi E^{ij}\partial_i\partial_j\delta^3(\mathbf{x}) + \\ & + 4\pi M E^{ij}\left(\hat{r}^i\partial_j\delta^3(\mathbf{x}) + \hat{r}^j\partial_i\delta^3(\mathbf{x})\right) - E^{ii}\left(\frac{M^3}{r} - 4\pi M\delta^3(\mathbf{x}) + \frac{2M^2}{r^2}\right)\Bigg\}\frac{e^{-Mr}}{4\pi}\,. \end{aligned} \tag{C.3}$$

where

$$\begin{aligned}
\mathbf{A} &\equiv \frac{\boldsymbol{v}_1\times\boldsymbol{\sigma}'}{4m_1}-\frac{\boldsymbol{v}_2\times\boldsymbol{\sigma}}{4m_2}+\frac{\boldsymbol{v}_1\times\boldsymbol{\sigma}}{2m_2}-\frac{\boldsymbol{v}_2\times\boldsymbol{\sigma}'}{2m_1}\,,\\
B^{ij} &\equiv \frac{(\boldsymbol{v}_1\cdot\boldsymbol{\sigma})}{4}\boldsymbol{v}_1^i\sigma'^j+\frac{(\boldsymbol{v}_2\cdot\boldsymbol{\sigma}')}{4}\boldsymbol{v}_2^i\sigma^j+\frac{(\boldsymbol{v}_1\times\boldsymbol{\sigma}')^i(\boldsymbol{v}_1\times\boldsymbol{\sigma})^j}{4}-(\boldsymbol{v}_1\times\boldsymbol{\sigma})^i(\boldsymbol{v}_2\times\boldsymbol{\sigma}')^j+\frac{(\boldsymbol{v}_2\times\boldsymbol{\sigma})^i(\boldsymbol{v}_2\times\boldsymbol{\sigma}')^j}{4}\,,\\
C &\equiv -\frac{(\boldsymbol{v}_1\cdot\boldsymbol{\sigma})(\boldsymbol{v}_1\cdot\boldsymbol{\sigma}')}{4}-\frac{(\boldsymbol{v}_2\cdot\boldsymbol{\sigma}')(\boldsymbol{v}_2\cdot\boldsymbol{\sigma})}{4}\,,\\
D &\equiv -\frac{\boldsymbol{\sigma}\cdot\boldsymbol{\sigma}'}{16m_1^2}-\frac{1}{4m_1m_2}\,,\\
E^{ij} &\equiv \frac{\sigma^i\sigma'^j}{16m_1^2}\,.
\end{aligned} \tag{C.4}$$

Pseudotensor-Pseudotensor

Expanding at the NLO of the non-relativistic limit gives the following amplitude

$$\begin{aligned}
\mathcal{M} =&\frac{4g_1^{\tilde{T}}g_2^{\tilde{T}}}{|\mathbf{q}|^2+M^2}\Bigg\{-(\mathbf{q}\cdot\boldsymbol{\sigma})(\mathbf{q}\cdot\boldsymbol{\sigma}')\left[1+\frac{|\mathbf{q}|^2}{8}\left(\frac{1}{m_1^2}+\frac{1}{m_2^2}\right)+\frac{|\mathbf{P}|^2}{2m_1^2}+\frac{|\mathbf{P}'|^2}{2m_2^2}\right]+\\
&+|\mathbf{q}|^2\left[\left(\frac{\mathbf{P}}{m_1}\cdot\frac{\mathbf{P}'}{m_2}\right)(\boldsymbol{\sigma}\cdot\boldsymbol{\sigma}')-\left(\frac{\mathbf{P}}{m_1}\cdot\boldsymbol{\sigma}'\right)\left(\frac{\mathbf{P}'}{m_2}\cdot\boldsymbol{\sigma}\right)\right]-\mathbf{q}\cdot\left(\frac{\mathbf{P}}{m_1}\times\boldsymbol{\sigma}\right)\mathbf{q}\cdot\left(\frac{\mathbf{P}'}{m_2}\times\boldsymbol{\sigma}'\right)\Bigg\}=\\
&=\frac{4g_1^{\tilde{T}}g_2^{\tilde{T}}}{|\mathbf{q}|^2+M^2}\left(q^iq^jA^{ij}+B|\mathbf{q}|^2+C^{ij}q^iq^j|\mathbf{q}|^2\right)\,,
\end{aligned} \tag{C.5}$$

with

$$\begin{aligned}
A^{ij} &\equiv -\sigma^i\sigma'^j\left(1+\frac{|\boldsymbol{v}|^2}{2}+\frac{|\boldsymbol{v}'|^2}{2}\right)-(\boldsymbol{v}\times\boldsymbol{\sigma})^i\left(\boldsymbol{v}'\times\boldsymbol{\sigma}'\right)^j\,,\\
B &\equiv \left(\boldsymbol{v}\cdot\boldsymbol{v}'\right)\left(\boldsymbol{\sigma}\cdot\boldsymbol{\sigma}'\right)-\left(\boldsymbol{v}\cdot\boldsymbol{\sigma}'\right)\left(\boldsymbol{v}'\cdot\boldsymbol{\sigma}\right)\,,\\
C^{ij} &\equiv -\frac{\sigma^i\sigma'^j}{8}\left(\frac{1}{m_1^2}+\frac{1}{m_2^2}\right)\,.
\end{aligned} \tag{C.6}$$

It follows the potential

$$\begin{aligned}
V(\mathbf{x}) =&4g_1^{\tilde{T}}g_2^{\tilde{T}}\left(A^{ij}\partial_i\partial_j+B\nabla^2-C^{ij}\partial_i\partial_j\nabla^2\right)\left(\frac{e^{-Mr}}{4\pi r}\right)=\\
&4g_1^{\tilde{T}}g_2^{\tilde{T}}\Bigg\{-A^{ii}\left(\frac{M}{r^2}+\frac{1}{r^3}+\frac{4\pi}{3}\delta^3(\mathbf{x})\right)+A^{ij}\hat{r}^i\hat{r}^j\left(\frac{M^2}{r}+\frac{3M}{r^2}+\frac{3}{r^3}\right)+B\left(\frac{M^2}{r}-4\pi\delta^3(\mathbf{x})\right)+\\
&-C^{ij}\hat{r}^i\hat{r}^j\left[\frac{M^4}{r}-4\pi\delta^3(\mathbf{x})\left(\frac{M}{r}+M^2\right)+\frac{4M^3}{r^2}+\frac{6M^2}{r^3}\right]+4\pi C^{ij}\partial_i\partial_j\delta^3(\mathbf{x})+\\
&-4\pi MC^{ij}\left(\hat{r}^i\partial_j\delta^3(\mathbf{x})+\hat{r}^j\partial_i\delta^3(\mathbf{x})\right)+C^{ii}\left(\frac{M^3}{r}-4\pi M\delta^3(\mathbf{x})+\frac{2M^2}{r^2}\right)\Bigg\}\frac{e^{-Mr}}{4\pi}
\end{aligned} \tag{C.7}$$

Pseudo-tensor Tensor

The mixed currents, with the NLO corrections, give the amplitude

$$\mathcal{M}=4\frac{g_1^{\tilde{T}}g_2^{T}}{|\mathbf{q}|^2+M^2}\left[A^{ij}q^iq^j|\mathbf{q}|^2+B|\mathbf{q}|^2+C^{ij}q^iq^j+\mathbf{D}\cdot i\mathbf{q}|\mathbf{q}|^2+E|\mathbf{q}|^4+\mathbf{F}\cdot i\mathbf{q}|\mathbf{q}|^4\right] \tag{C.8}$$

and the resulting potential is

$$
\begin{aligned}
V(\mathbf{x}) &= -4g_1^{\tilde{T}} g_2^T \left(A^{ij}\partial_i\partial_j\nabla^2 - B\nabla^2 - C^{ij}\partial_i\partial_j - \mathbf{D}\cdot\boldsymbol{\nabla}\nabla^2 + E\nabla^4 + \mathbf{F}\cdot\boldsymbol{\nabla}\nabla^4\right)\frac{e^{-Mr}}{4\pi r} = \\
&= -4g_1^{\tilde{T}} g_2^T\Bigg\{A^{ij}\hat{r}^i\hat{r}^j\left[\frac{M^4}{r} - 4\pi\delta^3(\mathbf{x})\left(\frac{M}{r}+M^2\right) + \frac{4M^3}{r^2} + \frac{6M^2}{r^3}\right] - 4\pi A^{ij}\partial_i\partial_j\delta^3(\mathbf{x}) + \\
&+ 4\pi M A^{ij}\left(\hat{r}^i\partial_j\delta^3(\mathbf{x})\hat{r}^j\partial_i\delta^3(\mathbf{x})\right) - A^{ii}\left(\frac{M^3}{r} - 4\pi M\delta^3(\mathbf{x}) + \frac{2M^2}{r^2}\right) - B\left(\frac{M^2}{r} - 4\pi\delta^3(\mathbf{x})\right) + \\
&+ C^{ii}\left(\frac{M}{r^2} + \frac{1}{r^3} + \frac{4\pi}{3}\delta^3(\mathbf{x})\right) - C^{ij}\hat{r}^i\hat{r}^j\left(\frac{M^2}{r} + \frac{3M}{r^2} + \frac{3}{r^3}\right) + \mathbf{D}\cdot\left(\frac{M^2}{r^2}\hat{\mathbf{r}} + \frac{M^3}{r}\hat{\mathbf{r}} + 4\pi\boldsymbol{\nabla}\delta^3(\mathbf{x}) + \right. \\
&\left. - 4\pi M\delta^3(\mathbf{x})\hat{\mathbf{r}}\right) + E\left(\frac{M^4}{r} - 8\pi M^2\delta^3(\mathbf{x}) - 4\pi\nabla^2\delta^3(\mathbf{x}) + 8\pi M\boldsymbol{\nabla}\delta^3(\mathbf{x})\cdot\hat{\mathbf{r}}\right) - \mathbf{F}\cdot\left(\frac{M^5}{r}\hat{\mathbf{r}} + \right. \\
&\left. - 8\pi M^3\delta^3(\mathbf{x})\hat{\mathbf{r}} - 4\pi M\nabla^2\delta^3(\mathbf{x})\hat{\mathbf{r}} + 8\pi M^2(\boldsymbol{\nabla}\delta^3(\mathbf{x})\cdot\hat{\mathbf{r}})\hat{\mathbf{r}} + \frac{M^4}{r^2}\hat{\mathbf{r}} + 8\pi M^2\boldsymbol{\nabla}\delta^3(\mathbf{x}) + 4\pi\boldsymbol{\nabla}\nabla^2\delta^3(\mathbf{x}) + \right. \\
&\left. - 8\pi M\boldsymbol{\nabla}(\boldsymbol{\nabla}\delta^3(\mathbf{x})\cdot\hat{\mathbf{r}})\right)\Bigg\}\frac{e^{-Mr}}{4\pi}\,,
\end{aligned}
\tag{C.9}
$$

where

$$
\begin{aligned}
A^{ij} &= -\frac{P^i\epsilon^{kjl}\sigma'^k\sigma^l}{8m_1^3} + \frac{\sigma'^i\epsilon^{jkl}P^k\sigma^l}{16m_1m_2^2} + \frac{\sigma^i\epsilon^{jkl}P'^k\sigma'^l}{8m_1^2m_2}\,, \\
B &= \frac{\mathbf{P}\cdot\boldsymbol{\sigma}\times\boldsymbol{\sigma}'}{m_1} + \frac{\mathbf{P}\cdot\boldsymbol{\sigma}\times\boldsymbol{\sigma}'|\mathbf{P}'|^2}{4m_1m_2^2} - \frac{(\mathbf{P}'\cdot\boldsymbol{\sigma}')\mathbf{P}'\cdot\mathbf{P}\times\boldsymbol{\sigma}}{2m_1m_2^2}\,, \\
C^{ij} &= -\frac{\epsilon^{ikl}P_1^k\sigma^l\sigma'^j}{m_1} - \frac{\epsilon^{ikl}P^k\sigma^l\sigma'^j|\mathbf{P}'|^2}{4m_1m_2^2} + \frac{\epsilon^{ikl}P^k\sigma^lP'^j(\mathbf{P}'\cdot\boldsymbol{\sigma}')}{2m_1m_2^2} + \frac{\epsilon^{ikl}P'^k\sigma'^l\sigma^j}{m_2} + \frac{\epsilon^{ikl}P'^k\sigma'^l\sigma^j|\mathbf{P}|^2}{2m_1^2m_2}\,, \\
\mathbf{D} &= -\frac{\mathbf{P}'\times(\mathbf{P}\times\boldsymbol{\sigma})}{4m_1m_2^2} - \frac{\boldsymbol{\sigma}}{2m_2} - \frac{|\mathbf{P}|^2\boldsymbol{\sigma}}{4m_1^2m_2}\,, \\
E &= -\frac{\mathbf{P}\cdot\boldsymbol{\sigma}\times\boldsymbol{\sigma}'}{16m_1m_2^2} \\
\mathbf{F} &= -\frac{\boldsymbol{\sigma}}{16m_1^2m_2}\,.
\end{aligned}
\tag{C.10}
$$

BIBLIOGRAPHY

[1] G. Apollinari et al. "High Luminosity Large Hadron Collider HL-LHC". In: *CERN Yellow Rep.* 5 (2015). Ed. by G Apollinari et al., pp. 1–19.

[2] Georges Aad et al. "Observation of a new particle in the search for the Standard Model Higgs boson with the ATLAS detector at the LHC". In: *Phys. Lett. B* 716 (2012), pp. 1–29.

[3] Serguei Chatrchyan et al. "Observation of a New Boson at a Mass of 125 GeV with the CMS Experiment at the LHC". In: *Phys. Lett. B* 716 (2012), pp. 30–61.

[4] Jon Butterworth. "The Standard Model: How far can it go and how can we tell?" In: *Phil. Trans. Roy. Soc. Lond. A* 374.2075 (2016). Ed. by C. David Garner, p. 20150260.

[5] Hyun Min Lee. "Lectures on physics beyond the Standard Model". In: *J. Korean Phys. Soc.* 78.11 (2021), pp. 985–1017.

[6] Roberto D. Peccei. "The Strong CP Problem and Axions". In: *Lecture Notes in Physics*. Springer Berlin Heidelberg, 2008, pp. 3–17.

[7] Bob Holdom. "Two U(1)'s and Epsilon Charge Shifts". In: *Phys. Lett. B* 166 (1986), pp. 196–198.

[8] Basudeb Dasgupta and Joachim Kopp. "Sterile Neutrinos". In: *Phys. Rept.* 928 (2021), pp. 1–63.

[9] E. G. Adelberger, Blayne R. Heckel, and A. E. Nelson. "Tests of the gravitational inverse square law". In: *Ann. Rev. Nucl. Part. Sci.* 53 (2003), pp. 77–121.

[10] Asimina Arvanitaki and Andrew A. Geraci. "Resonantly Detecting Axion-Mediated Forces with Nuclear Magnetic Resonance". In: *Physical Review Letters* 113.16 (Oct. 2014).

[11] Pavel Fadeev et al. "Revisiting spin-dependent forces mediated by new bosons: Potentials in the coordinate-space representation for macroscopic- and atomic-scale experiments". In: *Phys. Rev. A* 99 (2 Feb. 2019), p. 022113.

[12] Bogdan A. Dobrescu and Irina Mocioiu. "Spin-dependent macroscopic forces from new particle exchange". In: *Journal of High Energy Physics* 2006.11 (Nov. 2006), p. 005.

[13] G. Feinberg and J. Sucher. "Long-Range Forces from Neutrino-Pair Exchange". In: *Phys. Rev.* 166 (5 Feb. 1968), pp. 1638–1644.

[14] J. Sucher. "LONG RANGE FORCES IN QUANTUM THEORY". In: *Cargese Lect. Phys.* 7 (1977). Ed. by M. Levy, pp. 43–110.

[15] Sylvain Fichet. "Quantum Forces from Dark Matter and Where to Find Them". In: *Physical Review Letters* 120.13 (Mar. 2018).

[16] R. Essig et al. *Dark Sectors and New, Light, Weakly-Coupled Particles*. 2013.

[17] Joerg Jaeckel and Andreas Ringwald. "The Low-Energy Frontier of Particle Physics". In: *Annual Review of Nuclear and Particle Science* 60.1 (Nov. 2010), pp. 405–437.

[18] Joseph D. Lykken. *Beyond the Standard Model*. 2011.

[19] Gianfranco Bertone and Dan Hooper. "History of dark matter". In: *Rev. Mod. Phys.* 90 (4 Oct. 2018), p. 045002.

[20] Jihn E. Kim and Gianpaolo Carosi. "Axions and the strong CP problem". In: *Rev. Mod. Phys.* 82 (1 Mar. 2010), pp. 557–601.

[21] Steven Weinberg. "A New Light Boson?" In: *Phys. Rev. Lett.* 40 (1978), pp. 223–226.
[22] R. D. Peccei and Helen R. Quinn. "CP Conservation in the Presence of Pseudoparticles". In: *Phys. Rev. Lett.* 38 (25 June 1977), pp. 1440–1443.
[23] "Cosmology of the invisible axion". In: *Physics Letters B* 120.1 (1983), pp. 127–132.
[24] R. D. Peccei and Helen R. Quinn. "Constraints Imposed by CP Conservation in the Presence of Instantons". In: *Phys. Rev. D* 16 (1977), pp. 1791–1797.
[25] Frank Wilczek. "Problem of Strong P and T Invariance in the Presence of Instantons". In: *Phys. Rev. Lett.* 40 (1978), pp. 279–282.
[26] John Preskill, Mark B. Wise, and Frank Wilczek. "Cosmology of the Invisible Axion". In: *Phys. Lett. B* 120 (1983). Ed. by M. A. Srednicki, pp. 127–132.
[27] L. F. Abbott and P. Sikivie. "A Cosmological Bound on the Invisible Axion". In: *Phys. Lett. B* 120 (1983). Ed. by M. A. Srednicki, pp. 133–136.
[28] Michael Dine and Willy Fischler. "The Not So Harmless Axion". In: *Phys. Lett. B* 120 (1983). Ed. by M. A. Srednicki, pp. 137–141.
[29] Edward V. Shuryak. "Theory and phenomenology of the QCD vacuum". In: *Phys. Rept.* 115 (1984), p. 151.
[30] C. A. Baker et al. "An Improved experimental limit on the electric dipole moment of the neutron". In: *Phys. Rev. Lett.* 97 (2006), p. 131801.
[31] C. Abel et al. "Measurement of the Permanent Electric Dipole Moment of the Neutron". In: *Physical Review Letters* 124.8 (Feb. 2020).
[32] Stefan Scherer. "Introduction to chiral perturbation theory". In: *Adv. Nucl. Phys.* 27 (2003). Ed. by John W. Negele and E. W. Vogt, p. 277.
[33] G. Ecker. "Chiral perturbation theory". In: *Prog. Part. Nucl. Phys.* 35 (1995), pp. 1–80.
[34] Luca Di Luzio et al. "The landscape of QCD axion models". In: *Physics Reports* 870 (July 2020), pp. 1–117.
[35] Georg G. Raffelt. "Astrophysical axion bounds". In: *Lect. Notes Phys.* 741 (2008). Ed. by Markus Kuster, Georg Raffelt, and Berta Beltran, pp. 51–71.
[36] Luca Di Luzio et al. "Stellar evolution confronts axion models". In: *JCAP* 02.02 (2022), p. 035.
[37] J. E. Moody and Frank Wilczek. "New Macroscopic Forces?" In: *Phys. Rev. D* 30 (1 July 1984), pp. 130–138.
[38] Stefano Bertolini, Luca Di Luzio, and Fabrizio Nesti. "Axion-mediated forces, CP violation and left-right interactions". In: *Phys. Rev. Lett.* 126.8 (2021), p. 081801.
[39] Luca Di Luzio. "CP-violating axions". In: *PoS* EPS-HEP2021 (2022), p. 513.
[40] Pavel Fadeev et al. "Revisiting spin-dependent forces mediated by new bosons: Potentials in the coordinate-space representation for macroscopic- and atomic-scale experiments". In: *Physical Review A* 99.2 (Feb. 2019).
[41] Ciaran A. J. O'Hare and Edoardo Vitagliano. "Cornering the axion with CP-violating interactions". In: *Phys. Rev. D* 102 (11 Dec. 2020), p. 115026.
[42] Igor G. Irastorza and Javier Redondo. "New experimental approaches in the search for axion-like particles". In: *Progress in Particle and Nuclear Physics* 102 (2018), pp. 89–159. ISSN: 0146-6410.
[43] Georg Raffelt. "Limits on a CP-violating scalar axion-nucleon interaction". In: *Phys. Rev. D* 86 (1 July 2012), p. 015001.
[44] N. Crescini et al. "Improved constraints on monopole–dipole interaction mediated by pseudo-scalar bosons". In: *Physics Letters B* 773 (2017), pp. 677–680.
[45] Pierre Sikivie. "Invisible axion search methods". In: *Rev. Mod. Phys.* 93 (1 Feb. 2021), p. 015004.
[46] Andrea Caputo et al. "Dark photon limits: A handbook". In: *Phys. Rev. D* 104.9 (2021), p. 095029.
[47] Jun John Sakurai. *Modern quantum mechanics; rev. ed.* Reading, MA: Addison-Wesley, 1994.
[48] Albert Messiah. *Quantum Mechanics 1.* Series in physics. North-Holland, 1961.
[49] M.D. Schwartz. *Quantum Field Theory and the Standard Model.* illustrated. Quantum Field Theory and the Standard Model. Cambridge University Press, 2013.
[50] Michael Edward Peskin and Daniel V. Schroeder. *An Introduction to Quantum Field Theory.* Reading, USA: Addison-Wesley (1995) 842 p. Westview Press, 1995.

[51] P. Caldirola. "Eden, R. J. - High Energy Collisions of Elementary Particles". In: *Scientia* 64.5 (1970), p. 344.
[52] Steven Weinberg. *Quantum theory of fields. Foundations Volume 1*. 1st ed. Cambridge University Press, 1995.
[53] Ramamurti Shankar. *Principles of Quantum Mechanics, Second Edition*. 2nd. Springer, 1994.
[54] David J. Griffiths. *Introduction to Electrodynamics*. 3rd ed. Prentice Hall, 1999.
[55] Ryuji Daido and Fuminobu Takahashi. "The sign of the dipole–dipole potential by axion exchange". In: *Physics Letters B* 772 (Sept. 2017), pp. 127–129.
[56] Xun-Jie Xu and Bingrong Yu. "On the short-range behavior of neutrino forces beyond the Standard Model: from 1/r5 to 1/r4, 1/r2, and 1/r". In: *Journal of High Energy Physics* 2022.2 (Feb. 2022).
[57] P. Munro-Laylim, V. A. Dzuba, and V. V. Flambaum. *Effects of the long-range neutrino-mediated force in atomic phenomena*. 2022.
[58] Nicholas Orlofsky and Yue Zhang. "Neutrino as the dark force". In: *Phys. Rev. D* 104 (7 Oct. 2021), p. 075010.
[59] Philippe Brax, Sylvain Fichet, and Guillaume Pignol. "Bounding quantum dark forces". In: *Physical Review D* 97.11 (June 2018).
[60] Hannah Banks and Matthew McCullough. "Charting the fifth force landscape". In: *Physical Review D* 103.7 (Apr. 2021).
[61] Alexandria Costantino, Sylvain Fichet, and Philip Tanedo. "Exotic Spin-Dependent Forces from a Hidden Sector". In: *JHEP* 03 (2020), p. 148.
[62] Mario Trigiante (auth.) Riccardo D'Auria. *From Special Relativity to Feynman Diagrams: A Course of Theoretical Particle Physics for Beginners*. 1st ed. UNITEXT. Springer, 2012.

ACKNOWLEDGEMENTS

I am deeply grateful to my supervisor Dr. Luca Di Luzio for his invaluable advices, continuous support, and patience during the thesis work. His supervision was really influential in shaping my methods of analysis and research. My gratitude goes to all my family and friends who supported me and stood by me in the most difficult times. It is their kind help and support that have made my life a wonderful time. Lastly, I would like to thank all the professors who passionately guided me through the most fascinating discoveries of modern physics.